

# Design and Validation of an MR Conditional Upper Extremity Evaluation System to Study Brain Activation Patterns after Stroke

Rubing Xu  
*Marquette University*

---

## Recommended Citation

Xu, Rubing, "Design and Validation of an MR Conditional Upper Extremity Evaluation System to Study Brain Activation Patterns after Stroke" (2010). *Master's Theses (2009 -)*. Paper 51.  
[http://epublications.marquette.edu/theses\\_open/51](http://epublications.marquette.edu/theses_open/51)

DESIGN AND VALIDATION OF AN MR CONDITIONAL UPPER EXTREMITY  
EVALUATION SYSTEM TO STUDY  
BRAIN ACTIVATION PATTERNS  
AFTER STROKE

By:

Rubing Xu, B.S.

A Thesis submitted to the Faculty of the Graduate School,  
Marquette University,  
in Partial Fulfillment of the Requirements for  
the Degree of Masters of Science

Milwaukee, Wisconsin

August 2010

# ABSTRACT

## DESIGN AND VALIDATION OF AN MR CONDITIONAL UPPER EXTREMITY EVALUATION SYSTEM TO STUDY BRAIN ACTIVATION PATTERNS AFTER STROKE

Rubing Xu, B.S.

Marquette University, 2010

Stroke is the third leading cause of death and second most frequent cause of disability in the United States. Stroke rehabilitation methods have been developed to induce the cortical reorganization and motor-relearning that leads to stroke recovery. In this thesis, we designed and developed an MR conditional upper extremity reach and grasp movement evaluation system for the stroke survivors to study their kinematic performances in reach and grasp movement and the relationship between kinematic metrics and the recovery level measured by clinical assessment methods. We also applied the system into the functional MRI experiments to identify the ability to study motor performance with the system inside the scanner and the reach, grasp and reach-to-grasp movements related brain activation patterns.

Our experiments demonstrate that our system is an MR conditional system in a 3.0 Tesla magnetic field. The system is able to measure the stroke survivors' reach and grasp movement in terms of grasp aperture and elbow joint angles. We used the Mann Whitney U test to examine the significant metrics in each tasks and principle component analysis to decide the major metrics that are associated with the outcome. Then we used the linear regression analysis to create the regression models between the recovery scores and the kinematic metrics. The regression models suggest that functional recovery for reach and/or grasp tasks is predictable with maximal and mean velocities, maximal movement, error in reach, grasp and reach-to-grasp tasks. We discovered that low functioning subjects generally showed smaller movement velocity, smaller maximal movement, larger error and longer time to peak velocity in reach, grasp and reach-to-grasp tasks. In addition to these metrics, time to maximal angle, time to target and time to peak velocity could also be used as additional metrics to help predict the recovery, assess robot-assisted therapy and optimize task-oriented rehabilitation strategy. We also applied the system into an fMRI case series and proved that we are able to capture the brain activation patterns after stroke with our system and experiment set up.

## ACKNOWLEDGEMENTS

Life is a journey and we never know what is going to happen next. In looking back on my journey of graduate study at Marquette University, there are so many important individuals that helped me with every step. I would like to first thank Dr. Michelle J. Johnson, my academic and research advisor, for providing me with the opportunity to study in the United States, and for believing that I could carry out the work. Dr. Johnson has been generous and patient in her help, encouragement and guidance. I will always be grateful for that.

Thanks also go to all my committee members: Dr. Robert Scheidt, Dr. Sheila Schindler-Ivens and Dr. Sandra Hunter for their generous time and valuable advice.

I am grateful for the help, suggestions and comments provided by staff and colleagues at the Medical College of Wisconsin (MCW), especially Mr. Matthew Verber, Dr. Yu Liu, Mr. Wolfgang Gaggl, Mr. Timothy Thelaner, Dr. Thomas Prieto, Dr. Andrew Nencka, Dr. Aniko Szabo and Ms. Qun Xiang.

I would also like to thank Dr. Dean Jeutter for his help with the encoder board and electronics, Mr. Sheku Kamara at Milwaukee School of Engineering (MSOE) for his excellent work on the orthosis; Mr. Raymond Hamilton and Mr. Dave Gibas at Discovery Learning Center at Marquette University for their help in the mechanic shop.

I would also like to thank all past and present staffs at Rehabilitation Robotics Lab at the Clement J. Zablocki VA for their generous help and suggestions, support and encouragement, especially Jeff Melbye, DSci, Dominc E. Nathan, MS, Elaine Strachota, Ph.D, OTR, Rohit Ruperal, Shantanu Karnik, Yuniya Shakya Bishop, MS, Ping Bai, Ph.D, Jerome McGinnis, Yasser Mallick, Ph.D and Linda Telfered.

I thank the Neuro-Motor Control Lab for providing us with the Simulink programs and devices. I also thank all subjects who took part in the study and provided me with valuable feedback.

I would also like to thank our funding source: National Institutes of Health Career Award K25NS058577 - 01A1 and the Advancing a Healthier Wisconsin Grant #5520015 with infrastructure support from the Zablocki VA Medical Center. I will always be grateful for the priceless treasure I gained from the Rehabilitation Robotics Lab – the knowledge, skills, experience and much more.

Special thanks go to Songrui for standing by my side through everything, believing me and encouraging me even when I did not believe in myself and for never letting me lose hope.

And finally, my sincere gratitude goes to my parents Ruodou Xu and Shanglei Zuo. Words alone cannot express how much I owe you and how much I love you.

To my parents, I would like to dedicate this thesis.

## TABLE OF CONTENTS

ACKNOWLEDGEMENTS .....	i
LIST OF TABLES .....	viii
LIST OF FIGURES .....	x
LIST OF ABBREVIATIONS.....	xii
 CHAPTER	
1. THESIS OVERVIEW.....	2
1.1. Introduction.....	2
2. BACKGROUND .....	6
2.1. Stroke and its rehabilitation .....	6
2.2. Retraining Reach and Grasp Movements .....	7
2.2.1. Robot Assisted Therapy for Retraining Reach and Grasp Movements.....	9
2.2.2. Evaluating Reach and/or Grasp Motor Performance .....	11
2.2.2.1. Clinical assessment tools .....	11
2.2.2.2. Biomechanical assessment tools .....	13
2.3. Brain Function after Stroke.....	14
2.3.1.Theories of cerebral plasticity.....	14
2.3.2.Assessing brain function using fMRI .....	15
2.3.2.1. fMRI techniques.....	15
2.3.2.2. fMRI study design.....	16
2.3.2.3. fMRI task design and results.....	17
2.4. Summary .....	18
3. UPPER EXTREMITY REACH AND GRASP (UE R/G) SYSTEM	

DEVELOPMENT .....	21
3.1. Introduction.....	21
3.2. System development .....	23
3.2.1. System Requirements.....	23
3.2.2. System Overview .....	25
3.3. System Components.....	27
3.3.1 Hardware.....	28
3.3.1.1. Hand glove.....	28
3.3.1.2. Elbow orthosis .....	31
3.3.2. Software .....	32
3.3.2.1. Data acquisition .....	32
3.3.2.2. Task control .....	33
3.3.2.3. Task display .....	38
3.4. Elbow Orthosis Calibration Study .....	41
3.4.1. Calibration Experiment Set-up .....	41
3.4.2. Data analysis .....	44
3.4.3. Elbow Calibration Results and Discussion.....	44
3.5. MR Safety Validation Study.....	49
3.5.1. MR Validation Procedure .....	50
3.5.2. Data Analysis .....	51
3.5.3. Results and Discussion .....	53
3.5.3.1. Phase image .....	53
3.5.3.2. Image Quality.....	55

3.5.3.3. Device .....	55
3.6. Conclusion .....	57
<b>4. A CORRELATION STUDY BETWEEN REACH AND GRASP MOVEMENT AND THE STROKE IMPAIRMENT LEVEL .....</b>	<b>59</b>
4.1. Abstract .....	59
4.2. Background .....	60
4.3. Methods.....	65
4.3.1. Apparatus .....	66
4.3.2. Experiment protocol.....	66
4.3.3. Data analysis method .....	69
4.3.3.1. Clinical data .....	70
4.3.3.2. Performance metrics .....	71
4.4. Result and discussion.....	72
4.4.1. Clinical measurement results .....	72
4.4.2. Movement performance results.....	77
4.4.2.1. Movement trajectories .....	77
4.4.2.2. Kinematic metrics .....	80
4.4.3. Comparison of two movements in the only and combined movements .....	95
4.4.4. Coordination between reach and grasp movement .....	100
4.5. Discussion .....	101
4.5.1. Clinical assessment .....	101
4.5.2. High and low function subjects performance differences.	102
4.5.3. Evaluation of movements and kinematic .....	106
4.6. Conclusion and future directions .....	109

5. UE R/G SYSTEM USABILITY TESTING INSIDE MR ENVIRONMENT WITH INSIGHTS INTO BRAIN ACTIVATION PATTERNS AFTER REACH AND GRASP TASKS: A CASE SERIES .....	111
5.1. Overview .....	111
5.2. Background .....	112
5.2.1. Study goals .....	116
5.3. Method .....	117
5.3.1. Subjects .....	117
5.3.2. Experiment procedure .....	119
5.3.3. Experiment set up .....	120
5.3.4. Data acquisition .....	121
5.3.4.1. Movement data acquisition .....	121
5.3.4.2. Image data acquisition .....	122
5.3.5. Data analysis .....	124
5.3.5.1. Performance data analysis .....	124
5.3.5.2. Image data analysis .....	124
5.4. Results .....	126
5.4.1. Movement performance .....	126
5.4.2. Brain Activation .....	128
5.4.2.1. Model fitting .....	128
5.4.2.2. Brain activation patterns .....	129
5.4.3. Head movement .....	133
5.5. Discussion .....	135
5.6. Conclusion .....	138
6. CONCLUSIONS AND FUTURE DIRECTIONS .....	141

REFERENCES .....	144
APPENDIX.....	155
Appendix A: Detailed description of clinical measurements .....	155
Appendix B: Diagram of device set up.....	158
Appendix C: Compatibility test result .....	159
C.1. B field change in the compatibility test.....	159
C.2. SNR of magnitude image .....	160
Appendix D: Sensors' reading in the compatibility test .....	161
D.1. Grasp aperture in the non-movement conditions .....	161
D.2. Grasp aperture in the movement conditions .....	161
D.3. Encoder reading in the movement conditions.....	162
Appendix E: Kinematic metrics used to evaluate movements.....	163
Appendix F: Task results .....	165
F.1. Reach task results .....	165
F.2. Grasp task results.....	167
F.3. Reach movement results in the reach to grasp task .....	168
F.4. Grasp movement in the reach to grasp task .....	169
F.5. Kinematics results by groups.....	170
Appendix G: The location of activation areas .....	172
Appendix H: Inclusion/exclusion criterion of subjects in the fMRI case study	173
Appendix I: Comparison of kinematics measure of reach-to-grasp movement between inside and outside the scanner .....	174

## LIST OF TABLES

Table 3.1 Comparison between encoder reading and the designed angles of four subjects .....	46
Table 3.2 ANOVA result on the phase image B field change .....	54
Table 3.3 ANOVA result on the magnitude image.....	55
Table 3.4 Two-way ANOVA result for the glove and sensors.....	57
Table 4.1 Standard outcome measurement tools for stroke.....	61
Table 4.2 Kinematic metrics for evaluating movements .....	64
Table 4.3 Subject information.....	66
Table 4.4 Clinical measurement for low functioning subjects* .....	74
Table 4.6 Mann Whitney U test result of the performance metrics in the reach movement .....	82
Table 4.7 Principle components among the kinematic metrics in the reach task .....	83
Table 4.8 Mann Whitney U test result of the performance metrics in the grasp movement .....	86
Table 4.9 Mann-Whitney U test result of the performance metrics in the grasp movement excluding subject 2 .....	88
Table 4.10 Principle components among the kinematic metrics in the grasp task .....	89
Table 4.11 Mann Whitney U test result in reach-to-grasp task .....	93
Table 4.12 Mann Whitney U test result in reach-to-grasp task .....	94
Table 4.13 Mann Whitney U test result for reach movement in reach only and reach-to-grasp tasks.....	97
Table 4.14 Mann Whitney U test result for grasp movement in grasp only and reach-to-grasp tasks.....	98
Table 4.15 Paired T test results between reach only and the reach portion in reach-to-grasp tasks.....	99
Table 4.16 Paired T test results between grasp only and the grasp portion in reach-to-grasp tasks.....	99
Table 4.17 Mann-Whitney U test result of the time ratio metrics in the grasp movement .....	100

Table 5.1 Subject information.....	118
Table 5.2 fMRI scan type and time.....	123
Table 5.3 The cross-correlation results of single inside vs. outside the scan. ....	128
Table 5.4 Head movement range of each subject .....	134

## LIST OF FIGURES

Figure 3.1 Basic configuration of the system .....	27
Figure 3.2 System flow .....	27
Figure 3.3 The hand glove. Four bend sensors (sensor 1-4) are inserted into the sleeves to cover index and thumb PIP and MCP joint. ....	29
Figure 3.4 The hand model to calculate the grasp aperture ( $\beta$ ). ....	30
Figure 3.5 The equations to calculate grasp aperture ( $\beta$ ). ....	30
Figure 3.6 Configuration of elbow orthosis. ....	31
Figure 3.7 The data configuration of hand glove. ....	33
Figure 3.8 Experiment flowchart .....	34
Figure 3.9 The blank trial and three tasks display. ....	35
Figure 3.10 Flowchart of the grasp task control .....	36
Figure 3.11 Five states of the grasp task. ....	37
Figure 3.12 Four states of the reach to grasp movement. ....	39
Figure 3.13 Example results of grasp movement. ....	40
Figure 3.14 Example results of reach movement. ....	40
Figure 3.15 Example results of reach to grasp movement. ....	41
Figure 3.16 Elbow orthosis calibration fixture .....	43
Figure 3.17 Elbow orthosis calibration experiment set up .....	43
Figure 3.18 The position and velocity curve for a typical elbow calibration movement. ....	45
Figure 3.19 Comparison between the average encoder readings and the designed angles. ....	47
Figure 3.20 The linear correlation between encoder reading and the designed angles. ....	47
Figure 3.21 Experiment set up of elbow calibration task .....	49
Figure 3.22 Region of interest in the phantom image. ....	52
Figure 3.23 B field magnitude of phase image in two control conditions. ....	54
Figure 4.1 Snapshot of the experiment set up .....	68
Figure 4.2 Flowchart of the task procedures. ....	69
Figure 4.3 Recovery score vs. FM score for all the 12 subjects .....	77
Figure 4.4 Representative trajectories in reach, grasp and reach to grasp movements ....	79

Figure 4.5 The four low function subject' grasp aperture .....	79
Figure 4.6 The comparison among Subject 2's performance metrics, low to medium group and high functioning group.....	87
Figure 4.7 An example of grasp movement velocity .....	89
Figure 4.8 The time ration in reach to grasp movement. ....	101
Figure 5.1 Lesion imaging for three stroke survivors.....	118
Figure 5.2 Snapshot of experiment set up in the scanner .....	120
Figure 5.3 Snapshot and Diagram of experiment set up in the MR scanner. ....	121
Figure 5.4 Comparisons of movement trajectory and velocity in grasp and reach movement inside and outside of the scanner. ....	128
Figure 5.5 Model fit of reach-to-grasp movement.....	129
Figure 5.6a Examples of brain activation in a normal and a stroke subject's grasp movement.....	132
Figure 5.6b Examples of brain activation in a normal and a stroke subject's reach movement.....	132
Figure 5.6c Examples of brain activation in a normal and a stroke subject's reach-to-grasp movement.....	133
Figure 5.7 Subject 5's head movement in reach to grasp movement .....	135

## LIST OF ABBREVIATIONS

ADL: Activity of Daily Living  
ADLER: Activities of Daily Living Exercise Robot  
ANOVA: Analysis of variance  
BBT: Box and Block Test  
BOLD: Blood Oxygen Level dependent  
Ct: Contralateral  
CRB: Cerebellum  
DTI: Diffusion tensor Imaging  
fMRI: Functional Magnetic Resonance Imaging  
FMA: Fugl-Meyer Assessment  
FT: Functional Test  
JTHF: Jebsen Taylor Hand Function Test  
LI: Laterality Index  
NHPT: Nine Hole Peg Test  
M1: Primary motor cortex  
PCA: Principle Component Analysis  
PMA: pre-motor area  
R/G: Reach/Grasp  
RAT: Robot assisted therapy  
S1: Primary sensor cortex  
SIS: Stroke Impact Scale  
SMA: supplementary motor area  
UE R/G: Upper Extremity Reach and Grasp  
UE: Upper extremity

## Chapter 1

### Thesis Overview

# **1. Thesis Overview**

## **1.1. Introduction**

Stroke is the third leading cause of death and the second most frequent cause of disability in the United States [American Heart Association (AHA) 2009]. Stroke can result in the impairment of body function at different levels from body paralysis to weakness, limited range of motion, abnormal muscle tone, abnormal posture, abnormal movement synergies and loss of accurate coordination that will impede proper reach and grasp movement. Although no direct cure for stroke exists, recent stroke rehabilitation strategies such as Intensive Occupational Therapy (OT), Constraint Induced Movement Therapy (CIMT) and device-based strategies such as Robot-Assisted Therapy (RAT) have been proved to induce cortical reorganization and motor re-learning that lead to recovery and function gains. RAT is designed to provide convenient, effective and high intensity therapy with control through the electrical-mechanical systems. However, the advantages of RAT still need to be investigated. Studies on the effects of the RAT should focus on kinematics analysis in order to differentiate between neural repair based recovery and the compensation strategies based recovery [Kwakkel et al 2009].

There are three ways to evaluate stroke recovery which could benefit the development of rehabilitation strategies. Firstly, stroke impairment/recovery can be evaluated through a series of clinical measurement tools from the perspective of impairment including consciousness, cognition, sensorimotor scales, timed motor performance, the ability of activities of daily living, and participation in daily life.

Secondly, movement after stroke can be evaluated through the kinematic metrics such as movement time, velocity, accuracy, efficiency and kinetic measurements of forces in particular tasks such as reach/grasp movement. Thirdly, recovery could also be evaluated through the neuro-imaging methods. Studies have demonstrated the cerebral plasticity of adult brain, which implies neural changes in activation patterns and connectivity. Functional Magnetic Resonance Imaging (fMRI) is such a technique that allows us to investigate the brain function. With high temporal and spatial resolution, fMRI is used to detect brain activation based on the changes in deoxyhemoglobin in response to the neural firing. The activation reflects the Blood Oxygen Level Dependent (BOLD) signal changes that are related to the neural activities. Experiments have been performed on the neural reorganization after stroke. The results could be summarized into two aspects: a) over activation of areas belong to the physiological neural network for a specific task; and b) activation of unusual areas that tends to compensate the function of damaged areas [Rossini et al, 2007].

Our long-term goal is to assess the effectiveness of RAT with the Activities of Daily Living Exercise Robot (ADLER) developed by Johnson and colleagues at Zablocki VA medical center [Johnson et al, 2006]. The system is used to train the recovery of reach and/or grasp activities after stroke. Although the kinematics of reach-to-grasp movement have been studied and the brain activation of this kind of movement has also been studied in the fMRI studies, very few devices exist that allow us to evaluate the motor performance of reaching and grasping movements both inside and outside the scanner. We developed an MR conditional Upper Extremity Reach and Grasp (UE R/G) evaluation system at the Rehabilitation Robotic Research and Design Lab to evaluate

stroke survivors' function inside and outside the MRI environment. The main purpose of this thesis is to develop the system, to provide the calibration study and correlation study that verifies and validates the system, and to demonstrate that it is feasible to conduct an experiment using the system in the MRI environment to study the brain activation patterns of reach and grasp movements of stroke survivors. The thesis is organized into five main sections: Chapter 2: Background; Chapter 3: System development; Chapter 4: System validation: A correlation study; Chapter 5: fMRI case study and Chapter 6: Conclusion and future directions. The three main aims are as follows:

**AIM 1 (Chapter 3):** To develop an MR-conditional upper arm evaluation system to assess the reaching and grasping movement. The UE R/G evaluation system includes a hand glove to measure hand grasp aperture, an elbow orthosis to measure elbow flexion and extension angle, and a display and control environment. MR-safety will be objectively determined using a phantom in the 3.0 Tesla General Electric (3T GE) MR scanner. The device performance is evaluated outside and inside the magnetic field.

**AIM 2 (Chapter 4):** To validate that the UE R/G system when utilized outside the fMRI is sensitive to differences in motor performance due to stroke impairment and functional recovery. A secondary goal is to characterize the observed motor performance on reach, grasp, and reach-to grasp tasks by recovery level using time, velocity, and quality of movement metrics.

**AIM 3 (Chapter 5):** To validate that the developed system when utilized inside the fMRI is usable and stable, i.e., exhibits similar trends observed inside scanner and identify the movement related brain activations after stroke.

## Chapter 2

### Background

## **2. Background**

### **2.1. Stroke and its rehabilitation**

Every year, about 795,000 people in the U.S experience new or recurrent stroke, 600,000 of which are first attacks and 185,000 are recurrent attacks with an average of one individual stroke occurring every 40 seconds and about one death happening out of every 17 stroke patients. In other words, one person dies from stroke every 3 to 4 minutes. The estimate expenditure of stroke for 2008 is \$65.5 million. Approximately 85% of patients survived the stroke, living an average of seven years thereafter. Most are left with significant disabilities [American Heart Association (AHA) 2009]. According to the mechanism and location of the vascular damage in the brain, strokes can be divided into two classifications: ischemic and hemorrhage. Ischemic stroke, which is caused by the block in the blood vessel, accounts for about 87% of all stroke onsets [AHA 2009, GCNKSS, NINDS 1999]. Hemorrhage stroke, caused by the blood bleeding outside of the vascular space, accounts for 13% of all strokes [Woodson, 1995]. Hemorrhagic stroke can cause more severe consequence than ischemic. 37-38% of Hemorrhage stroke survivors at the age of 45-64 die within 30 days, while only 8-12% of ischemic stroke survivors die [AHA 2009]. Since stroke affects people differently depending on the type of stroke, the location of the infarct and the extent of the brain injury, developing patient-specific rehabilitation strategies are very important.

Rehabilitation strategies often vary. For example, occupational therapy (OT) focuses on training and re-educating the patients with their daily living skills and function

ability through a practice of ADL tasks. Physical therapy (PT) trains the patients with the basic joint movements, walk, balance, and reintegrate sensation [Wieber, 2006]. In the past decade, newer rehabilitation strategies such as CIMT and RAT have been developed. CIMT, based on “learned non-use” theories, retrains the brain by constraining the use of the less-affected arm and forces the patient to utilize the more-affected arm [Taub, 1999]. RAT, discussed in detail in section 2.3, is based on automating some traditional OT and PT training paradigms and uses electro-mechanical machines to actively or passively assist the more-affected limb [Aisen et al, 1997]. It is commonly accepted that the stroke recovery is realized through motor re-learning and motor adaptation [Krebs et al, 2009]. The key ingredients needed in successful rehabilitation strategies include highly repetitive and intense practice of specific tasks that require problem-solving and engagement [Kwakkel et al., 2003]. In addition, providing feedback, typically muscle level knowledge of performance or information about accuracy, is important for error detection, error correction, motivating patients and guiding them to perform desired movements better. Krebs and colleagues also found that intensity, task specificity, active engagement, and focusing training on motor coordination are key factors enabling effective recovery [Krebs et al, 2007].

## **2.2. Retraining Reach and Grasp Movements**

Because arm and hand movements play crucial roles in independent daily living, the recovery of upper extremity is a major focus of rehabilitation. In the upper extremity, the severity of hemiparesis is typically greater in proximal (upper arm) than in distal part (hand); the rehabilitation is more effective for the proximal disability than distal disability

[Lang et al., 2006]. Voluntary reach and grasp movements recruit the entire motor system. The cerebellum and basal ganglia receive the sensory input and modulate the movement timing and trajectory, which are important for accurate and smooth movement. The cerebellum initiates and times the movement; the brain stem and thalamic motor nuclei mediate the cerebellum and basal ganglia [Kandel et al., 2000]. The dysfunction of voluntary movement could vary regarding to the location of brain damage in the motor system. Developing special motor re-learning/recovery strategies for different types of stroke is quite important.

Reaching movements have been extensively studied in the two-dimensional (horizontal plane) and in the three-dimensional point to point reach tasks as well as in the reach-to-grasp tasks. The movements can be classified into two types: with support (gravity compensation) and without support (no gravity compensation). Both kinds of studies show that stroke survivors, compared to normal subjects have decreased movement velocity [Wing et al., 1990, Kamper et al., 2002], increased initial movement direction error [Beer 2000], increased off-axis force against the support face [Reinkensmeyer, 1999], increased segmentation [krebs, 1999], decreased movement distance and increased trajectory curvature [Levin, 1996], increased path length of hand trajectory (Kamper et al., 2002). Chae and colleagues show that stroke survivors tend to have more delayed movement in their more-affected hand than normal hand; and the delay is significantly correlated with the motor impairment severity [Chae et al., 2002].

Studies have also been performed to understand the neuroscience of grasp [Castiello, 2005]. The grasp movement is generally studied in a reach-to-grasp movement. Results indicate that in the normal reach-to-grasp movement, the hand is pre-

shaped to the object during reaching. Stroke survivors tend to segment the reach and grasp movement so that reaching occurs before grasping. Stroke survivors also show an inter and intra variability in the affected hand movement with decreased hand transportation velocity, decreased velocity of grasp aperture, and inaccurate grasp aperture with an extensive opening of the hand and inaccurate scaling of the peak grasp aperture [Lang et al, 2005, Johansson and Westling, 1984]. The coordination of reach and grasp movement is also impaired [Nowak et al, 2007].

Studying the vertical elbow flexion/extension movement with the hand grasp movement after stroke and then correlating them with the motor impairment level make our study unique and valuable. Insights gained from this thesis will allow us to shed some light on how to evaluate the stroke survivors' recovery kinematically and how stroke survivors coordinate elbow flexion/extension movement with hand grasp movement.

### **2.2.1. Robot Assisted Therapy for Retraining Reach and Grasp Movements**

Several RAT systems are focused on upper extremity, providing environments that deliver highly repetitive, task-oriented practice and objective quantification for reach and grasp training [Masire, Coote, Krebs, Kwakkel et al, 2008]. Typically, these RAT strategies involve training the impaired arm for 4-6 weeks with games and feedbacks used as the incentives to the subjects. Constraints are provided to optimize the required movement patterns. As a result, the complexity of a task can be learned procedurally and gradually [Kwakkel et al, 2008]. The clinical and kinematic assessments are provided before and after the RAT to assess the recovery. The literature supports the potential of effectiveness of the RAT on elbow/shoulder retraining to elicit improvements in proximal upper limb function. However, the improvement of ADL cannot be sustained since the

measurements of ADL function are not precise enough to reflect the recovery. Kinematic measurement should be developed to differentiate the principles of recovery between neural repair compensation strategies [Kwakkel, et al, 2008].

Reach training examples include MIT-MANUS (Interactive Motion Technologies, Inc., Cambridge, MA) (now InMotion) and the Gentle/s systems. In the MIT-MANUS environment, the subject's more-affected arm is attached to a 2-DOF robot's end-effector to assist completing goal-directed reaching tasks in a horizontal plane. Force sensors and position encoders are used for force, position and reflection measurements [Krebs et al, 1998]. The GENTLE/s system uses a haptic Interface arm (Haptic Master, Fokker Control Systems) with 3 active DOF for wrist positioning and 3 passive DOF for wrist orientation to train the reach movement of stroke survivor's more affected arm in 3D space with the simple tasks with visual feedback [Coote, 2008]. Hand rehabilitation is more difficult because it requires fine motor control. Examples of hand RAT systems include the Rutgers Master II [Bouzit et al, 2002] and Hward (Hand Wrist Assisted Rehabilitation Device) [Takahashi et al, 2000]. The Rutgers master II uses four pneumatic linear actuators that could resist finger flexion and assist finger extension to help grasp movement. Feedback is provided with virtual reality environment [Bouzit, 2002]. HWARD is designed by Takahashi to assist hand in grasp and release movements with 3 pneumatic actuators [Takahashi et al, 2000].

Given the need to improve ADL function for real life, there has been a recent surge of robot-assisted devices for retraining both reaching and grasping movements. One of such devices, developed in the rehabilitation robotics lab at the Medical College of Wisconsin, is the Activity of Daily Living Exercise Robot (ADLER). ADLER uses the

Haptic Master robot as in the Gentle/s system for reaching assistance and a low-cost grasp glove with Functional Electrical Stimulation (FES) for grasping assistance [Nathan, Johnson, McGuire, 2009]. Subjects perform the task-oriented activities of daily living, such as drinking, combing, and feeding with or without support from the RAT system [Johnson, 2006].

One motivation for this thesis is to examine the effectiveness of robot-assisted training of reach and grasp using ADLER. Our hope is to examine the movement kinematic changes and brain changes after RAT. Therefore, we developed systems that allow us to evaluate reach and grasp movement performance and help elicit neural patterns sub-serving the reach and grasp control.

### **2.2.2. Evaluating Reach and/or Grasp Motor Performance**

In order to evaluate motor performance changes on reach, grasp, and reach-to-grasp tasks with an assessment tool, one must first validate the new tool against a gold standard one and determine its sensitivity to changes in performance. However, a clear gold standard tool does not exist for reach and grasp motor tasks. Therefore, we evaluate the sensitivity of our assessment tools against different clinical assessment scores as well as the composite “recovery” scores consisting of key clinical assessment tools. The following section reviews the clinical assessment tools and the typical biomechanical assessment tools used to score motor performance described in this thesis.

#### **2.2.2.1. Clinical assessment tools**

An assessment method needs to be valid and accurate enough to measure the underlying phenomena or disease with minimal errors, reliable with reasonable inter and

intra subject variability, sensitive enough to differentiate within subjects, simple, easy to operate and communicate. The Stroke assessment methods are such techniques using instruments to measure the impairment level of stroke as well as the effect of interventions. Three types of scales are used in clinical assessment: focal activity scale, activities of daily living scale, and instrumental activities of daily living scale. The Mobility Index (MI) [Rossier et al, 2001], the Motor Assessment Scale (MAS) [Park et al, 1994], the Nine Hole Peg Test (NHPT) [Kellor et al., 1971], the Fugl-Meyer assessment (FMA) [Fugl-meyer 1979] are examples measuring focal activity focused on providing the mobility and arm function for the intended study outcome. ADL function measurement scales, such as the functional independent measure (FIM) [Keith et al., 1987], Functional Test (FT) [Wilson et al., 1984], Box and Block Test (BBT) [Mathiowetz et al., 1985], and Jebsen Taylor Hand Function Test (JTHT) [Stern et al, 1992] are used to assess the clinical relevant changes on ADL. The tools using instrumental activities of daily living scales are for those stroke survivors with basic ADL function and are used to qualify the more complex daily tasks for safely living in the community. Such scales include Stroke Impact Scale (SIS) [Duncan et al, 1999], Rivermead activities of daily living assessment [Lincoln et al, 1990], and Motor Activity Log (MAL) [Taub et al, 2005]. In evaluating upper extremity movement, we focused on FMA, NHPT, MI FT, BBT, JTHT, FT, and the grip strength in this thesis (detail description in Appendix A). The clinical evaluation tools provide gross measures of function other than small motor changes during the recovery process and are highly dependent on the clinicians performing the evaluation. To understand the process of the recovery from a more incremental and finer movement perspective, biomechanical

assessment tools become very important.

#### 2.2.2.2. Biomechanical assessment tools

Many of the RAT systems have developed key biomechanical scales that have been shown to be sensitive to motor functional changes. Reach movement could be evaluated by repeated tracking tasks. Grasp movement could be evaluated within the reach-to-grasp movement with real/unreal objects. Krebs and colleagues found out that the point-to-point reaching movements of stroke survivors were separated into several small sub-movements, each with a bell-shaped speed profile, presumably because the motor control processes that would normally coordinate and overlap these segments were disrupted [Krebs et al, 1999]. The sub-movements are typically analyzed through a series of biomechanical scales. Examples of the scales include movement smoothness, evaluated by jerk, the third time derivative of position or counting peaks in speed [Rohrer et al, 2002, Krebs et al, 1999], movement speed [Roby-Brami et al 1997, Wing et al 1990], movement time [Wing et al, 1990], time to peak velocity [Wing et al, 1990], Root mean square jerk (RMSJ) [Song et al, 2008], movement trajectories, straightness, and direction of the hand path during reach movement [Kamper et al, 2002]. Scales for grasp movements also includes grasp aperture, velocity of grasp aperture, time to peak grasp aperture. Other scales include movement efficiency and efficacy. Efficacy is measured by computing the active movement index that is calculated from the percent of movement that subjects performed without robot's assistance. Efficiency is calculated by computing the path length of the trajectory traveled by the patient to each target. Greater length indicates greater energy expenditure than normal kinesiology movement patterns [Colombo, 2008].

## **2.3. Brain Function after Stroke**

### **2.3.1. Theories of cerebral plasticity**

Neural plasticity and cortical reorganization is the common accepted mechanism for stroke recovery. There are several theories offering explanations for the way the damaged brain regains its lost functions. Firstly, some inactive neuron could become active to respond to the action mediated by the damaged areas [He et al, 1995]; secondly, a neural system could change its function to accommodate for the damaged areas [Nudo et al, 1996]; thirdly, a behavior could be performed differently from its original method due to the substitution of the secondary input. The change of the underlying mechanism subserves the movement or the different strategies [Chollet, 1991]. The underlying mechanism of the neural plasticity could be originated from the increases in the synaptic strength. The pathway that is not damaged by the brain injury might be facilitated because of the high demand of neural activity [Kandel et al, 2000]. The preserved axons might sprout into the damaged lesions and innervate dendrites that have lost their synaptic inputs. The formation of new synapses which might appear after brain injury when there are loss of some other synapses connection; and the formation of new neurons or the dendrite sprouting which happens when a neuron nearby lost its function, the dendrite might sprout to compensate for the neural function. Among these mechanism, the functional reorganization is the most important one and it could be studied by the functional imaging techniques, including Positron Emission Tomography (PET), functional Magnetic Resonance Imaging Techniques (fMRI), Single Photon Emission Computerized Tomography (SPECT), Magnetic Resonance Spectroscopy (MRS),

Transcranial electrical and magnetic stimulation (TMS), Diffusion Tensor Imaging (DTI). We will focus on the fMRI technique with the experimental findings in this thesis.

### **2.3.2. Assessing brain function using fMRI**

#### 2.3.2.1. fMRI techniques

Based on the findings that the changes in blood flow and blood oxygenation in the brain are closely linked to the neural activity in 1890s [Roy et al, 1890], Kwong discovered the use of fMRI techniques in 1990 [Kwong et al, 1990]. The technique is able to detect the Blood Oxygen Level Dependent (BOLD) signal. Oxygen is carried by the hemoglobin in the local capillaries in the brain. Neural activities cause the oxygen consumption, which results in the blood vessel vasodilatation. Then the cerebral blood flow increases, more oxygenated hemoglobin are provided and the portion of deoxyhemoglobin is reduced. As a result, the BOLD signal decreases and the MR susceptibility decreases in the vicinity of venues veins [Huettel, 2004]. By calculating the signal changes, the movement related neural activities can be detected. Since 1990, this technique has been widely used in studying the motor, language, memory related activations. Motor tasks are focused on the upper and lower extremity movements including the wrist/elbow flexion/extension, hand gripping, finger tapping, finger tracking, and foot tapping. MR conditional/safe devices are built to control, record and evaluate these movements. MR conditional means an item has been demonstrated to pose no known hazard in a specified MR environment with specified conditions of use [Gassert et al, 2008a]. According to standard F2503-05 of the American Society of

Testing and Materials (ASTM), an MR system could be defined as MR safe, MR conditional or MR unsafe. MR safe means an item poses no known physical risks in all MR environments, not taking into account image artifacts. MR conditional means an item has been demonstrated to pose no known hazard in a specified MR environment with specified conditions of use. MR unsafe means an item is known to pose hazards in MR environments [Gassert et al., 2008a]. A system is MR conditional only when it does not bring any injury to person or to any other equipment when placed inside the scanner and the performance of the system is not affected by the static or switching magnetic fields. In addition, the use of the device does not affect the MR image quality [Kanal et al., 2007]. Such devices include a wrist pneumatic manipulandum used to measure the wrist flexion/extension movement [Suminski et al, 2007], a custom-made electrogoniometer braces used to measure the finger tracking movement [Carey et al, 2002], and a master and slave system with two optical force sensors, two shielded optoelectronic encoders and a hydrostatic transmission to measure the arm reach movement [Gassert et al, 2006]. More examples are described in chapter 3. However, we didn't find any device measuring both reach and grasp movement simultaneously in the MR scanner, which is very important for understanding the upper extremity recovery of stroke survivors. Hence, we are motivated to develop the (UE R/G) movement system.

#### 2.3.2.2. fMRI study design

Because of the good spatial and temporal resolution on the brain imaging, fMRI technique has been widely used in studying the brain reorganization of stroke recovery. There are two kinds of such studies: the longitudinal study which focuses on the intervention effect on the brain reorganization; and the cross-sectional study, which

investigates the difference of brain reorganization results of stroke survivors at different impairment level. Typically, in the cross-sectional study, subjects will receive one to two sessions of the clinical evaluation and fMRI scans. The results are compared between subjects at difference impairment levels. In the longitudinal study, stroke subjects who have already passed the spontaneous recovery periods will receive pre and post-intervention fMRI scans with the same motor tasks. The intervention between the two scans can vary to the types and duration according to the purpose of the studies. The activation patterns from the pre and post intervention will be compared to study the brain reorganization induced by the therapy.

#### 2.3.2.3. fMRI task design and results

Typically, to study the effects of upper extremity stroke rehabilitation, movements like sequential finger tapping [Dong, 2007], hand open and close [Johansen-berg, 2002], wrist flexion/extension movement [Loubinoux, 2003] or elbow flexion/extension [Feydy, 2001] are performed. There are two types of fMRI experiment design, block design with the alternation of blocks of task and rest; and the Event-Related (ER) design with inter-stimulus intervals. In the ER design, each task is of the same amount of time, but the interval between the tasks could be multiple times of the task time. Results showed the task related brain activations in motor and sensory areas [small 02, Carey 02, Ward 03], such as primary motor areas (M1), primary sensory areas (S1), pre-motor areas (PMA), secondary motor areas (SMA), cerebellum (CRB), thalamus, and optical lobe. Stroke survivors have different activation sites from the normal subjects due to the stroke lesion site, size and brain reorganization. Typically, the stroke lesion site can be classified into 5 locations, cortex, corona radiata (CR), internal capsule (IC), putamen, and thalamus.

Researchers showed that subjects with cortex infarct have more contralateral S1, M1 activation and better motor function than the subjects with CR infarct which show more activation in bilateral S1 and M1. Strokes with lesion in CR show better recovery in the internal capsule [Kwon 2007 Ward (06)]. Studies also found the impaired functional integrity of the CNS is associated with recruitment of secondary motor networks in both hemispheres in attempt to generate motor output to spinal cord motor neurons [Ward 06]. The primary motor cortex integrity is closely associated with the brain activation and recovery. Stroke survivors with more intact ipsilesional motor cortex will have more ipsilesional activation during the affected hand use and better recovery [Bhatt, 2007], while subjects with ipsilesional motor cortex damage will have more contralesional activation, indicating poor motor recovery [Stinear et al, 07]. The intact M1 and its descending pathway also showed decreased ipsilesional sensory motor cortex activation which was paralleled by an increase in intracortical excitability [Hamzei, 2006]. However, it is important to notice that the stroke recovery is not only related to the lesion site and location but also greatly affected by other factors such as medical conditions, psychological factors, and environmental and family support.

#### **2.4. Summary**

The understanding of neural mechanism of stroke recovery is a major research focus nowadays. It is crucial to develop efficient rehabilitation strategies according to the recovery mechanism. The rehabilitation strategies including RAT have been developed in the past decades, dedicating to the stroke recovery. One major focus of recovery is retaining the reach and grasp movement ability. Clinical tools, kinematic and kinetic

metrics are being used to understand the stroke survivor's recovery level and movement performance. fMRI techniques with the high spatial and temporal resolution has also been widely used to understand the way strokes respond to movements in the neural level. Devices and studies have been developed for this purpose. It is clear that the stroke have different movement patterns as well as brain activation patterns. To study stroke's recovery of reach and grasp movements from the perspective of clinical, kinematical and brain reorganization perspective, the following chapters detail our development of an MR conditional upper extremity reach and grasp evaluation system to study the reach/grasp movement, and demonstrate our ability to study the related brain activation.

## Chapter 3

Upper extremity reach and grasp evaluation system development

### **3. Upper extremity reach and grasp (UE R/G) System Development**

#### **3.1. Introduction**

Currently, there are several devices designed to assess the stroke survivors' elbow or hand movement [Rohrer et al., 2002, Song et al., 2008, Kamper et al., 2002, Colombo et al., 2008, Reinkensmeyer et al., 2000] with repetitive or tracking tasks. Typically, due to material and/or actuation properties, these devices are designed for the laboratory use only and they are often not usable in the MR environment. Given the increasing need to examine the brain activation pattern of motor tasks, several MR conditional or safe devices are designed to measure, monitor human movements or enable impaired movements for subjects with disabilities in the scanner. Wrist movement is measured by a wrist pneumatic-driven manipulandum and a force field resisting or assisting the movement [Suminski et al., 2007]. Finger tracking movements are measured by two custom-made electrogoniometer braces [Carey et al, 2002]. Hand grip force is measured and controlled by a Magnetic Resonance Compatible Hand Interfaced Rehabilitation Device (MR\_CHIROD) using electro-rheological fluids for control and force generation [Khanicheh et al., 2005]. Arm reach movement is measured by two optical force sensors and two shielded optoelectronic encoders as well as a hydrostatic transmission separated master and slaves system [Gassert et al., 2006]. Finger movement is also evaluated by a micro-electro-mechanical system (MEMS) gyroscope that measures angular velocity, finger position, acceleration, and jerk of each finger [Schaechter et al., 2006]. However, no device at this time measures hand and arm performance simultaneously in the MR

environment.

Due to our strong interests in studying the brain activity of stroke survivor and the recovery mechanism governing return of function after RAT using activities of daily living involving reaching and grasping, we are motivated to develop the MR conditional reach and grasp evaluation system. To build an MR conditional system, metal objects are strictly excluded from the scanner, where a strong magnetic field exists and is able to lift up even really heavy metal objects, and pull them up to the scanner bore at high speeds. In addition, metal objects embedded inside the body, such as aneurysm clip and cardiac pacemaker, are also excluded since they might be re-oriented during scanning causing serious mal-function or internal bleeding [Schenck et al., 1996]. Some other materials are excluded from the field such as the ferrous parts which might lose function in the strong magnetic field and cause the projectile effect; high impedance sensor which might introduce the radio frequency (RF) pulse; dielectric or conductive material which might affect the property of the antenna when attached to the RF probe; cables that are not RF shielded properly which might transmit noise from the control room; or gain controller of the signal receiver which might be mistuned in the presence of a large source of resonance signal when the image objects have weak signal [Chinzei, 1999]. Polymers such as polyoxymethylene, polyethylene terephthalate and polyetheretherketone, glass, beryllium-copper, and ceramic are easy to fabric and typically used as the MR conditional/safe materials. Brass or aluminum components are widely used as screws and fixtures.

Our goal is to create an MR conditional system that can enable stroke survivors to perform “simulated” reach (elbow joint movements key to reaching), grasp (hand

opening and closing key to grasping), and the combined reach-to-grasp movements inside and outside the scanner. The system would provide the visual stimulus to prompt stroke survivors to perform these movements in the MR scanner, monitor the movement during the scan and provide a bridge to correlate the movement measurement and the brain activation measurement.

### **3.2. System development**

The design of the upper extremity reach and grasp (UE R/G) evaluation system builds upon previous work in the Rehabilitation Robotics Research and Design Lab. Nathan and Johnson developed a low-cost, grasp glove that could be used with the ADLER during RAT [Nathan et al., 2009]. Static and dynamic validation studies with the glove suggested it a good tool for measuring hand opening and closing movement. However, no study was done to verify whether the glove was MR conditional. We therefore conducted a study to confirm this. A prototype of an elbow orthosis called the game-glove, built in the lab in a senior design project for children with cerebral palsy, was redesigned and modified. The two prototypes formed the hardware basis of the UE R/G evaluation system. The software design for the UE R/G was built upon previous work for providing and controlling visual tracking stimuli for a wrist manipulandum [Suminski et al, 2007].

#### **3.2.1. System Requirements**

Our UE R/G evaluation system is designed to be used both inside and outside an MR Scanning environment for stroke survivors. The system development had the following requirements:

a). *The system must be MR-conditional.* The system will be used in the 3.0 Tesla GE magnetic scanner located at Froedtert Hospital, Milwaukee. The device should not bring any injury to person or to any other equipment when placed inside the scanner and the performance of the device must not be affected by the static or switching magnetic field. In addition, use of the device should not affect the MR image quality evaluated from the signal to noise ratio. The device developed here must use MR-compatible materials and have a sensing architecture that is robust to noise. A validation study, which is reported in section 3.5, tested the UE R/G device inside and outside the fMRI scanner and proved the system was MR conditional.

b). *The device must fit inside the bore of the scanner.* The General Electric (GE) 3.0 Tesla short-bore excite MRI system features a 60cm bore diameter for maximal patient comfort. With the setup of our system, most of the subjects will be able to wear the devices on the elbow and hand, perform the hand fully open/close movement as well as elbow flexion/extension movement between 0 and 50 degrees.

c). The device must be *sensitive* to changes in elbow flexion/extension and hand open/close movements. Specifically, the elbow joint angle resolution is 1.4 degrees and hand grasp aperture resolution is 1 mm. The elbow joint angle can be measured from 0-90 degrees outside the scanner. In the scanner, an angle stop could be installed onto the orthosis to limit the movement in between 0-50 degrees to prevent the subject from hitting the scanner bore. The grasp aperture measurement is subjective to the subject's finger length.

d). *Measurements with the device must be accurate and repeatable.* The session with the system lasts up to 2 hours for each subject. It is crucial to ensure the

system is stable and able to report accurate measurements (resolution for grasp aperture: 1mm, for reach angle, 1.5°) over time and across subjects. We described a calibration study in chapter 3.5 to validate the elbow orthosis' accuracy and stability in terms of angle measures and a validation study in chapter 4 to prove that the system is valid in terms of quantifying movement performance.

a) ***The system must be able to provide visual stimuli to cue movements and feedback about movement.*** The software system must collect movement data, generate tracking tasks, and provide visual and audio cues for subjects.

b) ***The device must be portable with minimum set-up requirements (<30 lbs).*** We need to transport the system between different places; so it should be portable and convenient to set up and use in the MR scanner. Hence, we built our system easy to connect through custom made cables and easy to operate. Our goal is a total weight less than 30lbs and that all components fit in a travel size suitcase that is easy to transport.

c) ***The device must be easy to don on/off and comfortable to wear (<5minutes).*** Many stroke survivors have difficulties opening their hands or stretch their elbows to fit into the device, the system needs to be very convenient to don on and don off. We used stretchable hand glove prototypes, add several Velcro straps in both hand glove and elbow orthosis. The experiments with 12 stroke survivors using the system for 2 hours indicated no allergic reactions or itches on the skin. The average don on/off time is less than 5 minutes.

### **3.2.2. System Overview**

The resulting UE R/G evaluation system consists of four parts: the measurement portion, the data collection portion, the task control portion, and the task display portion.

The measurement portion includes two measurement devices, a hand glove that measures the grasp aperture defined as the distance between the Cartesian end point position of the tip of index finger and thumb during the grasp movement [Nathan et al., 2009]; and an elbow orthosis that measures the elbow joint angle during the elbow flexion/extension movements, which we refer to as elbow reach in the thesis. The data collection portion includes two parts: a custom made circuit for the analog-to-digital signal conversion of the bend sensors and a PCI\_QUAD04 incremental encoder driver (Measurement Computing Co. Middleboro, MA) for the optical encoder reading of the orthosis. The task control portion is built on an xPC target system (MathWorks Inc. Boston, MA), including a target desktop personal computer (PC) that can collect the digital signal from the two devices and a host PC (a laptop) that has a Simulink® (MathWorks Inc. Boston, MA) model based on the real-time workshop to control the task execution as well as the data transmission. The target display portion is consisted of a display monitor that connects to the host PC and provides visual feedback to the subjects. During the MR scanning, only the hand glove and elbow orthosis will be placed inside the scanner. The tasks are back-projected and visible to the subjects via a reflective mirror placed over their eyes. Figure 3.1 is the basic hardware configuration of the system. Figure 3.2 is the overall system configuration. More detailed control flows for both MR-environment and non-MR environment diagrams are presented in Appendix B.

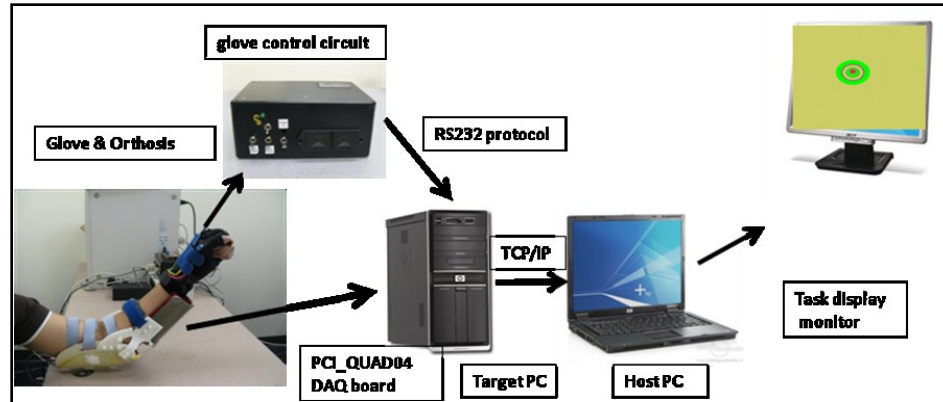


Figure 3.1 Basic configuration of the system

*(The glove is controlled by a control circuit with the microprocessor connected to the target PC through RS232 protocol. The elbow orthosis is controlled by PCI\_QUAD04 DAQ board inserted in the target PC. The target PC is connected to host PC through TCP/IP protocol. A monitor is connected to the host PC for task display).*

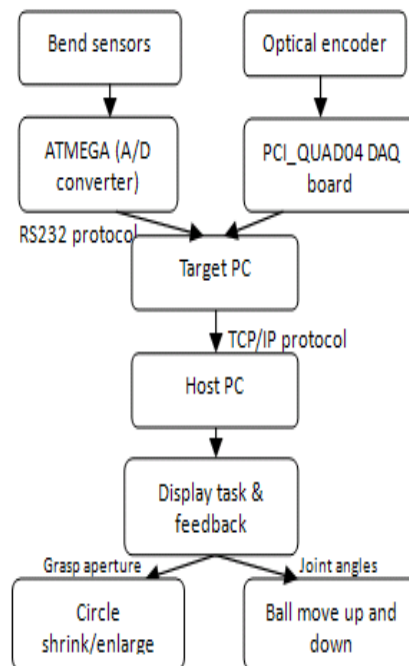


Figure 3.2 System flow

### 3.3. System Components

### 3.3.1. Hardware

We will discuss the hardware components for the hand glove and the elbow orthosis separately.

#### 3.3.1.1. Hand glove

The hand glove, originally designed for use with ADLER, is an FES sensorized glove that can measure index and thumb finger joint movements during static and dynamic tasks and deliver the functional electrical stimulation to help stroke survivors open and close their hands [Nathan et al., 2007, 2008, 2009]. We utilized the measurement portion of the glove and reserved its function of stimulation in this thesis. Four bend sensors (Flexpoint Sensor System Inc. Draper, UT) are connected to the microcontroller ATMEGA 8 (Atmel Inc. San Jose, CA), used for A/D conversion and data transmission. The data transmission occurs through the RS232 protocol via a RS232 chip (ST232, STMicroelectronics, IL, USA) connected between the microcontroller and the serial port of target PC. The bend sensor consists of a polyimide substrate as a plastic file coated with a proprietary carbon/polymer based ink. When the sensor is bent, the ink will separate into many micro cracks and result in the impedance changes [Flexpoint, 1997]. When the sensors are connected to the circuits, the impedance change will result in the voltage changes, which can be picked up by the microcontroller and converted into digital signals, from which joint angles can be calculated. The hand glove is made from a commercial available latex free glove (Carpal Tunnel Glove, Sammon Preston Inc. Boolingbrook, IL). Velcro straps are added to enhance the convenience of the donning on and off for stroke survivors. Two sleeves are attached to the index finger and thumb of

the glove with slices every half-inch. Each of the four sensors can be inserted into the slices depending on the subject's finger length to cover one of the four joints: index and thumb inter-phalangeal (PIP) and metacarpo-phalangeal (MCP) joint. The sensors are connected through a Radio Frequency (RF) shielded cable to the control panel between the control room and scan room, and ultimately connected to the control circuit placed in the control room. Figure 3.3 is the picture of the glove and sensors.

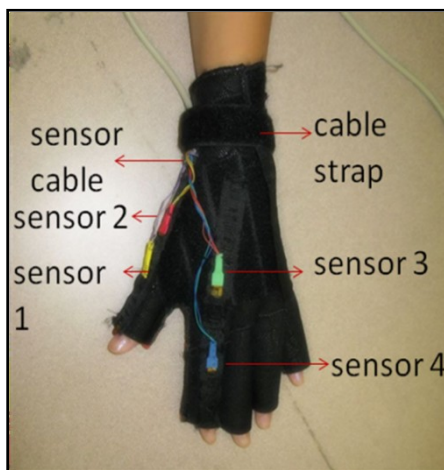


Figure 3.3 The hand glove. Four bend sensors (sensor 1-4) are inserted into the sleeves to cover index and thumb PIP and MCP joint.

A two-link hand robot model with 4-DOF was developed to transform finger joint measurements into Cartesian finger tip positions [Nathan, Johnson, McGuire, 2009]. The Index and thumb finger lengths with four joint angles were used in the model to calculate the grasp aperture (Figure 3.4 and 3.5). The hand model is based on three assumptions, the grasp movement can be model from the relationship of the index finger and thumb; the distal-phalange and inter phalange segment of index finger are considered as one single rigid body, the MCP joint of thumb is considered as a 1-DOF revolute joint. A

validation study was preformed to prove that the hand glove is sensitive, accurate and stable enough to capture the hand grasp aperture [Nathan, 2008, Nathan and Johnson 2009].

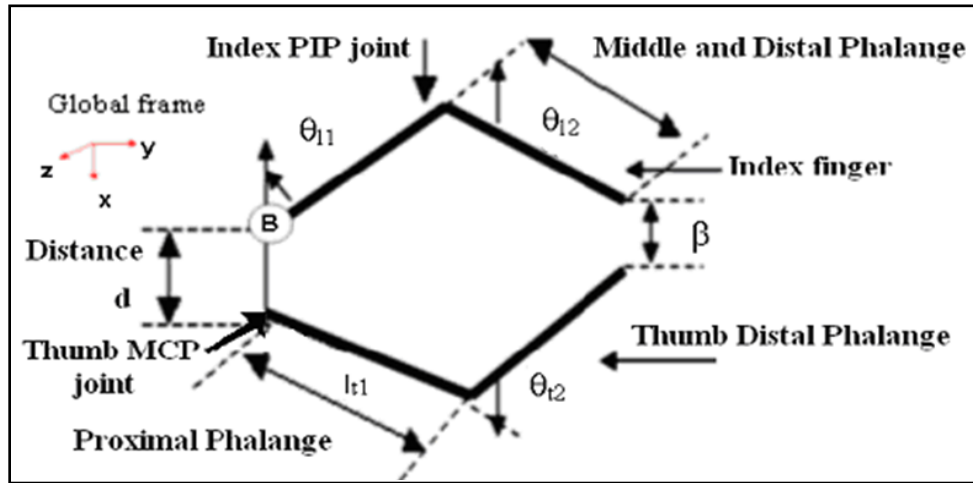


Figure 3.4 The hand model to calculate the grasp aperture ( $\beta$ ).  $\beta$  is defined as the distance between the tip of index finger and thumb [Nathan, 2008 and Nathan and Johnson 2009].

$$\begin{bmatrix} x_{thumb} \\ y_{thumb} \\ z_{thumb} \end{bmatrix} = \begin{bmatrix} c(\theta_{i1} + \theta_{i2})l_{i2} + c(\theta_{i1})l_{i1} + d \\ s(\theta_{i1} + \theta_{i2})l_{i2} + s(\theta_{i1})l_{i1} \\ 1 \end{bmatrix}$$

$$\begin{bmatrix} x_{index} \\ y_{index} \\ z_{index} \end{bmatrix} = \begin{bmatrix} c(\theta_{t1} + \theta_{t2} - 90)l_{t2} + c(\theta_{t1} - 90)l_{t1} \\ s(\theta_{t1} + \theta_{t2} - 90)l_{t2} + s(\theta_{t1} - 90)l_{t1} \\ 1 \end{bmatrix}$$

$$\beta = \sqrt{(x_{index} - x_{thumb})^2 + (y_{index} - y_{thumb})^2}$$

Figure 3.5 The equations to calculate grasp aperture ( $\beta$ ). ( $d$  is the distance between index finger and thumb MCP joint;  $l_{i1}$  is the distance from index MCP to PIP,  $l_{i2}$  is the distance from index PIP to TIP;  $l_{t1}$  is the distance from thumb MCP to PIP;  $l_{t2}$  is the distance from thumb MCP to PIP. The upper equation is the calculation of position of index and thumb finger derived from the hand mode; the lower equation is the calculation of the distance between the tip of index finger and thumb derived from the position of both fingers [Nathan, 2008 and Nathan and Johnson 2009]).

### 3.3.1.2. Elbow orthosis

The elbow orthosis (Figure 3.6) measures elbow joint angle via a reflective optical encoder (Avago Technology®, San Jose, CA). There are two pieces in the orthosis structure: the upper arm piece made from acrylic and the forearm piece made from polycarbonate.

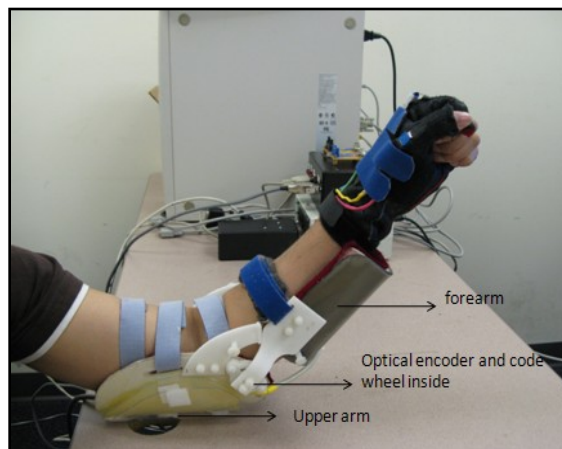


Figure 3.6 Configuration of elbow orthosis.

*(The orthosis consists of three parts: the forearm piece, the upper arm piece and the encoder housing at the hinge of two pieces).*

The prototype is designed for a medium-size upper and forearm. Velcro straps and foam padding are added in both pieces to keep the subject's arm stable. A custom-made encoder structure including the housing and code wheel is placed in the hinge part of two pieces. AEDR-8400-132 is placed on a custom made PCB board. A reflective code wheel with 127 lines is placed on top of the encoder, resulting in a conversion factor of 1.411 from digital counts to the angle. The encoder combines an emitter and a detector in a single surface mount leadless package. The encoder contains three parts: an LED

light source, a detector IC consisting photodiodes and lens to focus light beam from the emitter as well as light falling on the detector [Avago, 2006]. When the codewheel rotates, light will only be reflected in the reflective areas. The light pattern will fall on the detector IC and be decoded into the rotation angle. There are two channels outputting voltage information from the encoder, phase A and phase B, the differences between which can be used to calculate the angles. The magnitude of the signal is 2V, below the threshold of PCI-QUAD04 DAQ board, which is 3V. Hence, we amplify the signal by 1.5 times through two operational amplifier (TL062, Texas instrument, Dallas, TX) and four resistors (10K $\Omega$ , 15K $\Omega$ ).

### **3.3.2. Software**

The software for the system contains three parts, the data acquisition, task control, and task display.

#### **3.3.2.1. Data acquisition**

The glove sensor data is transmitted through the serial port of the target PC via RS232 protocol which is standard for serial binary data signals connecting between Data Terminal Equipment (DTE) and Data Circuit-terminating Equipment (DCE) [Nelson, 2000]. It defines the voltage level that corresponds to logic one and logic zero levels for the data transmission and the control signal lines. Valid signals are  $\pm 3$  to  $\pm 15$  volts. Logic one is defined as negative voltage and logic zero is positive voltage. In the Simulink model, we use the FIFO (First In First Out) method to detect the sensor data. The FIFO Read/Write block is used for the data streams transfer, which has the following sequences (Figure 3.7):

H e a d e r (255)	Sensor1 Thumb MCP	Sensor2 Thumb PIP	Sensor3 Index MCP	Sensor4 Index PIP	Stop bit (0)
----------------------	-------------------------	----------------------	----------------------	----------------------	-----------------

Figure 3.7 The data configuration of hand glove

The FIFO Read/Write can detect the header and stop bit of the data sequence and extract each sensor's information. Because the sensor readings are in the binary form; they are firstly transmitted into the decimals then converted into the joint angles. The hand model is then applied to calculate the grasp aperture, which is used for the data processing and display. For the elbow joint angles, as described in the hardware part, the data is transmitted to the DAQ board of target PC; and converted into angles in the Simulink model. Since the encoder is an incremental optical encoder, the joint angle reading is relative to the start position of the encoder other than an absolute change from the zero position. As a result, the joint angles are calculated in the data processing part of the program by subtracting the current angle with the angle at the beginning of the task.

#### 3.3.2.2. Task control

The task control system is built on the xPC real-time workshop platform. Following the inter-stimulus interval task paradigm of event-related task design in fMRI experiment, we have 75 tasks randomly spread out in 10 minutes. Each task is 4 seconds. The intervals between tasks may be 4s, 8s, 12s or multiple times of 4 seconds. A custom-made time trigger box is used to control the event onset time by starting with the MR

scanner and delivering a positive pulse every 4 seconds which could trigger the task onset. The duration of the pulse is 99 milliseconds, and the period is 4 seconds. The experiment flowchart is presented in figure 3.8.

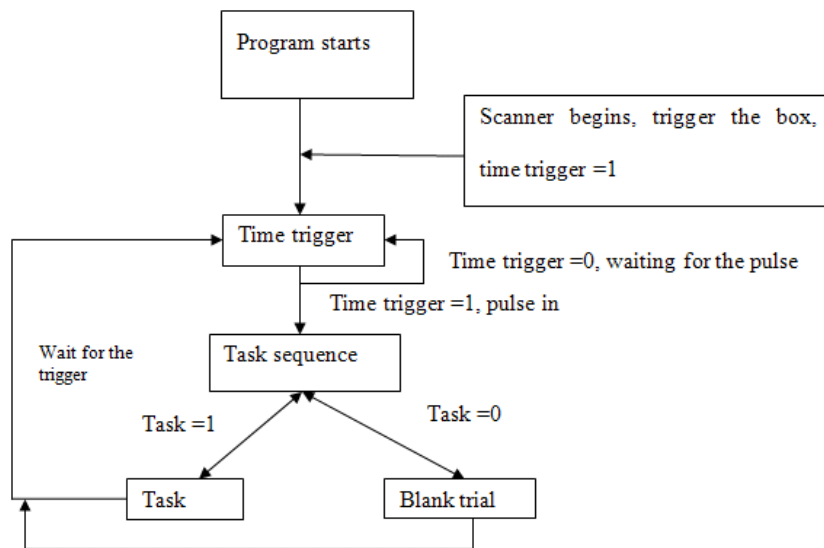


Figure 3.8 Experiment flowchart

*(The time trigger controls the onset of tasks, the task sequence controls the onset of task or blank trials).*

In the blank trial, a fixture cross will be displayed on the screen (figure 3.9a); subjects keep still. For the task trial, visual stimulus is shown depending on the type of tasks (elbow reach (figure3.9b), grasp (figure 3.9c), reach-to-grasp (figure 3.9d)) with an audio beep. There are 3.5 seconds from the time the target is displayed on the screen to the time target disappears. After the target disappears, the fixture-cross shows up on the screen again. Figure 3.9 shows the screen shots for all tasks.

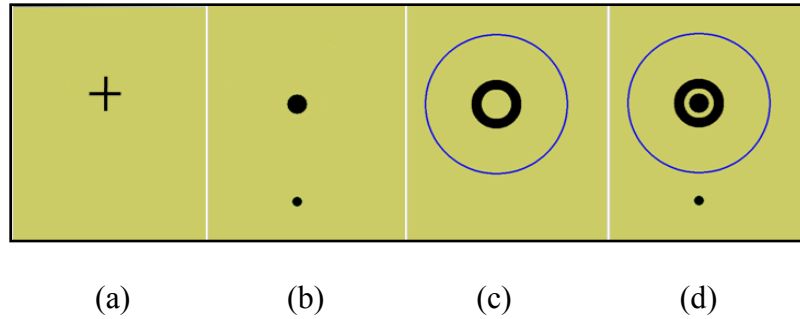


Figure 3.9 The blank trial and three tasks display.  
*(From left to right, the first picture is shown in the blank trials and at the end of all trials after the completion of tasks; the second, third and fourth picture shows at the beginning of reach, grasp and reach-to-grasp tasks and it is the go cue for each kind of movement.)*

Each task has four states: start, go, shoot/undershoot/overshoot target and return back. Take grasp task as an example. Figure 3.10 shows the flowchart of how the grasp aperture controls the tasks display.

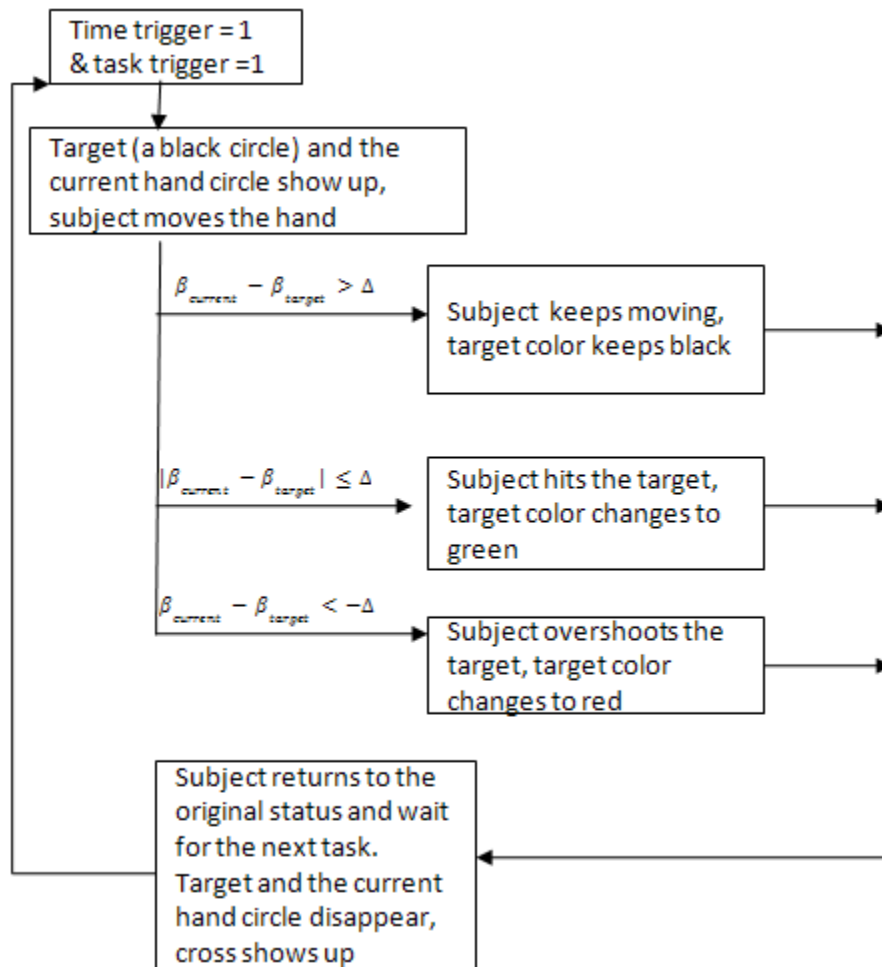


Figure 3.10 Flowchart of the grasp task control

Figure 3.11 demonstrates the visual feedbacks shown on the screen. Firstly when the system waits for the trigger, a fixture cross is shown (Figure 3.11a). When time trigger changes to 1 and a grasp task begins, a black circle scaled to the target grasp aperture ( $\beta_{target}$ ) and a blue circle ( $\beta_{current}$ ) scaled to the current grasp aperture appears (Figure 3.11b). Then as the subject closes his/her hand, the blue circle continuously becomes smaller (Figure 3.11c). If  $|\beta_{current} - \beta_{target}| \leq \Delta$ ,  $\Delta=0.2$  is the acceptable range, the target color will turn green, indicating the subject successfully hit

the target (Figure 3.11d); If  $\beta_{current} - \beta_{target} < -\Delta$  the target color will turn red, indicating the subject overshoot the target (Figure 3.10e); otherwise, if, the target color keeps black, indicating the subject hasn't hit the target (Figure 3.11c). After the hand close movement, subject opens his/her hand and returns back to hand open position, the target and hand circle disappear and the fixture cross shows on the screen again. The subject is instructed to perform a single hand close movement per trial.

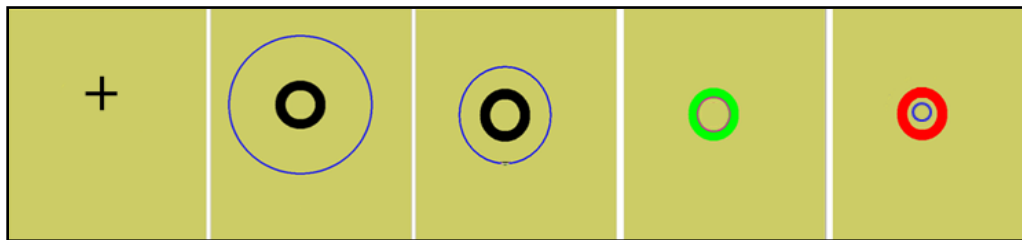


Figure 3.11 Five states of the grasp task.

*(From left to right, the figures represents waiting for the trigger, grasp task begins with target and current hand circles shows up; hand moving with undershoot state; the target successfully hit; and the target is overshoot.)*

For the reach task, the elbow joint angle  $\theta$  is used as the movement criterion.  $\theta_{current}$  represents the current joint angle and  $\theta_{elbow}$  represents the target angle. If  $|\theta_{current} - \theta_{elbow}| \leq \Delta$  ( $\Delta = 2$ ), the subject hits the target, target color turns green. If the subject overshoots the target ( $\beta_{current} - \beta_{target} < -\Delta$ ) and the target color turns into red. When  $\beta_{current} - \beta_{target} > \Delta$ , the target is undershoot and kept black color. Subjects are instructed to perform an elbow flexion movement per trial. For the reach-to-grasp tasks, both the target for reach and grasp movements will be shown (see Figure 3.12) with both grasp aperture and joint angle used as the movement criteria. Only when both the grasp aperture and joint angle are within its own target range, the target will change color to green, if either reach or grasp movement overshoots its own target, the target color changes to red, otherwise, the color stays black. The flowchart in Figure 3.10

holds for all tasks.

### 3.3.2.3. Task display

The task display portion is controlled by the “s-function (s-fun)” in the Simulink model, which is used for real time experiment display. As described in the task control portion, there are different states in the experiment. Different visual cues will be shown on the screen correspondingly (see Figure 3.9). The s-fun uses figure handles to plot different figures. In the blank trials, the task-control sends command =1 to the s-function, which calls the fixture cross handle. When the task starts, the task control sends the command = 2 to the s-fun, which calls the handles controlling the target and hand circle. During the tasks, the command state remains at 2; and the color of target depends on the relationship between the target and grasp aperture/joint angles. Figure 3.12 shows examples of the reach-to-grasp states at different times in the task trial experiment.

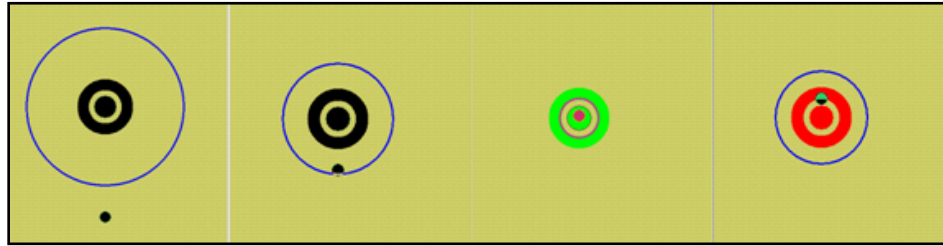


Figure 3.12 Four states of the reach to grasp movement.

*(From left to the right, A. task starts, target and current hand/elbow joint shows up; B. task in progress, subject squeeze the hand and move elbow up; C. subject hit the target, both hand and elbow are in their target; D. subject overshoot. In this case, the subject's elbow joint moves over the target; result in the overshoot.)*

Each kind of task is customized for individual at the beginning of their tasks for the target size and location. A calibration procedure is used to determine each subject's minimum grasp aperture and maximum elbow joint angle. During the calibration procedure, each subject is asked to perform a reach or a grasp movement within 4 seconds for 10 times. 150% of their minimum grasp aperture will be scaled by 15 times for their target radius; 80% of their maximum elbow joint angle will be used as the elbow target distance. For low functional subjects, i.e., if their movements are very small, we set the target to be 40 degrees and apply a gain (between 1 and 5) to ensure they can hit the target. The principle of the target design is to guarantee the subjects successfully hit the target and make 75 voluntary movements without fatigue. Figure 3.13-3.15 illustrates the examples of grasp, reach and reach to grasp movements in undershoot, correct and overshoot conditions.

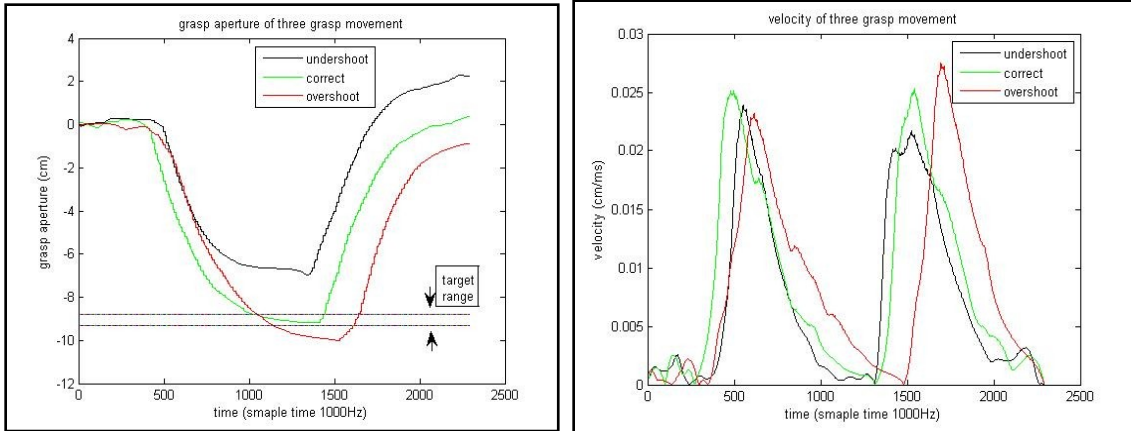


Figure 3.13 Example results of grasp movement.

(The left figure represents grasp aperture, the right figure represents grasp velocity. The grasp apertures are normalized to differentiate aperture by subtracting the baseline value. Green lines indicates subject hit the target, the maximal grasp aperture is in the target range; red line indicates subject overshoot the target and the black line indicates subject undershoot the target)

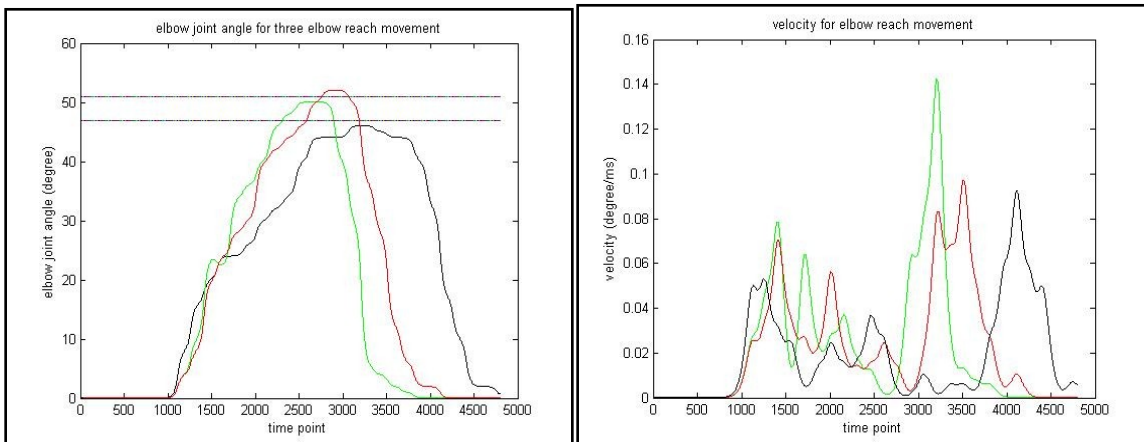


Figure 3.14 Example results of reach movement.

(The left figure represents elbow joint angle, the right figure represents reach velocity, Green lines indicates subject hit the target, the maximal grasp aperture is in the target range; red line indicates subject overshoot the target and the black line indicates subject undershoot the target)

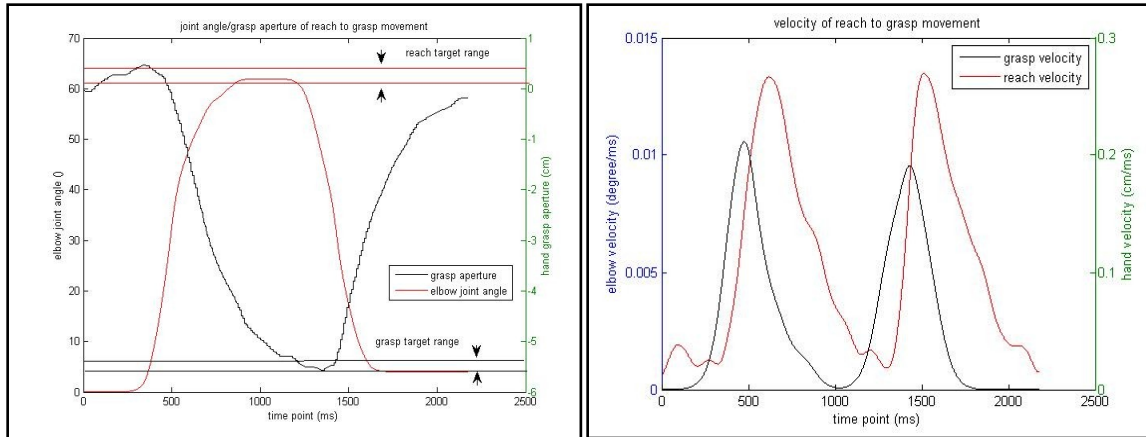


Figure 3.15 Example results of reach to grasp movement.

*(The left figure represent the movement angles (red line) and grasp aperture (black line); the right column represent the reach (red line) and grasp (black line) velocity. In the figure, the target was successfully hit; both the elbow angle and the grasp aperture are in their target range.*

### 3.4. Elbow Orthosis Calibration Study

The hand glove has been validated for static and dynamic accuracy in the previous studies [Nathan and Johnson 2009]. There is a need to evaluate the accuracy and repeatability of elbow orthosis. A calibration study was completed with 4 normal subjects (mean age 26 year-old,  $SD=\pm 2.45$ , 2 male and 2 female). The following part describes the calibration hardware, calibration procedure, and results from this analysis. We hypothesize that the joint angles measured by the orthosis could accurately reflect the subject's movement to 6 known angles between 0 to 90 degrees. We will compare our device reading with the goniometer reading and perform statistic test for agreement and stability.

#### 3.4.1. Calibration Experiment Set-up

An elbow calibration structure (Figure 3.16) consists of a jig where the elbow

orthosis will be positioned was made to stabilize the orthosis during the experiment. The upper arm was placed in the inclined panel where a mold was made for the shape of upper arm piece of the orthosis. Two clamps were installed in the bottom part of the inclined panel to prevent the orthosis from slipping down. The forearm piece was placed on the flat panel. The hinge between two pieces of the orthosis was lined up to the pivot point as marked in the figure 3.16. Seven holes were made in the plastic panel installed to the side of the structure, marked as  $0^\circ$ ,  $15^\circ$ ,  $30^\circ$ ,  $45^\circ$ ,  $60^\circ$ ,  $75^\circ$  and  $90^\circ$  from the pivot point, which could control the orthosis' movement to each specific angle by a stop pin inserted into the holes and held by the experimenter. Subjects were seated in a stationary chair in front of the table in a self-comfortable distance and move their elbows to each angle. The experiment set-up is shown in figure 3.17. An audio cue was given to the subject every 4 seconds indicating their movements. 10 movements were made for each angle.

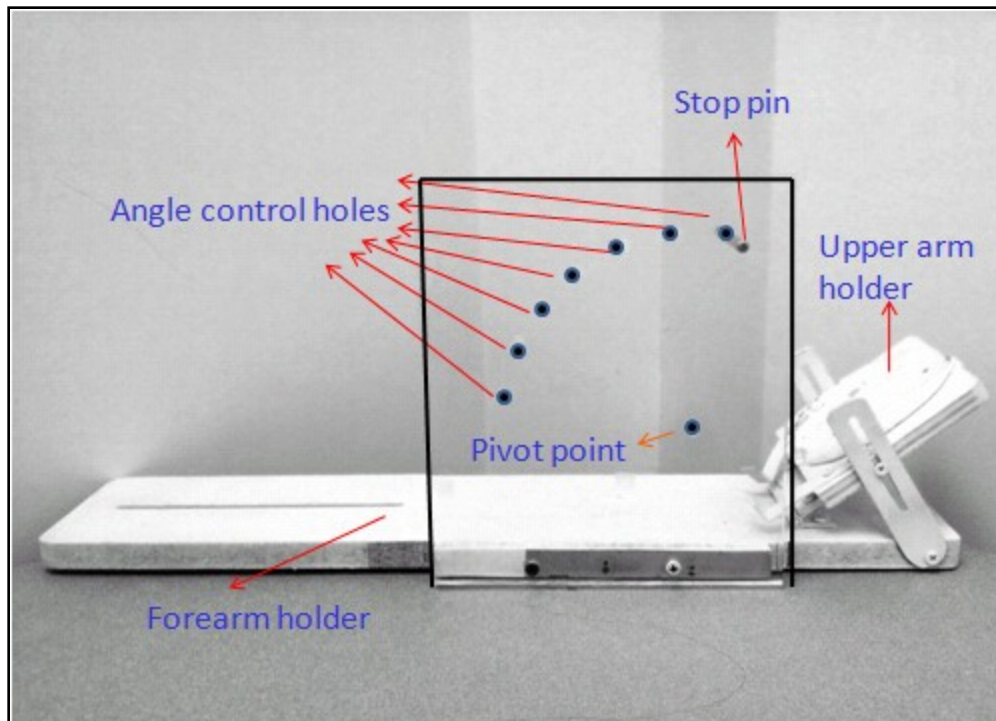


Figure 3.16 Elbow orthosis calibration fixture

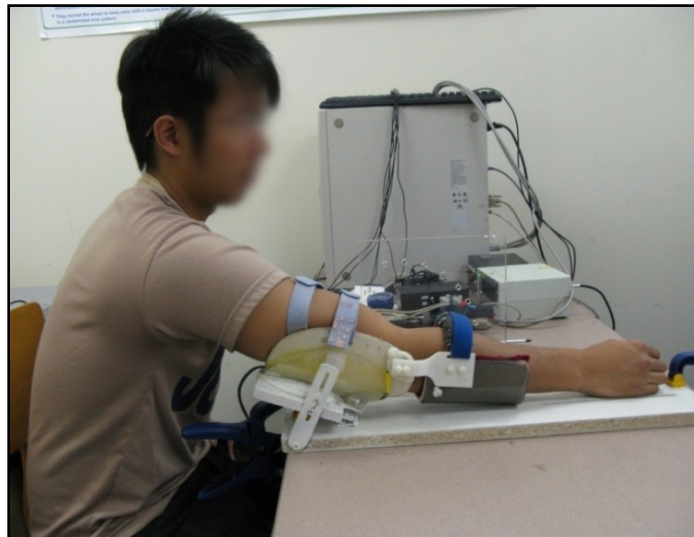


Figure 3.17 Elbow orthosis calibration experiment set up

### **3.4.2. Data analysis**

Elbow orthosis angles were recorded with MATLAB (MathWorks Inc, Boston, MA). Data was taken offline and analyzed with MATLAB and Microsoft Excel (Microsoft Corp, Redmond, WA). We calculated the mean and standard deviation for each subject at each angle across ten trials. An ANOVA test was performed for repeatability by examining if there is any significant difference between each subject's reading. The relationship between the encoder reading and the designed angles were studied with linear correlation analysis. Pearson's correlation  $r$  was calculated for the correlation between the encoder reading and designed angles. The velocity profile for each movement was also examined.

### **3.4.3. Elbow Calibration Results and Discussion**

The typical position and velocity curves for the elbow calibration tasks are shown in figure 3.18. The whole movement contains two sub-movements: an elbow extend to flex movement and a flex to extend movement. In the figure, the blue bell-shape line represents the joint angle trajectory; and the two green bell-shape lines represent the movement velocities for two sub-movements.

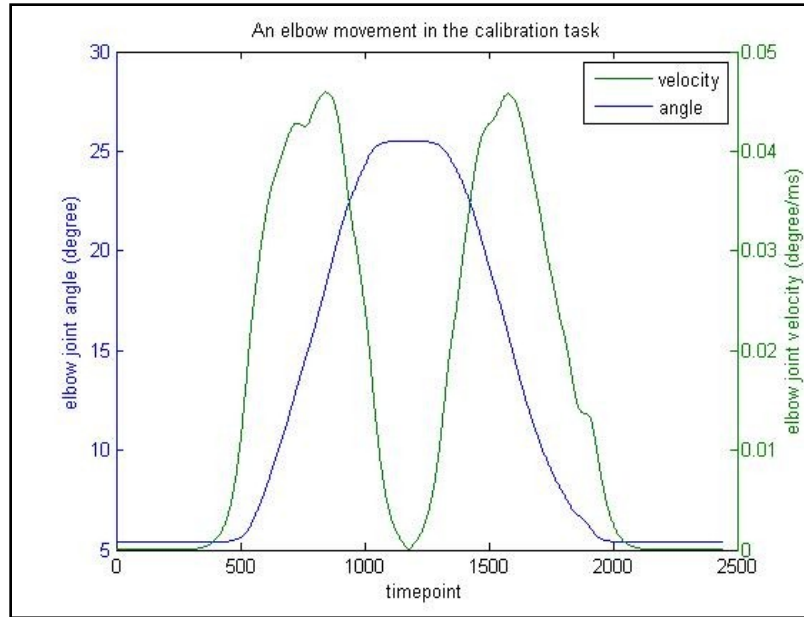


Figure 3.18 The position and velocity curve for a typical elbow calibration movement. (The green line represents the velocity profile, with the y-axis scale on the right; the blue line represents the joint angle profile, with the y-axis scale on the left.)

Results are presented in Table 3.1 with the mean and standard deviation for each subject at each angle. Subject 4's 15°, 45°, 60° movement encoder data are missing and the rest of his data is obviously different from the other subjects. From the video record of subject 4's experiment, we noticed that experiment set up was different from the designed routine. Specifically the orthosis was placed in the wrong position. Hence, we ruled out subject 4's data from our analysis. We then test the hypothesis that there is no significant difference between the three subjects by conducting a one-way ANOVA test across the subject. The p-value for the result is 0.907 ( $p > 0.05$ ). No significant difference was found between subjects. Figure 3.19 shows the averaged mean for each angle across the three subjects and the designed angle. In figure 3.19, the encoder readings are different from the designed angles. We then performed a Pearson product moment

correlation test. We hypothesize that the encoder reading is strongly linearly correlated with the designed angle. The result of Pearson Correlation coefficient is 0.998, indicating the strong linear correlation (eq. 3.1). Figure 3.20 showed the linear correlation.

$$Y = 1.03X + 13.9 \quad \text{Eq.3.1}$$

Y represents the encoder reading and X represents the designed angle. Then we can use this equation to calculate the actual movement angle based on the encoder reading from the following equation 3.2.

$$X = 0.98Y - 13.5 \quad \text{Eq.3.2}$$

Table 3.1 Comparison between encoder reading and the designed angles of four subjects  
(All units are in degree)

Angle (designed)	0		15		30		45		60		75	
	Mean	std										
sub1	7.59	0.00	28.45	0.00	42.11	3.66	60.32	1.96	75.03	3.02	93.62	2.90
sub2	10.62	4.04	28.35	2.55	41.35	3.32	58.99	2.79	71.88	4.68	86.11	5.86
sub3	18.50	1.63	36.92	1.55	51.46	4.43	62.68	2.62	78.96	1.06	91.11	4.33
Averaged	11.92	5.28	31.24	4.41	44.97	5.96	60.66	2.85	75.29	4.32	90.28	5.40

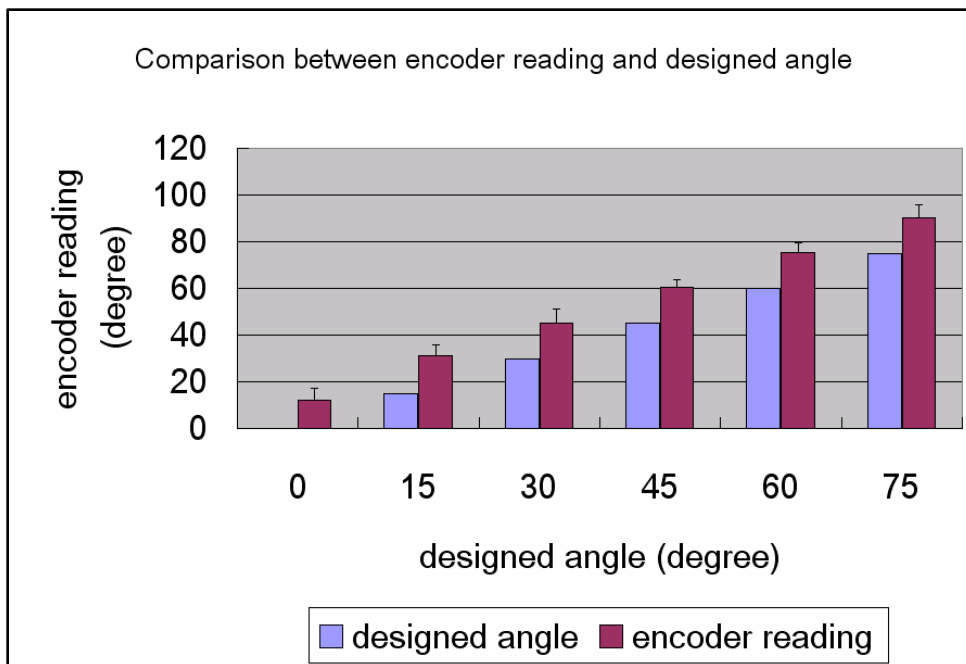


Figure 3.19 Comparison between the average encoder readings and the designed angles. The red bars represent encoder reading and the blue bars represent the designed angles. Error bars represent the standard deviation.

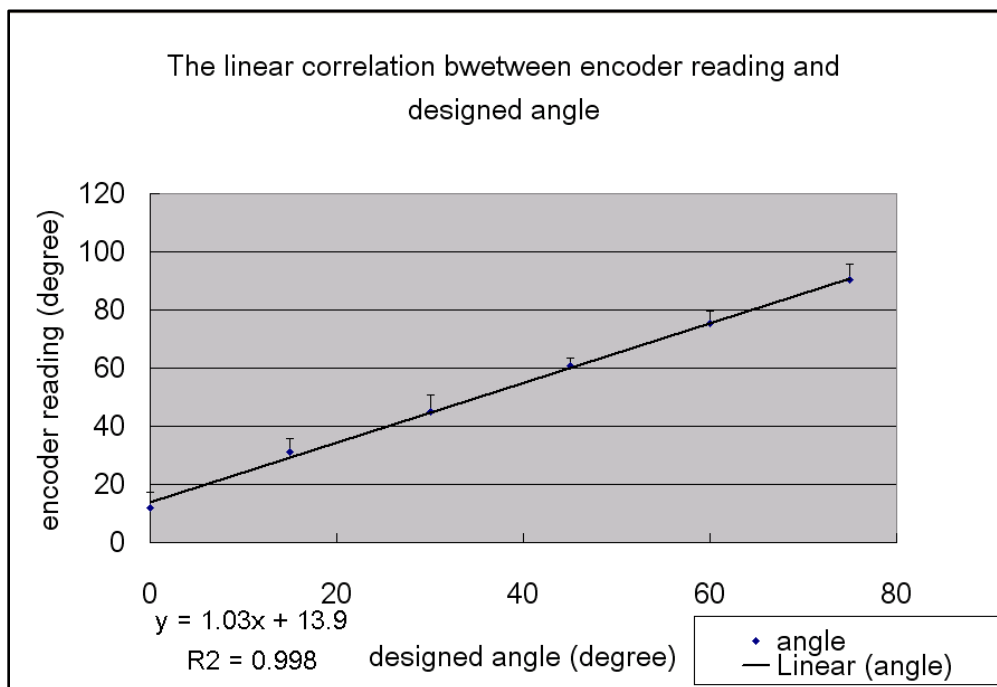


Figure 3.20 The linear correlation between encoder reading and the designed angles. (The dot presents the mean value; the error bar represents the standard deviation of angles.)

Based on the results, we discovered a strong linear correlation between the encoder reading and the designed angles ( $R^2 = 0.998$ ). However, we did notice the differences between the two, and the constant in the correlation equation showed a consistent offset at 13.9 degrees. The coefficient is 1.0278, which suggests the strong linear correlation between encoder and the true angle. We think the offset is due to our experimental set up. Figure 3.21 presents the device set up. When the subject's arm was placed in the orthosis and the orthosis was placed on the jig, there is an offset between the true  $0^\circ$  and the designed  $0^\circ$ . The offset is calculated as  $13^\circ$ . The offset should be applied when comparing the measured angle with the designed angle. We also noticed that during the calibration experiment, the pivot point of the orthosis (marked as the yellow dot) may shift with respect to the true pivot point on the side panel (marked as the black circle). And the possible exterior-interior elbow movement could also result in the inconsistency of the results.

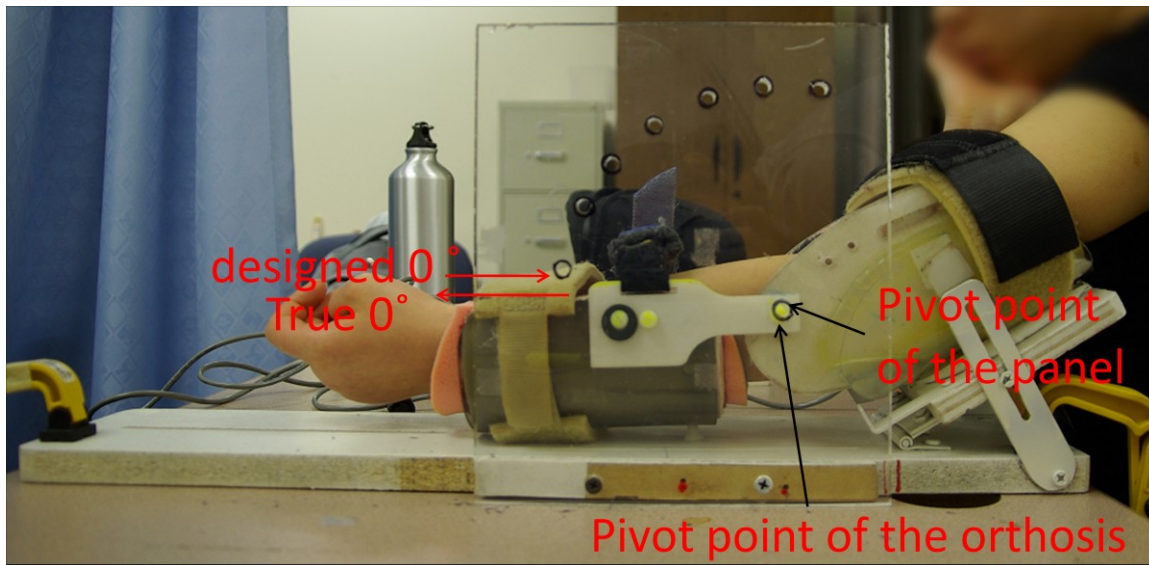


Figure 3.21 Experiment set up of elbow calibration task  
 (This figure displays the offset between the true 0° and the designed 0°. The alignment between pivot point of the panel and pivot point of the orthosis is also shown in the figure)

When we correct for the offset of 13 degrees, both the agreement and accuracy between the measured and designed angle are improved. Despite the errors noted in the experiment set-up, the results suggest that the system is able to accurately measure the subject's movements.

### 3.5. MR Safety Validation Study

One of the main requirements for the design of the upper extremity system was MR Safety. An MR conditional device will be usable in an MR scanner only when it will not be attracted to the magnet; operating it will not cause distortions in the brain images being collected, and its electromechanical function will not be affected. Phantom study is widely used to test if the device is applicable in particular scanner. Phantoms, spherical balloons filled with water or silicone, are placed inside the head coil and scanned using typical echo planar imaging (EPI) sequences. The effect of operating device statically or

dynamically on the MR image can be measured by defining regions of interests both inside and outside the phantom image, calculating the signal-to-noise ratios (SNR) in the magnitude image and comparing SNRs across different conditions [Suminski et al, 2007, Metha et al, 2009, Khnaicher et al, 2006] as well as calculating the B field changes in the phase image [Suminski et al, 2007]. The brightness of the magnitude images could also be compared with the phantom images of each condition to assess if there are any differences in the images [Metha et al, 2009]. The impact of magnetic field on the device's ability to function normally in the MR environment is evaluated by comparing the device results recorded when the device is inside the scanner at locations close or far from the head coil to device results recorded outside of the scanning environment. Some studies have assessed the device's performance in different magnetic field: the static high magnetic field, the echo planar imaging (EPI) and the gradient echo EPI imaging sequences [Schaechter et al., 2006]. Only when the device and MR image are not affecting each other, we can conclude that the system is MR conditional in that particular MR field.

### **3.5.1. MR Validation Procedure**

To examine if our UE R/G system is MR conditional, we scanned a spherical, silicone head phantom (General Electric (GE) model 2359877) under several conditions. The phantom was placed in the center of a single-channel Quadrature head coil at the 3.0 Tesla short-bore GE excite magnetic resonance imaging system (Waukesha, WI) located at the Froedtert Hospital (Milwaukee, WI). The EPI sequence (38 continuous axial slices, TE=27ms TR=2s, flip angle = 77°, FOV=24cm, 64\*64 matrix and 3.75\*3.75\*4 mm spatial resolution) was used. Three independent variables were used to control the

experiment conditions: device (glove/orthosis/no device), movement (grasp movement/reach movement or no movement) and distance (in the control room ( $\infty$ )/55cm/35cm on the scanner bore from the center of the coil). Specifically, 26 cases with the combination of devices and movement and 2 control cases were applied in the scan sequence. Three blocks of movements were performed in the movement condition. Each movement block contains 10 movements performed by the same subject followed by a 20second resting block. A subject stood by the side of the scanner bore to hold/wear the devices and made the movements. In the grasp movement, the subject wore the hand glove and performed hand fully open to hand fully close movement; in the reach movement, the subject's two hands held the two sides of the orthosis and moved the upper arm piece of the elbow orthosis from 0 to 50 degree stopper installed by the side of the orthosis. The MR phase, magnitude data and device data were collected in each condition. We hypothesized that the devices and distance of device from the magnetic field will not cause the MR magnitude image quality and the  $B_0$  field to change significantly and the MR field will not affect the device's function.

### **3.5.2. Data Analysis**

We performed three steps of analysis to validate the image quality and system function: the SNR of magnitude image, the B field change of phase image and the measurement from the device. Both the magnitude and phase image data calculated in eight ROIs pre-defined, seven of which located inside the phantom image and one located outside of the phantom on the upper right of the image (see figure 3.22). Each ROI is 8 voxels large with approximately 4.5mL in volume. To examine the B field change, we first reconstructed the image from complex K-space into the B field and calculated the

averaged time series in each ROI. Then we calculated the differences between averaged B field value from the time series phase data and the B field in the control condition (no devices and movement in the scanner) as the B field change. To examine the magnitude image, we calculated the SNR for each ROI with Equation 3.3 [Hacckle, 1999].

$$\text{SNR}_{\text{roi}} = S_{\text{roi}} / (0.665 * \text{SD}_{\text{noise}}) \quad \text{Eq.3.3}$$

The signal is calculated from the averaged time series, and the noise is the standard deviation of the time series data in each ROI. Three-way ANOVA test was used with the three independent variables: device, movement and distance to test if each of the variables will affect the phase and magnitude image quality.

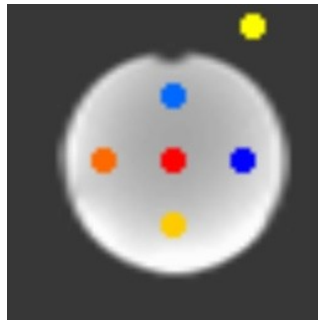


Figure 3.22 Region of interest in the phantom image  
*ROI 1 (blue dot), ROI 2 (light blue dot), ROI 4 (red dot), ROI 6 (yellow dot), ROI 8 (orange dot) are displayed inside the phantom, ROI 7 (lemon dot) is outside of the phantom image, ROI 3 and ROI 5 are not displayed in the picture. ROI 3 is located at the frontal part of the phantom sphere, ROI 5 is located at the rear part of the phantom sphere.*

From the device perspective, to determine if the magnetic field affects the normal operation of the devices, we compare the devices response both in stationary and movement condition. The averaged grasp aperture was calculated in the stationary condition from the rest blocks of the movement trials, the maximal grasp apertures were calculated from the move blocks in the movement trials. The orthosis angles were

calculated in each movement blocks. We then performed the one-way ANOVA to examine if the distance will affect the devices functioning in both stationary and movement conditions.

### **3.5.3. Results and Discussion**

#### **3.5.3.1. Phase image**

The B field change in each ROI is presented in the appendix C.1. The three-way ANOVA showed the device, distance, movement and their interactions caused no significant difference on the B field change (Table 3.2). The p-value for each variable and each interaction was close to 1. However, we did notice a B field shift as the experiment proceeded, i.e. between the two control conditions in the middle of experiment and at the end of the experiment. This might be caused by the increased temperature or overheating effects in the scanner. We also noticed a B field difference between stationary and movement conditions (Figure 3.23). We think the movement might cause some phase distortion. Two solutions could be applied to reduce this effect in future studies: 1) use the motion suppression algorithm developed by Menon [Menon, 2002] which estimates and removes the fraction of BOLD signal from motion by measuring their influence on the phase angle of the complex valued fMRI time series. The maximal likelihood estimator based on a linear least-squares fit of the BOLD signal phase to the BOLD signal magnitude in a voxel is determined and shown to efficiently suppress the BOLD effect from the larger veins. Baseline drift in the MR time course of each voxel was then removed by applying a band-pass filter. 2) The dynamic B field correction by measuring and correcting of MRI time series for effects of temporal dynamics in the main (static)

magnetic field. The method has shown impressive ability to restore statistical power to the complex constant phase fMRI activation model [Hahn et al, 2009].

Table 3.2 ANOVA result on the phase image B field change

Phase image B field change	ROI1	ROI2	ROI3	ROI4	ROI5	ROI6	ROI8	ROI7
Device	1	1	1	1	1	1	1	1
Distance	1	1	1	1	1	1	1	1
Movement	1	1	1	1	1	1	1	1
Device*distance	1	1	1	1	1	1	1	1
Device*movement	1	1	1	1	1	1	1	1
Distance*movement	1	1	1	1	1	1	1	1
Distance*device*movement	1	1	1	1	1	1	1	1

(*p*-values are reported in the table)

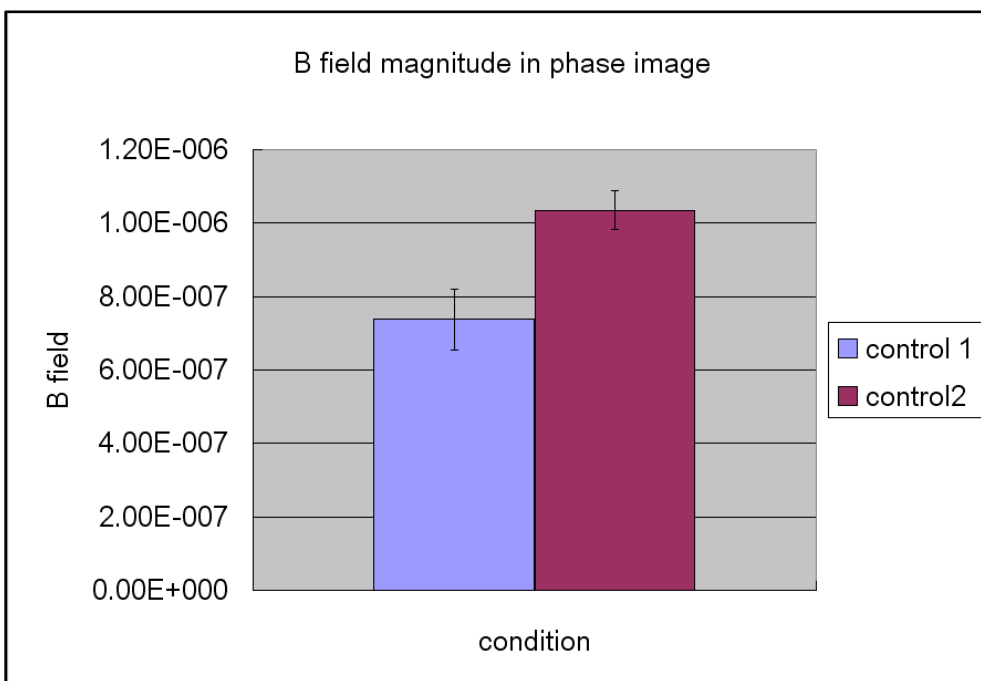


Figure 3.23 B field magnitude of phase image in two control conditions. Both conditions were scanned without any devices or movements. Control 1 was performed after a series of scans with devices in stationary conditions; control 2 was performed after a series of scans in movement conditions.

### 3.5.3.2. Image Quality

The original SNR for each ROI is show in appendix C.2 The ANOVA results showed the significant differences on the movement conditions (Table 3.3), and the Bonferroni post-hoc analysis showed the significant difference was between no movement vs. grasp movement and vs. reach movement. No significant differences were shown between grasp movement and reach movement results. Hence, we conclude that the device did not affect the magnitude image quality. To reduce the effect of movement in calculating the brain activations, we can include the motion parameters as the regressors in our general linear model.

Table 3.3 ANOVA result on the magnitude image

Magnitude SNR	ROI1	ROI2	ROI3	ROI4	ROI5	ROI6	ROI8	ROI7
Device	0.351	0.92	0.93	0.585	0.905	0.661	0.867	0.187
Distance	0.696	0.971	0.917	0.774	0.98	0.93	0.943	0.248
Movement	0.008*	0.029*	0.031*	0.024*	0.053*	0.017*	0.046*	0.003*
Device*distance	0.777	0.723	0.945	0.951	0.987	0.997	0.998	0.059
Device*movement	0.627	0.964	0.944	0.466	0.953	0.899	0.912	0.299
Distance*movement	0.73	0.927	0.964	0.843	1	0.991	0.985	0.2
Distance*device*movement	0.734	0.711	0.816	0.942	0.933	0.993	0.992	0.051

*P value was presented in the table. The values with (\*) indicates a significant difference.*

### 3.5.3.3. Device

In the stationary condition, the mean and standard deviation of grasp aperture were presented in Appendix D.1 and D.2. Two-way ANOVA showed no significant differences with the effect distance ( $F(2,14)=0.174$ ,  $p=0.84$ ), device ( $F(2,14)=2.02$ ,  $p=0.17$ ), and the interaction between distance and device ( $F(2,14)=0.658$ ,

$p=0.533$ ) on the glove sensors (Table 3.4). Therefore, we conclude that the bend sensor performance is consistent and not affected by the MR environment in stationary condition. The encoder reading is zero both inside and outside the scanner in stationary conditions. In the movement conditions, the encoder readings are represented in Appendix D.3. Two-way ANOVA on the grasp aperture also showed no significant differences on the effect of device (only orthosis move and orthosis move with the glove) ( $F(1,10)=2.17$ ,  $p=0.172$ ), distance ( $F(2,10)=1.9$ ,  $p=0.2$ ) and the interaction between distance and device ( $F(1,10)=0.065$ ,  $p=0.803$ ). Two-way ANOVA on the encoder reading in reach movement conditions also showed significant differences between the device ( $F(1,10)=0.124$ ,  $p=0.013$ ), distance ( $F(2,10)=14.091$ ,  $p=0.001$ ), but no significant difference on the interaction between device and distance ( $F(1,10)=4.749$ ,  $p=0.054$ ) (Table 3.4). Distance and devices significantly affects the encoder reading. The bonferroni post-hoc test showed the significant differences between the control room and 35cm, and between control room and 55cm. No significant difference was shown between 35cm and 55cm. From the encoder reading, we can see that the sensor reading inside the scanner was smaller than in the control room. We think this is due to the experiment control. An experimenter moved the forearm piece of the orthosis to the stopper for each trial. Inside the scanner, because of the limited space and her position, she reported that she had difficulties moving the orthosis to the designed angle. This might affect the results. From the other perspective, we didn't notice any noise on the encoder readings between conditions. Hence, we don't think the devices were affected by the distance from the center of coil. Therefore, we could conclude that the Magnetic field and the EPI sequence will not affect the device's function.

Table 3.4 Two-way ANOVA result for the glove and sensors

	Stationary				Movement			
	Glove		Orthosis		Glove		Orthosis	
	F	sig	F	sig	F	sig	F	sig
Distance	0.174	0.842	/	/	1.9	0.2	9.124	0.013
Device	2.02	0.17	/	/	2.17	0.17	14.091	0.001
Distance*Device	0.658	0.533	/	/	0.065	0.803	4.749	0.054

To sum up, the MR compatibility test result shows us that the image quality is not affected by the device operation and the device itself is not affected by the magnetic field.

### 3.6. Conclusions

This chapter presented the UE R/G system development, component, both the hardware and software design, the elbow orthosis calibration study and the MR compatibility test. The system uses bend sensors in a hand glove to measure the hand grasp aperture and an optical encoder in an elbow orthosis to measure the elbow joint angle. The system is designed for the reach/grasp movement with visual feedback to provide the task environment for the event-related fMRI scanning. The calibration study proved that the orthosis was able to accurately measure elbow movement and the compatibility test illustrated that the system is MR-conditional.

## Chapter 4

A correlation study between reach and grasp movement and the stroke  
impairment level

## **4. A correlation study between reach and grasp movement and the stroke impairment level**

### **4.1. Abstract**

To evaluate stroke recovery, it is important to develop assessment and training devices that are sensitive to the functional changes and able to measure the biomechanical kinematics of movement. This chapter examines motor performance on reach, grasp and reach-to-grasp tasks newly developed UE R/G system and determines how sensitive kinematic metrics derived to assess this performance correlate and predict stroke recovery levels. A group of 12 stroke survivors performed reach, grasp and reach-to-grasp movements with the system. Their stroke impairment was assessed by a series of clinical assessment tools and their motor performance by kinematic measures including the velocity, maximal movement, time, and smoothness metrics. We used Mann Whitney U test to examine the significant metrics in each task, and Principal Component Analysis (PCA) to decide the major metrics that could associate with the outcome. Linear regression analysis was then used to create the regression model between the clinical recovery score and the metrics extracted from the PCA. When compared with higher functioning subjects, low functioning subjects generally showed smaller movement velocity, smaller maximal movement, larger error and longer time to peak velocity in reach, grasp and reach-to-grasp tasks. The regression model suggests that functional recovery for reach and/or grasp tasks is predictable with maximal and mean velocities, maximal movement, error in reach, grasp and reach-to-grasp tasks. Additional to this

metrics, time to maximal angle, time to target and time to peak velocity could also be used as additional metrics to help predict the recovery and for assessing robot-assisted therapy and optimizing task-oriented rehabilitation strategy.

## **4.2. Background**

Rehabilitation is the most effective way to help stroke survivors re-gain their motor functions. To develop better rehabilitation strategies, it is important to determine how best to quantify the motor performance affected by stroke, to evaluate the effectiveness of rehabilitation strategies or the longitudinal performance changes over the time of stroke, to predict the possible potential for the recovery and to develop the best strategy for individual subject [Nowark et al, 2008]. Outcome measurement for motor function after stroke plays a critical role in quantifying the motor performance and the effectiveness of rehabilitation. Clinically, outcome measures are designed to measure three main issues: impairment, activity/disability, and participation. Table 4.1 is a summarization of clinical measurement tools. The stroke affects motor performance in a generalized manner and the different scales are not isolated from each other. Principle Component Analysis (PCA) has been used to study the relationships between these clinical metrics; by defining the most important eigenvalues that correlate to the clinical measures an overall recovery score representing the stroke survivor's function level can be derived and used to evaluate changes after a rehabilitation intervention [Ward et al 2003].

Table 4.1 Standard outcome measurement tools for stroke

Measurement criterion		Measurement tools
Impairment	Consciousness	Rancho Los Amigos Level of cognitive Function
	Cognition	Neurobehavioral cognitive status examination
	Sensorimotor scales	Grip strength, Fugl-Meyer Assessment of Motor Control, Ashworth scale of spasticity
	Timed performance	Nine hole peg test, Jebsen taylor hand function test, box and block test
	Instrumented evaluations	Strength: dynamometry Range of motion: goniometry
Activity/Disability	Activities of daily living	Barthel index, Functional independence measure
	Instrumental activities of daily living	Frenchay Activities index
Participation	Overall recovery	Stroke impact scale

Kinematic and kinetic measurements evaluating specific movements such as reach, grasp tasks from velocity, trajectory or force by the motion analysis system or force and position sensors. These measurements are promising and reliable ways to discriminate the motor function after stroke, to assess compensatory strategies of the motor system, to capture performance changes over time after stroke and to evaluate therapy induced changes in performance [Nowak et al 2008]. Reach tasks are often studied using point-to-point reach movements with force and position sensors [Colombo et al., 2002, Krebs et al., 1999, et al., 2002] or goniometers [Mirbagheri et al 2008, Song, et al, 2008]. Grasp movement, typically studied within the reach-to-grasp movement, is analyzed with the motion-analysis systems and optical tracking system [Paulette et al., 2007, Lang et al., 2006, 2006, Gentilucci et al, 2001, Schneiberg et al, 2002, Grosskopf et al., 2006, Nowark et al., 2007] separately or in combination with special hand gloves such as the 5DT Data Glove series (Fifth Dimension Technologies, Inc; Irvine, California), the CyberGlove (Immersion Corp; San Jose, California), and the ShapeHand (Measurand Inc, Fredericton, Canda).

Kinematic metrics evaluating movement velocity, accuracy, effectiveness, efficiency, smoothness and time are used to evaluate upper limb movements (Table 4.2). The studies of voluntary reach movements after stroke showed a decreased movement velocity [Kamper et al, 2002, Wing 1990], increased movement direction error [Beer et al., 2000], increased segmentation [Krebs et al., 1999], decreased movement distance, increased trajectory curve [Levin et al., 1996], increased reaction time and movement time [Chang et al 2005]. A correlation study revealed strong correlations between the Chedoke-McMaster (CM) stroke assessment score and significant degradation in all performance measures including distance, velocity, smoothness, straightness and direction of the hand path during each reach movement [Kamper et al 2002]. Strong correlations were also shown between the Action Research Arm Test (ARAT) score and decreased wrist velocity, increased movement time, decreased time of peak grip aperture, increased peak grip aperture, and increased amount of the grip force overshoot in affected hand and also decreased peak wrist velocity and increased movement time in the reach-to-grasp movement [Nowak et al, 2007]. Grasp movements were usually studied with the reach-to-grasp movement, which could be divided into two components: the hand transportation component which is transporting the hand from the start position to the target and the hand grasp component which is shaping the hand for the object [Jeannerod et al 1981]. It has been found that the peak grasp aperture occurred at about 70% of the time needed for the hand transport [Jeannerod, 1981, Castiello, 2005] and the amount of peak grasp aperture exceeded the actual object size by 20% [Jeannerod et al, 1981]. Stroke survivors with more severe impairment showed an intra and inter variability in the affected hand movement [Lang et al., 2005]; decreased hand transportation velocity,

decreased velocity of grasp aperture, inaccurate grasp aperture with an extensive opening of the hand, inaccurate scaling of peak grasp aperture, decoupling of the spatio-temporal coordination between the hand transport and the grasping [Lang et al., 2005, Nowark et al., 2007], a delay in initiating the formation of grasp aperture during the deceleration phase of the hand transporting component [Johansson and Westling 1984]. Studies have also found the subjects with more severe impairment had problems opening the fingers accurately when approaching the objects [Lang et al., 2005].

Table 4.2 Kinematic metrics for evaluating movements

(See Appendix E for definitions)

Metrics		Study	Movement
Velocity	Mean velocity	Wing et al,1990 Kamper et al 2002 Colombo et al, 2008	Reach, grasp
	Peak velocity	Lang et al 2006	
Accuracy	Direction error	Beer et al, 2000	Reach
	Root mean square error	Song et al., 2008	Reach
	Percent time in target (PPT) Dwelling percent time in target (DPTT)	Feng, 2007	Tracking tasks
Efficiency	Path length ratio	Colombo et al., 2008, Levin et al., 1996, Kamper et al., 2002 Schneiberg et al, 2002, Lang et al., 2006	Reach
Smoothness	Segmentation	Krebs1999, Kamper 2002	Reach, grasp
	Speed smoothness	Rohrer et al, 2002	Reach , grasp
Maximal movement	Maximal joint angle	Nowark et al., 2007, Kamper et al 2007	Reach
	Maximal grasp aperture	Lang et al, 2005, Noward et al, 2007, Gentilucci et al, 2001	Grasp
Time	Reaction time	Johansson and Westling, 1984	Reach, grasp
	Movement time	Lang et al., 2006, Nowark et al, 2007, Chang et al., 2005	Reach, grasp
	Time to maximal movement	Gentiluchi et al., 2001 Lang et al., 2006	Reach, grasp
	Time to peak velocity	Gentiluchi et al., 2001, Lang et al 2005, 2006, Chang et al., 2005	Reach, grasp
	Relationship between time to reach Peak velocity and grasp peak velocity	Hu et al, 2005, Lang et al, 2006	Reach to grasp

This chapter describes a study undertaken to evaluate the performance the UE R/G system with twelve stroke survivors of varying functional levels as they performed

reach, grasp and reach-to-grasp tasks. Their stroke impairment was assessed by the series of clinical assessment tools (Appendix A) performed by a physical therapist and a series of derived kinematic measures (Appendix E) including the velocity, maximal movement, time and smoothness metrics. Movement performances on reach, grasp and reach-to-grasp tasks were characterized by examining differences between low and high functioning stroke survivors. We hypothesize that the UE R/G system when utilized outside the fMRI will be sensitive to differences in motor performance due to stroke impairment and functional recovery. Specifically, the derived kinematic metrics will correlate to recovery scores. In addition, we will characterize the observed motor performance on reach, grasp, and reach-to grasp tasks by recovery level using time, velocity, and quality of movement metrics and determine which of the derived metrics best predicted level of recovery.

### **4.3. Methods**

Thirteen stroke survivors aged from 38-63 (mean age: 56.1 year-old, SD:  $\pm 7$ ) were recruited from the local community. One subject withdrew from the study. Within the 12 subjects, seven subjects were female (mean age: 55.8 year-old, SD= $\pm 8.5$ ) and 5 were male (mean age: 55.2 year-old, SD= $\pm 4.9$ ). All subjects have unilateral stroke for more than 6 months with no visual neglect and are able to understand the instructions and sit up right for 2 hours. According to the Edinburgh Handedness Survey [Oldfield, 1971], eight subjects are right-hand dominant and 4 are left hand-dominant. The detailed information of subjects is presented in Table 4.3.

Table 4.3 Subject information

Subject #	Gender	Age	Time post stroke	Affected	Handedness	FMA
1	F	55	14 years	R	L	48/66
2	F	59	19 years	R	L	58/66
3	M	51	7 years	L	R	27/66
4	M	63	2 years	L	R	23/66
5	M	55	4 years	R	L	28/66
6	F	60	24 years	L	R	24/66
7	F	54	3 years	L	R	66/66
8	M	56	2 years	L	R	41/66
9	F	63	29 years	R	L	31/66
10	M	51	3 years	L	R	24/66
11	F	38	17 years	R	R	65/66
12	F	62	7 years	L	R	64/66

#### 4.3.1. Apparatus

The UE R/G system is designed with a measuring portion including a hand glove with four bend sensors that could measure the index and thumb MCP and PIP joints and calculate the grasp aperture, defined as the distance between tip of index finger and thumb; an elbow orthosis with optical encoders which could measure the elbow joint angles; a data collection and task control portion which is built on xPC target system and real-time workshop, and a task display portion which includes a second monitor placed in front of the subject that provides tasks and visual feedback. Details of the system can be found in chapter 3.

#### 4.3.2. Experiment protocol

All subjects signed written consent forms approved by the Institution Review Board of Marquette University. They were evaluated by a physical therapist with nine

clinical assessment methods including Fugl-Meyer assessment (FMA), Function Test (FT), Jebsen Taylor Hand Function (JTHT), Box and Block Test (BBT), Nine Hole Peg Test (NHPT), Grip strength, Range of Motion (ROM), Functional Independence Measure (FIM) and Stroke Impact Score (SIS). They then performed a series of motor tasks, including hand grasp (from hand open to hand close), elbow reach (from elbow flexion to extension) and reach-to-grasp movement with the UE R/G system at the Falk Neurorehabilitation Laboratory at Marquette University. Figure 4.1 is a snapshot of the experiment set up. Subjects were seated upright in a stationary chair in front of a table as comfortable as possible. The subject's arm/hand to be tested was placed inside the orthosis and glove, placed onto a wooden fixture on the table. The fixture was locked at the position with respect to the table by three clamps. The other arm was rested at a comfortable position. Velcro straps were used to stabilize the upper arm with the fixture. Subjects were able to move the forearm up and down, open and close their hands without any restraint. A display screen was centered along the subject's middle line and 64 cm from the front edge of the table. The data acquisition devices were placed on the left side of table outside the workspace. Six EMG electrodes were placed on the triceps, biceps and extensors on the subject's upper and forearm to calculate the muscle activities for the mirror movement monitoring. Future analysis of EMG signals is not reported in this thesis.

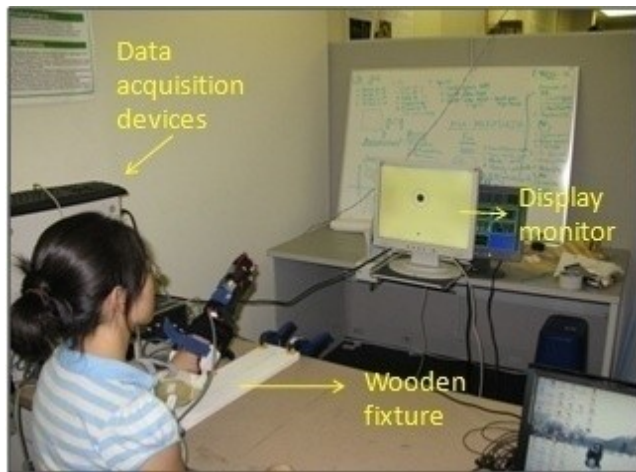


Figure 4.1 Snapshot of the experiment set up.  
*(Subject is seated in front of a table with hand and elbow in the devices. A display monitor is placed 64cm from the front edge of the table, aligned to the subject's center-line.)*

The tasks were designed following event related task design paradigm in the function MRI experimental design. Each task block contained 160 trials with 75 movement trials and 85 blank trials. Each trial was 4 seconds long. The tasks were randomly arranged among the whole sequences following the inter-stimulus-interval task design. Before subject performed the tasks, their minimal grasp aperture and elbow movement angles were measured with the hand and elbow calibration tasks. The grasp and reach target in the task were scaled to 150% of minimal grasp aperture and 80% of the maximal reach angle to ensure the subject's ability to perform tasks without fatigue. Before each task block, subjects were given enough practice until they were comfortable. Rests were given upon request between the blocks but not within the block. Figure 4.2 is a flowchart of the experiment procedures.

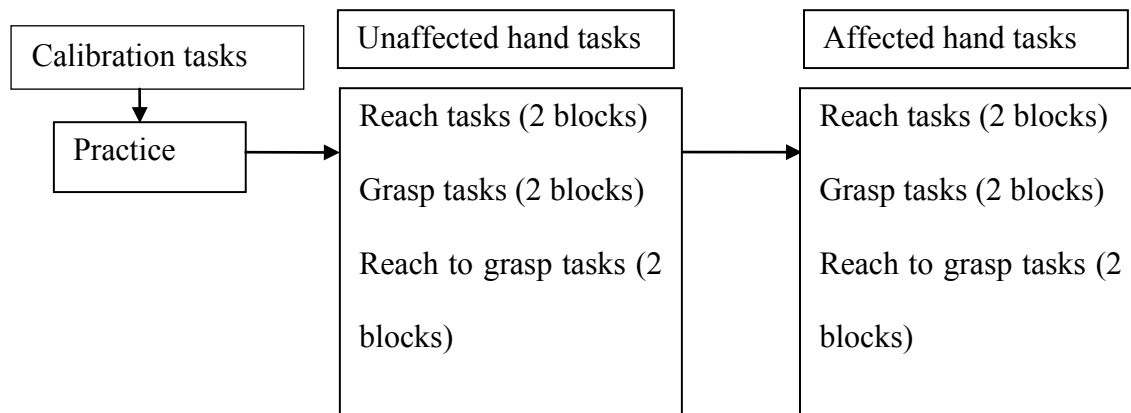


Figure 4.2 Flowchart of the task procedures

### 4.3.3. Data analysis method

The clinical assessment data was first normalized to unit mean and variance. PCA was performed for the 9 assessment types to generate the main components. The component coefficients were then used as the weights to calculate the recovery score, with which, subjects were divided into low to medium and high function groups. With movement performances, grasp aperture data was first normalized for each trial by subtracting from the baseline which was calculated as the mean value of grasp aperture of the first 50 data points. All trials were visually checked to exclude the ones with irregular trajectories, or with the reaction time, movement time and error outside of the acceptable range ( $MEAN \pm 2 * STD$ ). Movement performance metrics were calculated from movement velocity, maximal movement angle/aperture, smoothness, accuracy, reaction time and movement time, time to peak velocity, time to target and time to peak movement in each tasks. Metrics with significant differences between low and high function groups were discovered based on the Mann Whitney U test for each task type. A

principal component analysis was used to analyze the relationships between metrics and identify which metrics explained the variance found across the stroke subjects. The PCA analysis resulted in eigenvalues describing the variance in key directions. The main components describing at least 80% of the variance in the data were used. The main metrics in each principle component was used to calculate the PCA scores. Regression analysis was performed between the recovery scores and these PCA scores and ultimately defined the relationship between the recovery and the kinematic metrics. The coefficient in the equation was set to  $\pm 1$  to indicate the trend of the metric. The significance level for statistical analyses was set as 0.05. Data analysis was performed with MATLAB [Mathworks Inc, Boston, MA, USA], Microsoft Excel [Microsoft Corp, Redmond, WA, USA] and SPSS [SPSS Inc, Chicago, IL, USA].

#### 4.3.3.1. Clinical data

The Upper extremity FMA uses a scale between 0-66 to evaluate the movement coordination and reflex action. The NHPT tests the hand dexterity through measuring the amount of time to place nine pegs into nine holes in a vertical panel. The FT uses a scale from 1 to 7 to test the subjects' ability on activities of daily living. The FIM uses a scale from 1 to 7 with 5 items to measure the subject's level of disability in terms of burden of care. The BBT measures the amount of blocks the subject could transfer from a box to another within one minute. Time per block is calculated as the outcome. The JTHT measures the amount of time the subject used to complete several hand function tests with objects of different weights. The grip strength uses a hand dynamometer to measure the hand grip force. And the SIS score is a self-report questionnaire used to evaluate the subject's mobility, strength ADL and affected hand use. The BBT, JTHT, NHPT and grip

strength outcome is normalized by (unaffected hand – affected hand) / (unaffected hand + affected hand). Details of each scale are presented in Appendix A

#### 4.3.3.2. Performance metrics

Each task can be separated into two sub-movements; grasp task consists of hand open to close and hand close to open sub-movements, reach task consists of elbow flexion to extension and elbow extension to flexion sub-movements. Only the first sub-movements, defined from the time when velocity first reached 5% of the maximal velocity in the hand open to close process (elbow flexion to extension for reach) to the time when the subject reached 5% of the maximal velocity again in the hand close to open (elbow extension to flexion for reach) movement, were experimentally instructed and controlled with the subjects and analyzed with the following metrics:

**Velocity metrics:** The maximal velocity ( $V_{Rmax}$  for reach and  $V_{Gmax}$  for grasp task) and mean velocity ( $\bar{V}_R$  for reach and  $\bar{V}_G$  for grasp task) are calculated as the largest velocity and averaged velocity in the sub-movement. They are used to quantify the basic movement velocities.

**Movement metrics:** The maximal movement ( $\theta_{max}$  for reach and  $\beta_{max}$  for grasp task) is calculated in each trial, which is used to quantify the stroke survivor's movement abilities.

**Accuracy metrics:** The error ( $\bar{\theta}_{error}$  for reach task and  $\bar{\beta}_{error}$  for grasp task) is calculated as the square root of mean squared difference between the acquired angles to target angle normalized by the target angle in the task block across all the good task trials. Since the target is pre-defined for each individual according to their movement

abilities, the normalization process makes the error comparable between subjects.

**Smoothness metrics:** The movement unit ( $S_{Runit}$  for reach and  $S_{Gunit}$  for grasp task) is the number of peaks across movement, which is defined using the following method: local maximal and minimum velocity is searched; if the difference between the adjacent minimal and maximal velocity exceeds 15% of the maximal velocity, a peak is defined. The number of peaks is then counted as the number of movement units [Krebs et al, 1999]. Speed smoothness ( $J_R$  for reach and  $J_G$  for grasp task) is calculated from mean velocity divided by maximal velocity, which is also used to quantify the movement smoothness.

**Time metrics:** Reaction time ( $t_{Rreact}$  for reach and  $t_{Greact}$  for grasp) is calculated as the time from task begins to the time when velocity is larger than 5% of the maximal velocity of the movement. It is used to quantify how fast the subject responses to the tasks. Movement time ( $t_{Rmovt}$  and  $t_{Gmovt}$ ) is calculated from the movement onset to the movement offset defined with the sub-movements. Time to peak velocity ( $t_{Rvmax}$  and  $t_{Gvmax}$ ), time to peak movement ( $t_{\theta max}$  and  $t_{\beta max}$ ) and time to target ( $t_{\theta target}$  and  $t_{\beta target}$ ) are the time between movement onset to the time when  $v = v_{max}$ , when  $\theta = \theta_{max}$  or  $\beta = \beta_{max}$ , and when  $\theta = \theta_{target}$  or  $\beta = \beta_{target}$ . The relationships between time in reach movement and in grasp movement is calculated from time performance in reach tasks divided by the performance in the grasp tasks to quantify the coordination between the two movements in the reach-to-grasp tasks.

## 4.4. Result and discussion

### 4.4.1. Clinical measurement results

The FM, FT, NHPT, BBT, grip strength, FIM, JHPT, and SIS scores of each subject are reported in table 4.4. The component 1 from PCA results representing 70.7% of the total variance and the component coefficient (Row PCA1 in table 4.5) is then multiplied by the clinical results to generate the recovery scores (Last row in table 4.4). The FM, FT, NHPT, BBT, Grip strength, SIS-physical problems, JHPT scores are the major measurements affecting the recovery scores. The twelve subjects show a clustered pattern in their recovery scores (figure 4.3); subject 6,3,4,5,9,10 are classified into the low to medium group and subject 1, 7, 12, 11 belongs to the high functioning group. We will use the grouping methods for our analyses in the following chapters.

Table 4.4 Clinical measurement for low functioning subjects

	<b>Subject LOW</b>	<b>6</b>	<b>3</b>	<b>4</b>	<b>5</b>	<b>9</b>	<b>10</b>	<b>2</b>	<b>8</b>	<b>Mea n</b>	<b>St_d ev</b>	
Sensori motor scale	FMA	24	27	23	28	31	24	48	41	<b>30.7 5</b>	<b>9.07</b>	
	FT	3	3	3	5	3	3	4	5	<b>3.63</b>	<b>0.92</b>	
	Grip strength	0	0	0.19	0.06	0.39	0.12	0.15	0.22	<b>0.14</b>	<b>0.13</b>	
	ROM	0.72	0.29	0.61	0.78	0.45	0.76	0.99	0.19	<b>0.60</b>	<b>0.27</b>	
Timed perfor mance	BBT	0	0	0	0	0.08	0.04	0.14	0.29	<b>0.07</b>	<b>0.1</b>	
	NHPT	0	0	0	0	0	0	0	0.14	<b>0.02</b>	<b>0.05</b>	
	JTH T	Page turn	0.02	0	0	0	0	0	0.27	0.28	<b>0.07</b>	<b>0.13</b>
		Small objects	0.02	0	0	0	0	0	0	0.28	<b>0.04</b>	<b>0.1</b>
		Feeding	0.08	0	0	0	0	0	0	0.01	<b>0.01</b>	<b>0.03</b>
		Checker	0	0	0	0	0	0	0	0.09	<b>0.01</b>	<b>0.03</b>
		Large light object	0.02	0	0.08	0	0.05	0	0	0.13	<b>0.03</b>	<b>0.05</b>
Large heavy object	0.01	0	0.12	0	0.14	0	0	0.31	<b>0.07</b>	<b>0.11</b>		
ADL	FIM	31	33	35	30	31	34	35	32	<b>32.6 3</b>	<b>1.92</b>	
Particip ation	SIS	Physical problem	50	43.7 5	37.5	43.7 5	62.5	50	68.7 5	43.7 5	<b>50</b>	<b>10.5 6</b>
		ADL	90	88.8 9	64.3	80	92.5	77.5	95	72.5	<b>82.5 9</b>	<b>10.8</b>
		Mobility	66.7	100	88.9	63.9	88.9	88.3	86.1 1	94.4 4	<b>84.6 6</b>	<b>12.7 4</b>
		Affected hand use	0	15	0	50	10	80	35	80	<b>33.7 5</b>	<b>33.2 5</b>
	Calculated Score	-	-	-	-	-	-	-	-	- 4.78	1.68	
	Recovery	6.35	6.39	6.07	5.38	4.78	4.74	2.66	1.93			

Table 4.4 cont'd Clinical measurement for high functioning subjects\*

	<b>Subject HIGH</b>	<b>1</b>	<b>7</b>	<b>12</b>	<b>11</b>	<b>Mean</b>	<b>Stdev</b>	
Sensorimotor Scale	FMA	64	66	58	65	<b>63.25</b>	<b>3.59</b>	
	FT	6	7	7	7	<b>6.75</b>	<b>0.5</b>	
	Grip strength	0.4	0.58	0.69	0.88	<b>0.64</b>	<b>0.2</b>	
	ROM	1.06	0.99	0.92	1.06	<b>1.01</b>	<b>0.07</b>	
Timed performance	BBT	0.66	0.68	0.86	0.94	<b>0.79</b>	<b>0.14</b>	
	NHPT	0.18	0.71	0.53	0.87	<b>0.57</b>	<b>0.3</b>	
	JTHT	Page turn	0.54	0.61	0.61	0.78	<b>0.64</b>	<b>0.1</b>
		Small objects	0.61	0.61	0.7	0.94	<b>0.72</b>	<b>0.16</b>
		Feeding	0.48	0.52	0.49	0.71	<b>0.55</b>	<b>0.11</b>
		Checker	0.16	0.35	0.62	1.03	<b>0.54</b>	<b>0.38</b>
		Large light object	0.48	0.72	0.58	1.01	<b>0.70</b>	<b>0.23</b>
Large heavy object	0.61	0.67	0.61	0.76	<b>0.66</b>	<b>0.07</b>		
ADL	FIM	33	35	30	35	<b>33.25</b>	<b>2.36</b>	
Participation	SIS	Physical problems	75	43.75	93.75	75	<b>71.88</b>	<b>20.73</b>
		ADL	87.5	75	87.5	87.5	<b>84.38</b>	<b>6.25</b>
		Mobility	91.67	77.78	97.2	91.67	<b>89.58</b>	<b>8.29</b>
		Affected hand use	55	60	95	55	<b>66.25</b>	<b>19.31</b>
	<b>Calculated Recovery Score</b>	4.82	6.49	8.24	11.72	<b>7.82</b>	<b>2.95</b>	

\*(All scores have been normalized by unit mean and variance)

Table 4.5 PCA Analysis

		Mean ALL	St_dev ALL	PCA1	
Sensorimotor scale	FMA	41.58	17.66	<b>0.91</b>	
	FT	4.67	1.72	<b>0.91</b>	
	Grip strength	0.31	0.29	<b>0.95</b>	
	ROM	0.74	0.3	<b>0.69</b>	
Timed performance	BBT	0.31	0.37	<b>0.98</b>	
	NHPT	0.2	0.32	<b>0.94</b>	
	JTHT	Page turn	0.26	0.3	<b>0.98</b>
		Small objects	0.26	0.35	<b>0.97</b>
		Feeding	0.19	0.27	<b>0.95</b>
		Checker	0.19	0.33	<b>0.92</b>
		Large light object	0.26	0.35	<b>0.96</b>
Large heavy object		0.27	0.31	<b>0.96</b>	
ADL	FIM	32.83	1.99	<b>0.43</b>	
Participation	SIS	Physical problems	57.29	17.44	<b>0.79</b>
		ADL	83.18	9.25	<b>0.41</b>
		Mobility	86.3	11.31	<b>0.44</b>
		Affected hand use	44.58	32.58	<b>0.67</b>

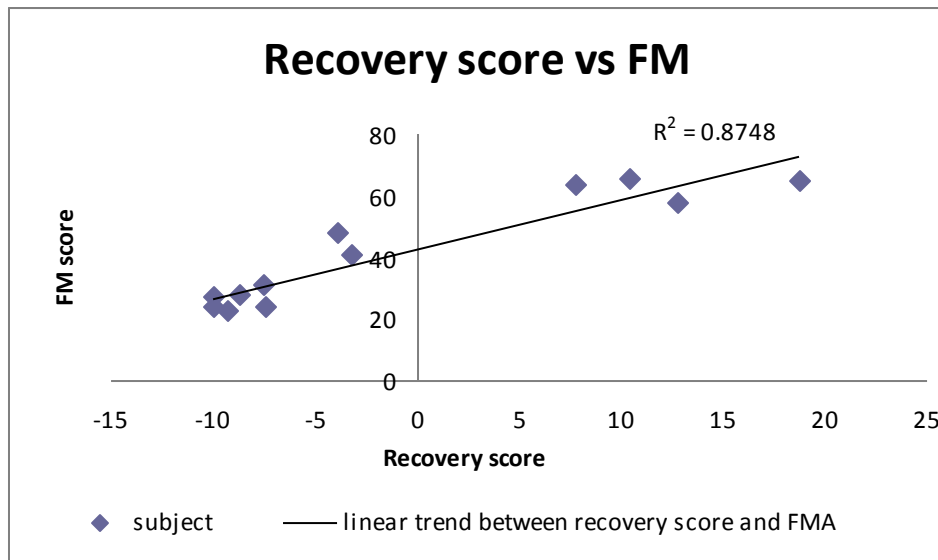


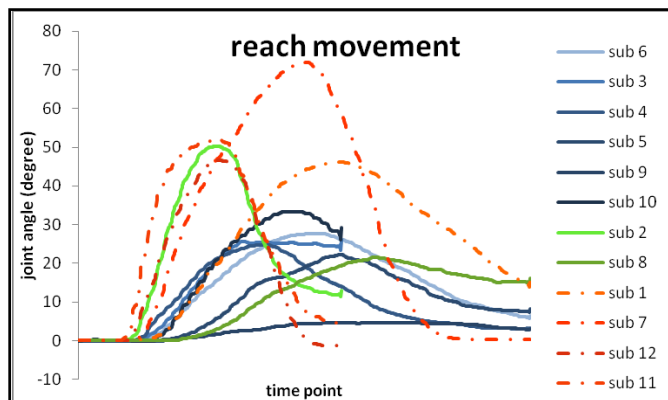
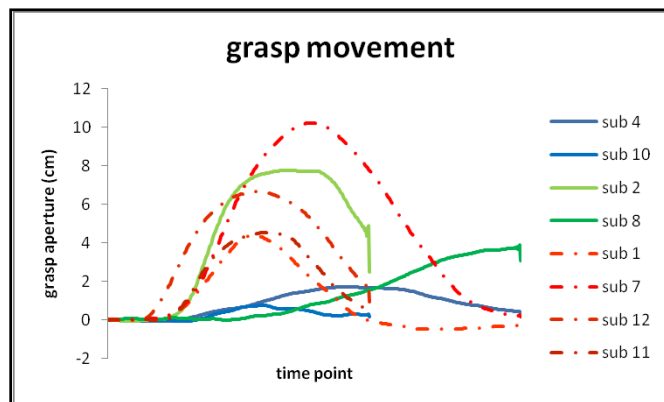
Figure 4.3 Recovery score vs. FM score for all the 12 subjects (X axis represents the recovery score generate from PCA, the y axis represents the FM score. Linear trend line was created between FM score and the recovery score. Each blue diamond represents a subject.)

#### 4.4.2. Movement performance results

##### 4.4.2.1. Movement trajectories

Representative low and high grasp and reach trajectories were presented for all subjects (figure 4.4). The bell shaped trajectory profile characterized both the hand open-close-open process and elbow flex-extend-flex process. In the grasp movements, high function subjects showed larger maximal grasp aperture in grasp tasks and larger maximal reach angles in reach tasks. In the reach-to-grasp task, the high function subject had larger reach and grasp target and showed he reached both targets earlier than the low function subjects with a better coordination between the two movements. The low function subject arrived at his reach target much earlier than he reached the grasp target

indicating a worse coordination between the two movements. There were four low functioning subjects (subject 3, 5, 6 and 9) that appeared to lack the ability to complete the grasp movements. Their clinical results had indicated little to no grasping ability (see table 4.4 BBT and NHPT). Their averaged grasp apertures were shown in figure 4.5. In an effort to determine the actual nature of these subjects grasping movements and whether their movements were usable, we further analyzed the results by comparing their movements to the sensor values obtained when the sensor was placed flat on the table and no movement was made (sensor flat). Subjects 5 and 6's movement trajectories were inside the sensor's fluctuation range and was not different from the noise ( $\pm 0.1$  cm). With the sensor's resolution being 0.1 cm, Subject 3's aperture firstly decreased to -0.1 cm then increased to 0.2 cm. Subject 9's aperture decreased to -0.3 cm first then increased to 0.2 cm.



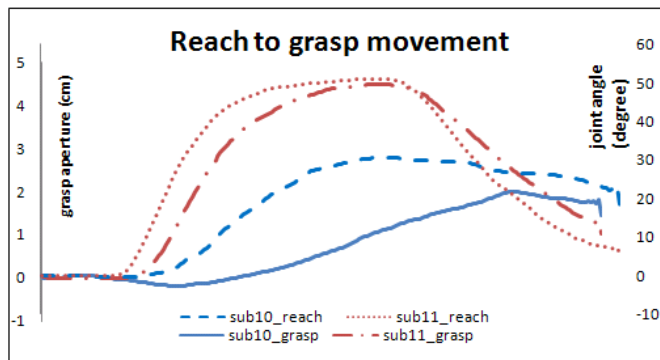


Figure 4.4 Representative trajectories in reach, grasp and reach to grasp movements ((1) grasp movement trajectories for 8 subjects; (2) grasp movement trajectories for 4 low functioning subjects (3): reach movement trajectories for 12 subjects; (5): reach to grasp movement trajectories for 2 subject (subject 10 –low functioning and subject 11-high functioning) The blue and green solid lines represents low to medium functioning subjects (subject 4, 10, 2, 8 in grasp movement, subject 6, 3, 4, 5, 9, 10, 2, 8 in reach movement); and the orange dash dot lines represents the high functioning subjects (subject 1, 7, 12, 11 ) in figure (1) and (3). In figure 4, blue dash dot line represents the reach movement of sub10; blue solid line represents grasp movement of subject 10; red dot line represent reach movement of subject 11; and red dash line represent grasp movement of subject 1. X axis is the time axis, y axis represents grasp aperture (grasp movement) in figure (1) and elbow joint angle (reach movement) in figure (3). Left Y axis represents grasp aperture (grasp movement) and right Y axis represents reach joint angle (reach movement) in figure 4.)

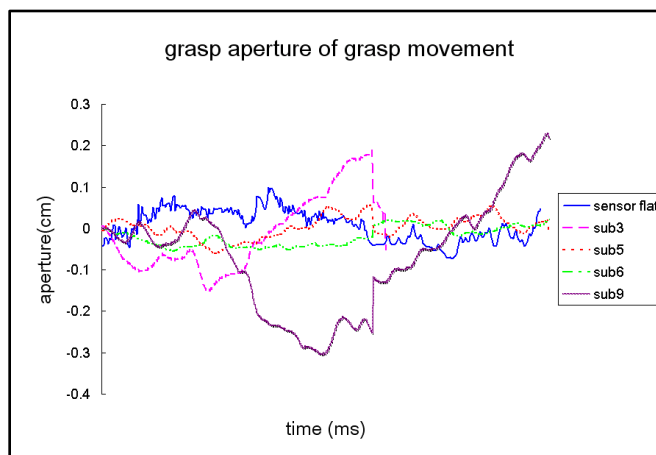


Figure 4.5 The four low function subject' grasp aperture (Grasp aperture of four low function subjects' grasp movement and when all sensors were placed flat and still. X axis represents the time (unit: ms), the Y axis represents the grasp aperture (unit: cm)).

The data indicate that when the task begun, subjects 6 and 9 attempted movement but were unable to open or close their hands. Movements seen was probably due to some squeezing movement that resulted in small grasp aperture changes. In comparison, the other 8 subjects with clear grasping movements performed the task with a hand close movement followed by a hand open movement with grasp apertures changing by at least 1.5cm, which were much larger than these subjects' movement. Based on the above reasons, subjects 3, 5, 6 and 9 movements were not analyzed further. These results indicate a need to improve the grasp glove's resolution and develop more accurate metrics to study low function subjects' limited movement.

#### 4.4.2.2. Kinematic metrics

Detail results of each kinematic metric for each kind of tasks are presented in the appendix F.

**Reach movement:** The Mann Whitney U test results (Table 4.6) showed significant differences in maximal and mean velocity, maximal angle, error, and reaction time, time to peak velocity and time to target metrics. Low function group showed lower maximal velocity, lower mean velocity, smaller maximal angle, smaller time to target, lower accuracy (larger error), larger time to peak velocity and larger reaction time compared to high function subjects. No significant difference was shown in movement unit, speed smoothness, time to peak angle and movement time. Using PCA the two principle components that accounted for 80% of the total variance were extracted (Table 4.7). Maximal and mean velocity, maximal angle, error, time to maximal angle and time to target were the main metrics contributing to component 1 and time to peak velocity was

the main metrics contributing to component 2. These metrics were used to calculate the PCA scores. Reaction time metric showed significant differences in U test only and time to maximal angle was a major metric in PCA result but not in U test. The other six metrics showed their significances in both metrics. Linear regression analysis between recovery score and the PCA scores showed a significant regression model (Eq. 4.1) with  $p = 0.01$  and adjusted  $R^2=0.74$ . Both components were significant ( $p= 0.003$  for component 1 and  $p=0.006$  for component 2). The beta coefficient was generated from the regression model ( $\beta_1 = 0.637, \beta_2 = 0.595$ ). However, because of the small sample size, the precision of coefficient was very low and the relationship between the recovery score and the components were more important; we used the coefficient of  $\pm 1$  in our results.

$$\text{Recover score} = \beta_1 * \text{component1} - \beta_2 * \text{component2} \quad \text{Eq.4.1}$$

Substituting component 1 and 2 with the kinematic metrics, we obtained the following equation (Eq. 4.2). The  $\beta$  value in the equation could also be calculated but not statistically precise ( $\beta_{11} = 0.53, \beta_{12} = 0.57, \beta_{13} = 0.60, \beta_{14} = 0.46, \beta_{15} = 0.56, \beta_{16} = 0.47, \beta_{21} = -0.50$ ).

$$\text{Recovery score} = \beta_{11} * V_{Rmax} + \beta_{12} * \bar{V}_R + \beta_{13} * \theta_{max} + \beta_{14} * t_{\theta max} + \beta_{15} * t_{\theta target} - \beta_{16} * \bar{\theta}_{error} - \beta_{21} * t_{Rvmax} \quad \text{Eq.4.2}$$

The recovery was positively correlated with the maximal velocity, mean velocity, maximal movement angle, time to maximal angle, time to target and negatively correlated with the error and time to maximal velocity. In other words, high function subjects had larger maximal velocity, mean velocity and maximal movement angle, longer time to maximal angle, longer time to target, smaller error and smaller time to peak velocity in the reach movement. The seven metrics could be used as the major

predictors to evaluate the strokes' reach movement kinematically.

Table 4.5 Mann Whitney U test result of the performance metrics in the reach movement

Metrics group	Metrics	U	Group	Mean Rank
Velocity	Max Velocity	5*	Low to medium	5.125
			High	9.25
	Mean Velocity	3*	Low to medium	4.875
			High	9.75
Accuracy	Error	0*	Low to medium	8.5
			High	2.5
Smoothness	Speed smoothness	11	Low to medium	5.875
			High	7.75
	Movement unit	15	Low to medium	6.625
			High	6.25
Maximal movement	Max angle	5*	Low to medium	4.75
			High	10
Time	Reaction Time	4*	Low to medium	8
			High	3.5
	Movement Time	16	Low to medium	6.5
			High	6.5
	Time to Peak Velocity	2*	Low to medium	8.25
			High	3
	Time to Peak Angle	11	Low to medium	5.875
			High	7.75
	Time to Target	2*	Low to medium	4.75
			High	10

*(Significant differences in U test are marked with (\*))*

Table 4.6 Principle components among the kinematic metrics in the reach task

	Component	
	1	2
Maximal velocity	0.834*	-0.121
Mean Velocity	0.902*	-0.118
Maximal Angle	0.944*	-0.079
Accuracy	-0.771*	0.06
Time to peak Velocity	-0.187	0.89*
Time to peak Aperture	0.735*	0.631
Time to target	0.887*	0.398
Reaction Time	-0.518	0.624

*The coefficient of each metrics in the two principle components. Main metrics are marked with (\*)*

**Grasp movement:** The four low function subject's movement data was not included in the analysis because of the limitation of our system (details described in movement trajectories section). Mann Whitney U test showed the low function group had significantly lower accuracy (higher error), larger time to peak aperture and smaller time to target. The other performance metrics didn't show any significant differences (Table 4.8). However, we noticed subject 2, who was in the low function group according to recovery score, had a different movement pattern in the movement performance comparing to the other subjects in the low group (Figure 4.6). We tested the results again with excluding subject 2 and found low to medium group demonstrated significantly smaller maximal velocity, smaller mean velocity, lower accuracy (higher error), more movement unit, smaller maximal grasp aperture, larger time to peak aperture, smaller time to target and smaller reaction time (Table 4.9). The reaction time showed an opposite trend to literatures that the low function subject should showed larger reaction time because of the damage in their center nerve system. We took a step further in

analyzing the reaction time, which was calculated as the time from the beginning of the task to the time when subject's velocity first reached 5% of the peak velocity. From the subject's movement velocity profile with low function subjects, such as in example figure 4.7, the 5% of maximal velocity is  $3E-05$  (cm/ms). With the sensor's resolution 1mm and the sampling frequency 100HZ; the velocity resolution is  $1E-03$ (cm/ms), larger than 5% of the maximal velocity. Therefore, we think the subject's movement was hard to differentiate from the sensor's fluctuation at the beginning of task for some low function subjects and as a result the calculated reaction time was very small and inaccurate. Because of our small sample size, every single subject might affect the statistics significantly. More studies are needed to prove the results. We then performed PCA with eight subjects and because of the limitation of reaction time; we didn't include this metrics in the analysis. Two components representing 73.4% of the total variances (Table 4.10) were selected. Maximal and mean velocity, maximal aperture, smoothness unit, error and time to peak velocity were the main metrics contributing to the first main components; time to target are the main metrics contributing to the second component. Except the fact that significance was shown in reaction time metrics but not in the PCA results, these two tests results selected the same metrics. These metrics from PCA and their component coefficients were used to calculate the PCA scores for each subject, which were used in the regression analysis to generate a recovery model between recovery score and the kinematic metrics with  $P=0.04$ , adjusted  $R^2= 0.724$ . Both components were significant with  $p=0.035$  for component 1 and  $p=0.048$  for component 2. The  $\beta$  was calculated from the regression analysis ( $\beta_1 = 0.68$ ,  $\beta_2 = 0.62$ ) but they were not precise that we could substitute them with  $\pm 1$  in our results.

$$\text{Recovery score} = -\beta_{11} * \text{component 1} - \beta_{12} * \text{component 2} \quad \text{Eq. 4.3}$$

By substituting the components with specific metrics, we obtained the following equation (Eq. 4.4).  $\beta_{11} = 0.62$ ,  $\beta_{12} = 0.65$ ,  $\beta_{13} = 0.61$ ,  $\beta_{14} = 0.59$ ,  $\beta_{15} = 0.59$ ,  $\beta_{16} = -0.57$ ,  $\beta_{21} = 0.55$  were calculated. Because the coefficients were not precise, we can use  $\pm 1$  to substitute them.

$$\begin{aligned} \text{Recovery score} = & \beta_{11} * V_{Gmax} + \beta_{12} * \bar{V}_G + \beta_{13} * \beta_{max} + \beta_{21} * t_{\beta target} - \beta_{14} * \\ & S_{Gunit} - \beta_{15} * \bar{\beta}_{error} - \beta_{16} * t_{Gvmax} \quad \text{Eq. 4.4} \end{aligned}$$

The recovery equation indicates a positive correlation between recovery scores and the maximal velocity, mean velocity, maximal aperture, time to grasp target and a negative correlation with movement unit, error and the time to peak velocity in the reach movement. Except the significance of movement unit, the relationship between recovery score and the other metrics are consistent with the grasp task results. This could also indicate that the high function subject will demonstrate larger maximal movement velocity, larger mean movement velocity with larger maximal aperture, longer time to target with smaller movement unit, smaller error and smaller time to peak aperture.

Table 4.7 Mann Whitney U test result of the performance metrics in the grasp movement

Metrics group	Metrics	U	Group	Mean Rank
Velocity	Max Velocity	4	Low to medium	3.5
			High	5.5
	Mean Velocity	4	Low to medium	3.5
			High	5.5
Accuracy	Error	1*	Low to medium	6.25
			High	2.75
Smoothness	Speed smoothness	8	Low to medium	4.5
			High	4.5
	Movement unit	4	Low to medium	5.5
			High	3.5
Maximal movement	Max aperture	3	Low to medium	3.25
			High	5.75
Time	Reaction Time	4	Low to medium	3.5
			High	5.5
	Movement Time	5	Low to medium	5.25
			High	3.75
	Time to Peak Velocity	5	Low to medium	5.25
			High	3.75
	Time to Peak Angle	1*	Low to medium	6.25
			High	2.75
	Time to Target	1*	Low to medium	2.75
			High	6.25

*(Significant differences in U test are marked with (\*))*

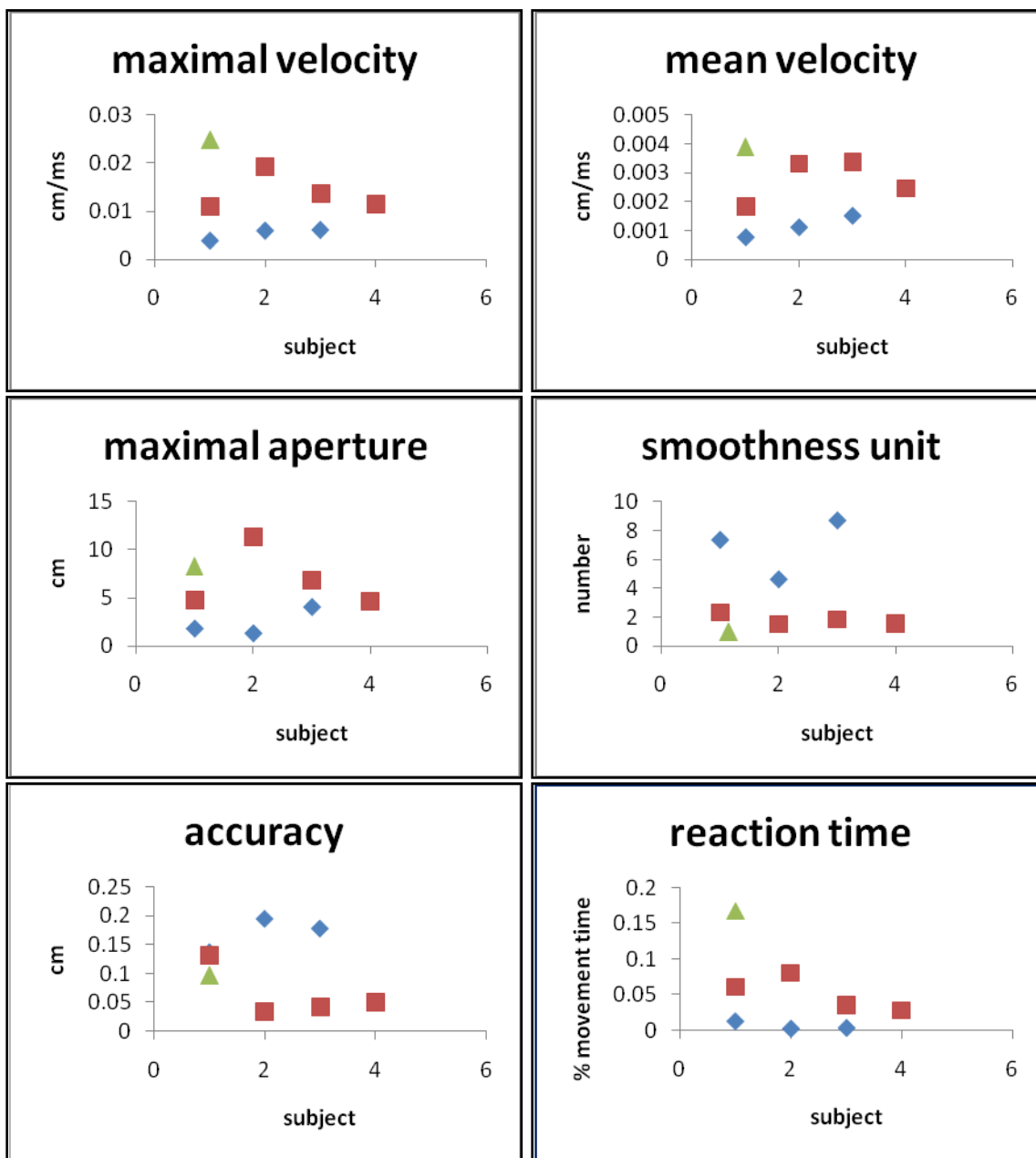


Figure 4.6 The comparison among Subject 2's performance metrics, low to medium group and high functioning group

(The blue diamond represents the low to medium group, the red square represents high functioning group and the green triangle represents subject2. Results of Maximal velocity, mean velocity, maximal aperture, smoothness unit, accuracy and reaction time are reported in the figure.)

Table 4.8 Mann-Whitney U test result of the performance metrics in the grasp movement excluding subject 2

Metrics group	Metrics	U	Group	Mean Rank
Velocity	Max Velocity	0*	Low to medium	2
			High	5.5
	Mean Velocity	0*	Low to medium	2
			High	5.5
Accuracy	Error	0*	Low to medium	6
			High	2.5
Smoothness	Speed smoothness	4	Low to medium	467
			High	3.5
	Movement unit	0*	Low to medium	6
			High	2.5
Maximal movement	Max aperture	0*	Low to medium	2
			High	5.5
Time	Reaction Time	0*	Low to medium	2
			High	5.5
	Movement Time	4	Low to medium	4.67
			High	3.5
	Time to Peak Velocity	2	Low to medium	5.33
			High	3
	Time to Peak Aperture	1*	Low to medium	5.67
			High	2.75
	Time to Target	1*	Low to medium	2.33
			High	5.25

(Significant differences in U test are marked with (\*))

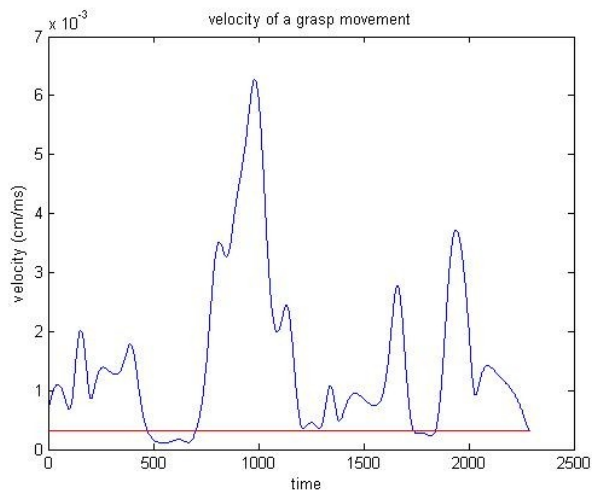


Figure 4.7 An example of grasp movement velocity  
(The blue line is the velocity profile, and the red line is 5% of the peak velocity.)

Table 4.9 Principle components among the kinematic metrics in the grasp task

	Component		
	1	2	3
Maximal Velocity	-0.912*	0.372	-0.014
Mean Velocity	-0.952*	0.145	0.227
Maximal Angle	-0.89*	-0.013	-0.003
Speed smoothness	0.292	-0.532	0.761*
Smoothness Unit	0.879*	0.001	0.258
Accuracy	0.87*	0.429	-0.09
Time to peak Velocity	0.832*	0.034	-0.367
Time to peak Aperture	0.695	0.475	0.256
Time to Target	0.124	-0.889*	-0.344

The coefficient of each metrics in the three principle components. Main metrics are marked with (\*)

**Reach to grasp movement:** Movements were analyzed with the grasp portion and reach portion separately with the same method in the reach and grasp movement. Significant

differences were shown in time to target in the reach portion and time to peak velocity in the grasp portion (Table 4.11) However, with our knowledge that subject 2's movement was different from the other subjects in the group; we re-tested our results without subject 2. Low function subjects showed significantly smaller maximal velocity, mean velocity, maximal angle in both reach and grasp portion and smaller time to target in the reach portion and larger time to peak velocity in the grasp portion. These implied that low function subjects performed slower movements; they arrived at their reach target earlier which might due to their reach target was smaller than the high function subjects; and they spent more time reaching to their maximal grasp velocity. PCA with the metrics also indicated similar results (Table 4.12). PCA with the reach portion extracted two principle components accounting for 80% of the total variance; maximal velocity, mean velocity, maximal angle, time to peak velocity, time to target, error were the major metrics contributing to component 1 and reaction time was the major metrics in component 2. The regression analysis generated a non-significant linear model with  $p=0.156$  and adjusted  $R^2=0.524$ . Both components were not significant with  $p=0.067$  of component 1 and  $p=0.451$  for component 2. The  $\beta$  were calculated from the regression analysis ( $\beta_1 = 0.75$ ,  $\beta_2 = 0.26$ ) but they were not precise in the equation that we could substitute them with 1 in our results.

$$\text{Recovery score} = \beta_1 * \text{component 1} + \beta_2 * \text{component 2} \quad \text{Eq. 4.5}$$

The equation 4.5 could be updated with the specific metrics. In our results, the coefficient were as follows:  $\beta_{11} = 0.59$ ,  $\beta_{12} = 0.66$ ,  $\beta_{13} = 0.68$ ,  $\beta_{14} = 0.71$ ,  $\beta_{15} = 0.66$ ,  $\beta_{16} = 0.64$ ,  $\beta_{21} = 0.23$ . Because they were not precision, we could substitute them with 1 in our results.

$$\text{Recovery score} = \beta_{11} * V_{Rmax} + \beta_{12} * \bar{V}_R + \beta_{13} * \theta_{max} + \beta_{14} * t_{\theta target} + \beta_{21} * t_{Rreact} - \beta_{15} * t_{Rvmax} - \beta_{16} * \bar{\theta}_{error} \quad \text{Eq. 4.6}$$

We substituted the coefficient of all the metrics to be  $\pm 1$  in the equation. But the coefficient for reaction time metrics was quite small (Beta = 0.2), we thought the effect of reaction time was not obvious. The model was insignificant, but the recovery score showed the potential to be positively correlated with the maximal velocity, mean velocity, maximal angle, and time to target and negatively correlated with time to peak velocity and accuracy. Therefore, we think the high function subject might show the trend to have larger maximal velocity, mean velocity, maximal angle and longer time to target and smaller time to peak velocity with smaller error. But because the recovery model only accounted from 52.4% of the total variance, we think there were some other variables that were related to the coordination between the reach and grasp movements and that were not evaluated in our analysis but affected the recovery level in reach-to-grasp movements.

In the grasp portion, two components were extracted, accounting for 79.7% of the total variance. Maximal velocity, mean velocity, maximal aperture, time to peak aperture, time to target and accuracy were the main metrics in component 1; smoothness unit, speed smoothness and time to peak velocity were the main metrics in component 2. The regression analysis generated an insignificant model with  $p=0.081$  and adjusted R square = 0.487 (Eq 4.7). Component 1 was significant with  $p=0.044$ ; component 2 was insignificant with  $p=0.214$ .  $\beta_1 = 0.72, \beta_2 = 0.39$  in the regression results. Because of the limited precision, we could substitute them with 1 in our results here.

$$\text{Recovery score} = \beta_1 * \text{component 1} - \beta_2 * \text{component 2} \quad \text{Eq. 4.7}$$

If we substituted the two components with specific metrics, we obtained the equation 4.8.  $\beta_{11} = 0.60, \beta_{12} = 0.67, \beta_{13} = 0.63, \beta_{14} = 0.54, \beta_{15} = 0.50, \beta_{16} = 0.56, \beta_{21} = 0.25, \beta_{22} = 0.32, \beta_{23} = 0.31$ . Because of the limited precision, we could substitute the  $\beta$  value with 1 in the results here.

$$\begin{aligned} \text{Recovery score} = & \beta_{11} * V_{Gmax} + \beta_{12} * \bar{V}_G + \beta_{13} * \beta_{max} + \beta_{14} * t_{\beta_{max}} + \beta_{15} * \\ & t_{\beta_{target}} - \beta_{16} * \bar{\beta}_{error} - \beta_{21} * S_{Gunit} - \beta_{22} * J_G - \beta_{23} * t_{Gvmax} \end{aligned}$$

Eq. 4.8

The insignificant model showed the potential that the recovery score might be positively correlated with maximal velocity, mean velocity, maximal aperture, time to peak aperture, time to target and negatively correlated with smoothness unit, speed smoothness and time to peak velocity. The result was consistent with the regression result of grasp only task except the time to maximal movement and speed smoothness were the main predictors in the grasp portion of reach-to-grasp task. The results also indicated subjects with better recovery might show the trend to have faster movement with larger grasp aperture, longer time to peak aperture, time to target and smaller error, smaller movement unit, smaller speed smoothness and smaller time to peak velocity. The insignificant of the model and the fact that the model only accounted for 48.7% of the total variance suggested that there might be some other kinematic metrics that affected the recovery level but were not evaluated in our experiments. As explained in the reach results, we think this might be related to the coordination of reach and grasp movement of the stroke survivors.

Table 4.10 Mann Whitney U test result in reach-to-grasp task  
(Eight subjects)

Metrics group	Metrics	U-Reach	U –	Group	Mean Rank-Reach	Mean Rank-Grasp
			Grasp			
Velocity	Max Velocity	4	4	Low to medium	3.5	3.25
				High	5.5	5.75
	Mean Velocity	4	3	Low to medium	2.75	3.5
				High	6.25	5.5
Accuracy	Error	3	4	Low to medium	5.75	5.5
				High	3.25	3.5
Smoothness	Speed smoothness	1	7	Low to medium	2.75	4.75
				High	6.25	4.25
	Movement unit	7.5	8	Low to medium	4.625	4.25
				High	4.375	4.75
Maximal movement	Maximal aperture/angle	3	3	Low to medium	3.25	3.25
				High	5.75	5.75
Time	Reaction Time	6	3	Low to medium	5	4
				High	4	5
	Movement Time	6	8	Low to medium	5	4.5
				High	4	4.5
	Time to Peak Velocity	4	0*	Low to medium	5.5	6.5
				High	3.5	2.5
	Time to Peak Angle/aperture	7	6	Low to medium	4.75	5
				High	4.25	4
Time to Target	0*	6	Low to medium	2.5	4	
			High	6.5	5	

Table 4.11 Mann Whitney U test result in reach-to-grasp task  
(Seven subjects without subject 2)

Metrics group	Metrics	U- Reach	U – Grasp	Group	Mean Rank- Reach	Mean Rank- Grasp
Velocity	Max Velocity	0*	0*	Low to medium	2	2
				High	5.5	5.5
	Mean Velocity	0*	0*	Low to medium	2	2
				High	5.5	5.5
Accuracy	Error	3	2	Low to medium	5	5.3
				High	3.25	3
Smoothness	Speed smoothness	1	4	Low to medium	2.3	4.7
				High	5.25	3.5
	Movement unit	4.5	5	Low to medium	4.5	4
				High	3.625	4
Maximal movement	Maximal aperture/angle	0*	0*	Low to medium	2	2
				High	5.5	5.5
Time	Reaction Time	5	3	Low to medium	4.3	2
				High	3.75	5.5
	Movement Time	3	6	Low to medium	5	4
				High	3.25	4
	Time to Peak Velocity	3	0*	Low to medium	5	6
				High	3.25	2.5
	Time to Peak Angle/aperture	5	6	Low to medium	4.3	4
				High	3.75	4
	Time to Target	0*	3	Low to medium	2	3
				High	5.5	4.75

To sum up, the movement performances in reach to grasp tasks generated insignificant models between the recovery scores and the kinematics metrics. The high function subjects showed the potential of larger maximal and mean velocity in both reach and grasp portion, larger maximal grasp aperture and reach angle, longer time to both reach and grasp target, smaller time to peak reach and grasp velocity with smaller error in both movements. They also had less smoothness unit and speed smoothness in grasp portion indicating smoother grasp movement and longer time to peak grasp aperture.

#### **4.4.3. Comparison of two movements in the only and combined movements**

We compared the reach/grasp movements in the reach/grasp only and reach-to-grasp movements to discover the possible differences among conditions. Based on the Mann Whitney U test result (Table 4.11 and Table 4.12), low function group showed smaller speed smoothness, larger movement unit and longer movement time; higher function group showed smaller mean velocity, smaller error, smaller speed smoothness and longer movement time in reach only tasks than in the reach-to-grasp tasks. Lower function group showed smaller mean velocity and higher function group showed smaller mean velocity, smaller error in grasp only task compared to reach-to-grasp tasks. We also performed the paired T-test for reach performance results between reach only and the reach-to-grasp tasks and for grasp performances between the two conditions (Table 4.15 and Table 4.16). With the Bonferroni correction of significant level for the 11 metrics, the significant level was set to  $p=0.05/11=0.0045$ . No significant difference was shown in the results of grasp tasks between two conditions. The mean velocity in reach tasks (Mean=0.0102degree/ms, SD=0.0048degree/ms) was smaller than in the reach portion of reach-to-grasp task (Mean=0.024degree/ms, SD=0.012degree/ms). The t-test showed the

significance beyond the 0.0045 level ( $t(7)=-4.52, p=0.003$ ). The speed smoothness in reach tasks (Mean $<0.001$ degree/ms, SD $<0.0001$ degree/ms) was smaller than in the reach-to-grasp task (Mean=0.18, SD=0.037) with a t-test significance ( $t(7)=-13.5, p<0.001$ ). The smoothness unit is significantly larger in reach only task (mean= 6.68, SD=2.07) than in the reach-to-grasp task (mean=3.09, SD=1.39) ( $t(7)=9.08, p<0.001$ ). The movement time is significantly larger in reach only task (mean=2.8s, SD=0.721s) than in reach-to-grasp task (mean=1.2s, SD=0.28s) ( $t(7) =7.47, p<0.001$ ). To sum up, we conclude that subjects tended to make slower and less smoothed reach movement with longer movement time in the reach only movement than reach-to-grasp movement. This is consistent with Lang who found higher peak velocities and smaller accuracy during the reach component of the reach-to-grasp movement compared to the reach alone [Lang et al, 2005]. The hand grasp movement doesn't differ significantly between in grasp only and in reach-to-grasp task in the low functioning group. Specifically, high function subjects had slower but more accurate movements in reach only and grasp only tasks than in the reach-to-grasp task. Low subject also showed the trend to have slower hand movement in grasp only than reach-to-grasp tasks.

Table 4.12 Mann Whitney U test result for reach movement in reach only and reach-to-grasp tasks

Metrics group	Metrics	U- Low	U - High	Group	Mean Rank low	mean Rank high	
Velocity	Max Velocity	8	4	Reach only	4.5	3.5	
				Reach to grasp	4.5	5.5	
	Mean Velocity	2	0	Reach only	3	2.5	
				Reach to grasp	6	6.5	
Accuracy	Error	2	0	Reach only	3	2.5	
				Reach to grasp	6	6.5	
Smoothness	Speed smoothness	0*	0	Reach only	2.5	2.5	
				Reach to grasp	6.5	6.5	
	Movement unit	0*	2	Reach only	6.5	6	
				Reach to grasp	2.5	3	
Maximal movement	Maximal aperture/angle	8	7	Reach only	4.5	4.25	
				Reach to grasp	4.5	4.75	
Time	Reaction Time	4	4	Reach only	5.5	5.5	
				Reach to grasp	3.5	3.5	
	Movement Time	0	0	Reach only	6.5	6.5	
				Reach to grasp	2.5	2.5	
	Time to Peak Velocity	8	2	Reach only	4.5	3	
				Reach to grasp	4.5	6	
	Time to Peak Angle/aperture	6	4	Reach only	4	3.5	
				Reach to grasp	5	5.5	
	Time to Target		5	7	Reach only	5.25	4.75
					Reach to grasp	3.75	4.25

Table 4.13 Mann Whitney U test result for grasp movement in grasp only and reach-to-grasp tasks

Metrics group	Metrics	U- Lo w	U – High	Group	Mean Rank- low	mea n Rank high
				Reach to grasp	3.75	3.5
	Mean Velocity	1*	0*	Reach only	2.75	2.5
				Reach to grasp	6.25	6.5
Accuracy	Error	4	1*	Reach only	3.5	2.75
				Reach to grasp	5.5	6.25
Smoothness	Speed smoothness	6	7	Reach only	4	4.25
				Reach to grasp	5	4.75
	Movement unit	7	8	Reach only	4.25	4.5
				Reach to grasp	4.75	4.5
Maximal movement	Maximal aperture/angle	7	5	Reach only	4.75	5.25
				Reach to grasp	4.25	3.75
Time	Reaction Time	4	7	Reach only	5.5	4.75
				Reach to grasp	3.5	4.25
	Movement Time	7	6	Reach only	4.75	5
				Reach to grasp	4.25	4
	Time to Peak Velocity	7	2	Reach only	4.25	6
				Reach to grasp	4.75	3
	Time to Peak Angle/aperture	6	6	Reach only	4	5
				Reach to grasp	5	4
	Time to Target	4	2	Reach only	3.5	6
				Reach to grasp	5.5	3

(Significant differences in U test are marked with (\*))

Table 4.14 Paired T test results between reach only and the reach portion in reach-to-grasp tasks

	P-value	Reach		Reach-to-grasp	
	Reach	Mean	Stdev	Mean	Stdev
Maximal velocity(degree/ms)	0.101	0.115	0.05	0.142	0.07
Mean velocity(degree/ms)	0.003*	0.01	0.005	0.024	0.012
Maximal angle(degree)	0.357	45.93	16.47	44.65	19.25
Speed smoothness	<0.001*	0	0	0.177	0.037
Smoothness unit	<0.001*	6.68	2.07	3.09	1.39
Accuracy	0.144	0.038	0.022	0.098	0.107
Time to peak velocity	0.3	0.227	0.083	0.263	0.07
Time to target	0.348	0.676	0.057	0.632	0.139
Reaction time	0.163	0.511	0.192	0.403	0.236
Movement time (s)	<0.001	2.79	0.721	1.21	0.28
Time to peak angle	0.41	0.903	0.024	0.918	0.03

*Significant level (p=0.0045)*

Table 4.15 Paired T test results between grasp only and the grasp portion in reach-to-grasp tasks

	p-value	Grasp		Reach-to-grasp	
	Grasp	Mean	Stdev	Mean	Stdev
maximal velocity (cm/ms)	0.068	0.012	0.007	0.011	0.007
mean velocity(cm/ms)	0.008*	0.002	0.001	0.011	0.007
maximal aperture (cm)	0.078	5.37	3.32	4.24	2.56
speed smoothness	0.622	0.204	0.036	0.222	0.077
smoothness unit	0.679	3.64	2.925	4.01	3.017
Accuracy	0.03	0.108	0.062	0.441	0.372
time to peak velocity	0.248	0.538	0.125	0.471	0.157
time to target	0.742	0.664	0.159	0.614	0.301
reaction time	0.68	0.05	0.055	0.037	0.058
movement time (s)	0.405	0.177	0.58	1.54	548.5
time to peak aperture	0.354	0.99	0.008	0.98	0.019

*Significant level (p=0.0045)*

#### 4.4.4. Coordination between reach and grasp movement

We studied the time to peak movement, time to peak velocity and time to target ratio between subjects (Figure 4.8). We found subject 4 had an extremely small time to target because of his limited hand grasp movement. Significant differences were found in time to peak velocity and time to target (Table 4.17). Low function subjects have lower time to peak velocity ratio and lower time to target ratio. Based on the subject's movement trajectories and velocity profile, we found that low function subjects obtained peak grasp velocity slower than reach peak velocity; while high function subjects obtained peak grasp velocity and peak reach velocity close in time. Low function subjects hit the reach target before the grasp target while the high function subjects hit both targets close in time. However, this time metrics didn't include the exact time information on how the subjects respond and coordinate between the two movements and how this coordination correlated with their recovery. In the future analysis, we will calculate the cross-correlation between the velocities of two movements to study the coordination.

Table 4.16 Mann-Whitney U test result of the time ratio metrics in the grasp movement

Metrics group	Metrics	U	Group	Mean Rank-Reach
Time ratio	Time to Peak velocity	0*	Low to medium	2
			High	5.5
	Time to Peak angle/aperture	1	Low to medium	2.33
			High	5.25
	Time to target	0*	Low to medium	2
			High	5.5

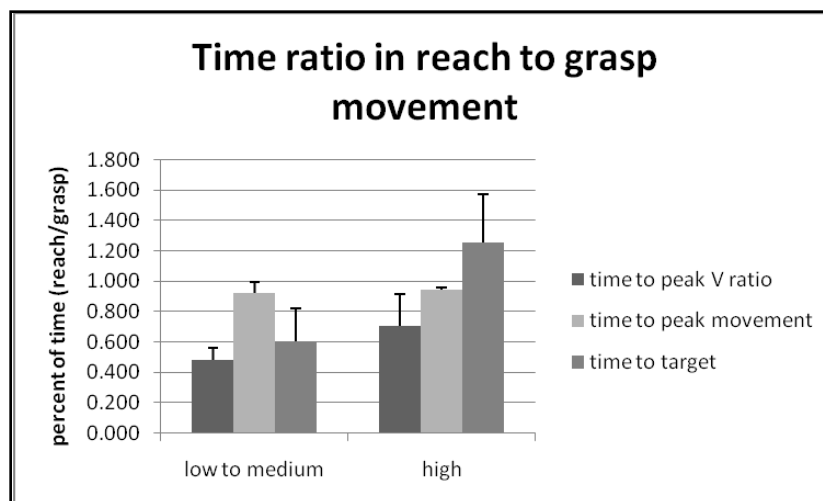


Figure 4.8 The time ration in reach to grasp movement.  
*(The time is calculated from time in reach movement divided by grasp movement. The first black bar represents the time to peak velocity ratio, the second grey bar represents the time to peak movement ratio and the third heavy grey bar represents the time to target ratio.)*

## 4.5. Discussion

### 4.5.1. Clinical assessment

The major prerequisites of successful rehabilitation are to understand the motor recovery mechanism, evaluate the recovery and develop the specific therapy strategies according to each individual's recovery. Our UE R/G system is developed to evaluate the stroke survivor's reach and grasp movements and shed some light on the relationship between reach, grasp and reach/grasp movement performance and recovery. We tested 12 stroke survivors with different functional levels and evaluated their movement performances with our UE R/G system. In doing so we discovered the key kinematic metrics that could be used to evaluate the spatial quality and timing of movements after

stroke. In addition these metrics may offer predictive insights into the recovery of reach, grasp and reach/grasp movements. Because stroke affects the patients in a more generalized manner, evaluating the recovery from one perspective is not sufficient. The recovery score generated with the PCA method calculated an overall score that could comprehensively evaluate their stroke recovery levels from their hand gross and fine motor function as well as elbow function. We observed (4.4-4.5) that of the 9 clinical measurements, the FT, NHPT, BBT, Grip, JTHT which evaluate the hand motor function, the elbow ROM which evaluates elbow impairment, and the FM which evaluates both the hand and elbow motor control were the major measurements contributing to our calculated recovery scores with FM being the most important one. Although the SIS and FIM are popular methods for recording the severity of patient disability, the results of medical rehabilitation and the impact on quality of life, they did not play a major role in the recovery score calculation since our subjects are long-time post-stroke and most have developed compensatory strategies.

#### **4.5.2. High and low function subjects performance differences**

Subjects were then divided into low and high function groups by the recovery scores and regression models were generated to evaluate how well derive kinematic metrics in each task type were able to predict the recovery scores. With our experiments results, we discovered significant differences between the low and high function subjects in terms of movement velocity, time, accuracy and smoothness metrics. The maximal velocity, mean velocity and maximal movement are the most sensitive metrics in all task types which are highly correlated with each other. Our results showed a significant larger mean and maximal velocity with high function subjects compared to the low subjects.

The decreased movement velocity after stroke and relative increase of movement velocity in the recovery were also found in other's studies in the reach movement (Kamper et al, 2002, Wing et al, 1990, Trombly et al, 1993).

The accuracy was another important metric which showed significant difference in the reach task and grasp tasks. High function subjects had smaller error resulting in higher accuracy. Increased movement errors were found in stroke survivors' reach movement (Beer et al 2000) and grasp movement (Lang et al, 2005, Nowark et al., 2007) compared to the normal subjects. However, no significant difference was show on accuracy in the U test of reach-to-grasp tasks. We think the differences between results from reach only or grasp only and reach-to-grasp tasks suggested the interlimb correlation of the stroke survivors played an important role in the reach-to-grasp tasks. It is important to develop a metrics in our future studies to characterize the coordination and the effect of the coordination on accuracy metrics. We also think the insignificance could partially due to our experiment design. Reach and grasp movement accuracy was calculated separately in the reach-to-grasp task. But in the experiment, visual feedback was given on both movements. When either the grasp or reach movement overshoot the target, the overshoot feedback would be given and implied the subject to return to home position without finishing the other part of movement. So the error for the reach portion or the grasp portion was affecting each other, which resulted in the insignificance in accuracy in reach-to-grasp movements. This was due to our experiment design and future investigation is needed to improve the accuracy evaluation metric in the reach-to-grasp tasks.

Maximal movement (reach angle and grasp aperture) showed significant

differences between the high and low function groups in both reach and grasp movements. This metric was directly correlated with the subject's movement abilities. Low function subjects tended to have little grasping ability, large spasticity and less control of movement and were only able to perform limited movements. Using the metrics was a direct and effective way to evaluate the stroke survivor's movement functions.

High function subjects have smaller time to peak velocity (between 10% to 20% of the movement time) in both the reach and grasp only tasks compared to the low function subjects (between 20% to 40%). A smaller time to peak velocity indicated more time spent in deceleration or a guided movement strategy was used [Chang et al, 2005]. Speed smoothness and smoothness unit were used to evaluate the stroke survivor's movement smoothness. More smoothness units indicated less smoothed movement, which was found in low functioning subjects' reach movements in the literatures (Kamper et al 2002). More severe strokes tend to have a series of shot, episodic sub-movement with the velocity profile composing of several peaks with deep valleys in between, representing the stops between sub-movements. Hence, their speed smoothness would be relatively higher than the low function subject, whose maximal velocity would be much larger than the mean velocity, resulting in smaller speed smoothness. However, in our experiment, we only analyzed one single sub-movement; this metric was not significant enough to differentiate between groups. In our reach U test and PCA results, both smoothness unit and speed smoothness didn't show any significant differences or were strongly correlated to the recovery results. We discovered the sensor artifacts affected the smoothness from the movement trajectories. With the sensor resolution 1.4

degrees, the variation in the reach velocity might be caused by the sensor fluctuation. Despite this the PCA analysis indicated that the speed smoothness and smoothness unit did played major roles in calculating the recovery level in the regression model of grasp movement, indicating their potential to be predictive of recovery.

The time to target metric was significant different across low and high functioning subjects in reach and grasp tasks. Lower function group showed smaller time to target (generally between 55% to 70%), while higher function group had larger time to target (generally between 65% to 80%). This might due to the fact that the high function subjects had a larger target distance or smaller target to grasp. Unexpectedly movement time did not play a strong role in differentiating across subjects. Typically, low functioning subjects move slower and take more time to complete tasks [Kamper et al 2002, Wing et la, 1990]. We think this is mainly due to the task design limitations. Since our target was displayed on the screen for a fixed time (4 seconds). When the target disappeared, the subjects moved their elbow back to the original position. Therefore, for the low functioning subject, even when they didn't reach their target, they would make the second sub movement – move back to the original condition once the target disappeared. In the future the subjects should be allowed to complete task at their own pace. Reaction time in the grasp movements also did not support the literature, which suggested that reaction times should be longer for lower functioning subjects. As explained in the grasp task results, we think the bend sensor resolution caused the insensitivity of the reaction time which made it an inappropriate metric for evaluating the grasp movement performances (fig 4.7).

In the reach-to-grasp tasks, significant differences were shown in time to peak

velocity and time to target ratio. Low function subjects showed higher percentage of time to peak grasp velocity. This indicated that lower functioning subject hit the reach target earlier than grasp target. Low function subject with significantly lower percent of time to peak velocity ratio and lower percent time to target ratio indicated that they obtained peak grasp velocity later than peak reach velocity and hit the grasp target later than the reach target. No difference was shown in time to peak aperture. This was consistent with Lang's study that they found the temporal coordination of reaching and grasping components, where peak aperture occurs near the time of peak arm deceleration, is relatively stable in healthy control subjects [Lang et al, 2005]. And this supported the idea that the coupling of reach and grasp component in a reach to grasp movement (quantified by the time of peak aperture) is reasonably preserved in people with different impairment [Michaelsen et al, 2004]. It is possible that the lower percent of time to peak velocity and time to target ratio could be explained as evidence of a breakdown in the central planning of the reach-to-grasp movements. The other metrics which didn't display significant differences were less sensitive with our system and might due to the system limitation and the small sample size.

#### **4.5.3. Evaluation of movements and kinematic**

The one major contribution of our study is providing another way to evaluate the recovery from the movement perspective and validating the evaluation method with the recovery models between the recovery score and the kinematic metrics. Although with our small sample size, some of the recovery models were not statistically powerful, the models and the U test results could provide us with some directions in our future studies when evaluating the stroke survivor's movement recovery. The recovery is positively

related to the mean velocity, maximal velocity, maximal reach angle, time to peak angle, time to target and negatively correlated with error and time to peak velocity in reach task. The fact that the regression model was significant indicates that a linear combination of these metrics have predictive value for recovery level and could account for up to 74 % of the variance in function levels seen across stroke survivors performing this task. In grasp tasks, recovery is positively correlated to the maximal and mean velocity, maximal grasp aperture, time to target and negatively correlated with smoothness unit, error and time to peak velocity in grasp task. The regression model was significant indicating that the a linear combination of these metrics does have predictive value for recovery and could account for up to 72.4% of the variance in function levels seen across stroke survivors performing this task. In the reach-to-grasp task, the recovery levels are positively correlated to the maximal and mean reach and grasp velocity, maximal aperture and angle, time to peak aperture, time to grasp and reach target, and negatively correlated with reach error and grasp error, speed smoothness and smoothness unit in the grasp task, time to peak grasp and reach velocity. The regression model for coordinated reach and coordinated grasp was not significant indicating that a linear combination of these metrics did not have predictive value for recovery and could account for only 48.7% for grasp portion and 52.4% for reach portion of the variance in function levels seen across stroke survivors performing this coordinated task. This suggests that other factors are influencing the reach and grasp performance when they are coupled. One factor could be cognitive load imposed on the dual task of reaching and grasping versus the single task of reach or grasp. Another factor could impair interlimb coordination with difficulty coordinating elbow and hand opening and closing. The third factor could be

experimental design, in that positive feedback was given to the subject only if they performed the coordinated movement and the visual feedback given was a bit more complex. These issues could have contributed the insignificance of the model and the incoordination seen. Further studies are needed to tease out the key kinematic variables for the combined reach to grasp movement.

With the knowledge of relationship between recovery and kinematic metrics, a key question in developing the rehabilitation strategies is to identify which motor recovery metrics might be most helpful. The high and low function subjects might have different responses to the same training and increase their performances in different aspects. Evaluating the movement with these metrics could help to identify the subject's movement and differentiate between low and high function group. It also helps to record the subject's performance during the therapy process to monitor the rate of the improvement overtime and modify the strategies that fits each individual. The regression model gives us some insight into how to monitor the subject's recovery in terms of their movement. It provides a way to compare the recovery between individuals. However, attention should be paid to each metric. Subjects might recover following difference paths, i.e. they might increase the velocity in the beginning process with increased error. Therapist needs to have a clear idea of the variety of movement pathways that will be appropriate for the selected activity that needs to be able to precisely monitor the progress of relearning process [Colombo et al, 2007]. But overall, the recovery model provides a general method to evaluate the subject's recovery from kinematic process and it can be used to record the differences between subjects. The study of learning rate in difference motor recovery components should be useful in detecting possible temporal hierarchies

or delays between components in the course of recovery that may play an important role in defining optimal rehabilitation strategies. Future studies are needed to provide additional support for the relationships we detected between performances and the recovery.

#### **4.6. Conclusion and future directions**

Despite the fact that our small sample size caused us to use non-parametric statistics, we were able to establish differences on key kinematic metrics and determine significant regression models governing the relationship between motor performance on reach and grasp tasks using the UE R/G system and clinical scores. The study described in this thesis supports the UE R/G system's ability to measure the upper extremity movement performance in reach and grasp tasks after stroke. Low functions subjects generally showed decrease movement velocity, movement angle/aperture, decreased accuracy, increased time to peak velocity and decreased time to target in reach, grasp and reach-to-grasp tasks. We also created the regression models to evaluate the recovery with a series of significant metrics. These metrics and model could be used in the future studies in recording and evaluating the recovery, differentiating between low and high function subjects and helping the therapist to design the optimized rehabilitation plans for the recovery.

## Chapter 5

Insights into brain activation patterns after reach and grasp tasks: A case series

## **5. UE R/G system usability testing inside MR environment with insights into brain activation patterns after reach and grasp tasks: A case series**

### **5.1. Overview**

To accomplish our long-term goal of examining subjects' brain patterns pre and post robot-assisted therapy practice of ADLs, we must design an appropriate experiment that allows the UE R/G system to be used in the MR environment by stroke survivors for reach, grasp or reach/grasp movements. Our immediate goal is to prove that our UE R/G system is usable by subjects in the MR environments and we are able to elicit appropriate brain activation patterns with our experiment. If the motor performance with the device is stable and the movements elicit reasonable brain activations without large head movements ( $<2\text{mm}$  per translation axis), then we will be confident that our system would be able to detect changes in activation patterns pre and post therapy. In this chapter, we reviewed fMRI, the motor task often used in the MR environment and the brain activation patterns along with reorganization patterns often seen and we discuss in detail the experimental set-up used in the scanning environment. We reported on a series of fMRI case studies with subjects performing the reach and grasp movement with the UE R/G system in the MR Scanner. We compared the motor performance results in the scanner to the result from chapter 4 to prove that our system was able to capture the movements in the MR environment and compare the preliminary results from normal and stroke impaired brain activations with the literature to determine how well we were able to elicit and evaluate brain activation patterns.

## 5.2. Background

Functional Magnetic Resonance Imaging (fMRI) plays an important role in studying the brain reorganization of stroke recovery. fMRI studies have been performed with acute stroke subjects, subjects in the recovery process, and chronic stroke subjects who have reached their recovery plateau. With both able-bodied and stroke survivors, upper extremity motor tasks have been studied extensively with or without fMRI compatible measuring/controlling devices. Finger tapping [Small et al, 2002, Dong et al, 2007, Szaflarski et al, 2006, Nair et al, 2005], finger tracking [Carey et al, 2002, Kimberly et al, 2004], wrist flexion/extension [Small et al, 2002, Loubinoux et al, 2003, Ward et al, 2006, Dechaumont-Palacin et al, 2007], hand gripping [Takahashi et al, 2008], hand opening and closing [Feydy et al, 2001, Kim, et al, 2004, Kwon, et al, 2007, Johansen-berg et al, 2002, Stinear, et al, 2006], elbow flexion/extension [Feydy et al 2001, Newton et al, 2002], shoulder flexion/extension [Feydy et al, 2001, Luft et al, 2004], and forearm supination/pronation [Takahashi et al, 2008] movement have been studied.

As a result of these tasks, brain activations have been seen in sensorimotor areas, cerebellum, thalamus, and basal ganglia. Based on the literature [Small et al, 2002, Levy et al, 2001, Carey et al, 2002, Ward et al, 2003, Fujii et al, 2003, Newton et al, 2002, Nari et al, 2005, Marshall et al, 2000], the following eight regions are typically activated: 1). Primary motor area (M1). It works in association with pre-motor areas to plan and execute movements. 2). Primary somatosensory area (S1). It receives sensory information from thalamic nerve projections. 3). Pre-motor area (PMA). It mainly participates in the initiation of skilled and delicate voluntary movements. 4). Supplementary Motor Area (SMA). It plays an important role in the programming of patterns and sequences of

movements. It is also implicated in the planning of motor actions and bimanual control [Carey et al, 2002]. 5). Dorsal prefrontal area. It is implicated in planning complex cognitive behaviors, personality expression, decision making and moderating correct social behavior. 6). The anterior cingulate motor area. It is involved in error and conflict detection processes such as go/no-go tasks; 7). Cerebellum. It plays an important role in the integration of sensory perception, coordination and motor control. Locations of these areas were presented in Appendix G. Other areas such as superior parietal cortex, inferior parietal cortex are also been shown to be involved with the motor movement.

Although brain activations have been mainly found in the brain areas listed above, the pattern of activation may differ. For example, healthy normal subjects and stroke survivors have different activation patterns. Stroke survivors' brain activation has been shown to change after therapy. The brain activation patterns, the activation volume as well as the intensity of activation are typically studied. As we described in chapter 2, the common thought is that brain recovery is based on the cerebral plasticity and reflected in brain reorganization. By comparing the activation pattern resulting from before and after an intervention, brain reorganization for stroke recovery has been attributed to the following: the peri-lesion neurons are activated after the reorganization; activation sites will be shifted to contralateral hemisphere with the reorganization process; and activations in some secondary motor areas are increased.

***Peri-lesional activation:*** Functional MRI and PET studies showed the increased activation around the lesion. This is possibly due to the axon sprouting [Kandle et al, 2000], decrease of the inhibition [Mountcastle et al, 1968] or recruitment of corticospinal tract from the alternative motor representation sites [Kwon et al, 07]. In Kwon's(07)

study, three subjects with cortex infarct showed activation in the peri-lesional area, supporting the notion that patient with cortical infarct may recover by means of peri-lesional re-organization [Kwon et al, 07]. Levy (02) also found the increased activation around the lesion area after 2 weeks constraint induced movement therapy [Levy, 02].

***Contralateral vs. ipsilateral activation:*** Voluntary movement is controlled by the corticospinal tract pathway. In the adults, 95% of the corticospinal tract are crossed, while only 5% are non-crossed [Kandle et al, 2000]. When the infarct in the corticospinal tract is disturbed from its normal function, the non-crossed pathway might be recruited to compensate for the damage of the crossed pathway [Cao, 1998]. This could partially explain the activation in the ipsilateral side. Several research studies have found the bilateral activation in the stroke survivors [Levy, 2002, Cao, 1998, Marshall, 2000]; and many of them have noticed that better recovery relates to more contralateral activation in motor areas such as M1, S1, in the cross-section study as well as in the longitudinal studies [Marshall et al, 2000, Feydy et al, 2002, Jang et al, 2007, Fuji et al, 2003, Ward et al, 2006, Nair et al, 2006, Carey et al, 2002]. On the contrary, more ipsilateral hemisphere activation is related to the poor recovery [Loubinoux et al, 2003]. Subjects with better recovery tend to have more focused activation patterns similar to the normal [Ward et al, 2003b].

***Secondary areas activation:*** When the neurons are damaged in the primary areas because of the infarct, the originally silent neurons in the secondary motor areas will be activated and compensate for the damage in the primary areas. Johansen-Berg found the therapy-related improvements in hand function correlated with increases in fMRI activity in the secondary somatosensory cortex contralateral to the affected hand [Johansen-Berg

et al, 2002]. The early recruitment and high activation of SMA and inferior Brodmann area 40 is correlated with faster and better recovery [Loubinoux et al, 2003]. Fujii also demonstrated that a high degree of connectivity between bilateral SMA activation was related to good recovery [Fujii et al, 2003]. Palacin proposed that increased contralesional activity in secondary sensorimotor areas likely facilitated control of recovered motor function by simple proprioceptive integration in the patient with poor recovery [Dechaumont-Palacin et al, 2008].

Most of these findings were discussed in terms of key metrics used to quantify the brain activations between individual subjects. These are the laterality index (LI), geometric center of the activation site, and the activation intensity. The Laterality Index (LI) is most often used. Defined in 1997 by Cramer and his colleagues, the index was first used to assess the ipsilateral over-activations in the first fMRI studies to assess cerebral reorganization in stroke patients. The LI is calculated as the differences between contralateral and ipsilateral hemisphere SM1 activation volumes divided by their sums.

$$LI = \frac{V_{\text{contralateral}} - V_{\text{ipsilateral}}}{V_{\text{contralateral}} + V_{\text{ipsilateral}}} \quad \text{Eq. 5.1}$$

LI ranges from +1 (exclusively contralateral) to -1(exclusively ipsilateral). A number of studies have found more ipsilateral activation of the SM1 in the poor recovered subjects [Luft et al, 2004, Jang et al, 2003, Scahechter et al, 2002, Ward et al, 2006]. Associated with LI, the voxel count or volume of activations are calculated and may be reported individually to reflect the reorganization. The activation site (geometric center of activation) is another important parameter to quantify the activation patterns [Dong et al, 2007, Pineiro et al, 2001, Szaflarski et al, 2006, Dechaumont-palacin et al, 2007]. The activation intensity is the third parameters used to quantify the reorganization

[Bhatt et al, 2007, Loubinoux et al, 2003, Kimberly et al, 2004, Hamzel et al, 2006], Percent signal changes are reported as the fMRI signal changes in the regions of interest [Dong et al, 2007]. With the application of these metrics, we can quantitatively evaluate the brain reorganization from the activation maps.

In addition to these brain-related metrics, motor performance inside the scanner is often analyzed. The motor performances such as reaction time, movement amplitude could be used to evaluate each response to a stimulus and to modulate the BOLD response amplitude. This motor performance could be used as regressors to study the brain activations which might vary proportionally to this Auxiliary Behavioral Information (ABI).

### **5.2.1. Study goals**

To demonstrate our ability to measure the motor performances in the fMRI scanner and to identify the movement related brain activation patterns, we recruited 5 subjects into the fMRI case series. They performed the reach and/or grasp movement with our MR-conditional UE R/G system in the 3.0T MR scanner. We examine the results to determine whether the following statements can be supported: 1) Stroke survivors will show the similar motor performance as demonstrated by movement trajectory and velocity; 2) We are able to identify the brain activation patterns from our system and experiment set up; 3) We will uncover confounding variables and issues that would influence the external and internal validity of future experiments, such as head movement, mirror movement and task design issues. Findings will allow us to finalize procedures for an impending study investigating changes in activations after RAT with ADLER.

## 5.3. Method

### 5.3.1. Subjects

Five subjects were recruited for the fMRI case series. Two of them were age controlled normal subjects (mean age: 64.5yr, SD: 0.7yr) including 1 male and 1 female, and three of them are stroke survivors (mean age: 55.3yr, SD: 4.5yr) including 2 male and 1 female. All of them were recruited from the local community or stroke center. One of these subjects was recruited from the previous experiment: subject 4 in fMRI study is also subject 2 in the correlation study. And her data was used to compare inside and outside movement performance. All the subjects signed the written consent form proved by Institutional Review Board of Medical College of Wisconsin and agreed to comply with the whole protocol. The inclusion and exclusion criterion of subjects were presented in Appendix H. Table 5.1 described the basic information on all the subjects. The three stroke survivors' lesion images were shown in figure 5.1. Subject 3 and 4 had ischemic stroke while subject 5 had a hemorrhagic stroke. Subject 3 had a wide lesion site on the motor cortex of right hemisphere including inferior frontal gyrus, Supramarginal gyrus, precentral gyrus, postcentral gyrus, Rolandic operculum, angular gyrus, SMA, Precuneus, middle cingulate cortex and insular lobe. Subject 4 have a lesion site on left hemisphere of motor cortex including inferior frontal gyrus, precentral gyrus, postcentral gyrus, Supramarginal gyrus, inferior parietal lobule and caudate nucleus. Subject 5 had a relative cortical lesion site on the left hemisphere including superior temporal gyrus, insula lobe and Rolandic operculum.

Table 5.1 Subject information

Subject #	Gender	Age	Time stroke post	Affected side	Dominant hand	Tested side	GDS	FMA
1 (normal)	F	65			R	R		
2 (normal)	M	64			R	R		
3s	M	51	7 years	L	R	L	3	27/66
4s	F	55	12 years	R	R	R	4	48/66
5s	M	60	1.5 years	R	R	R	0	N/A

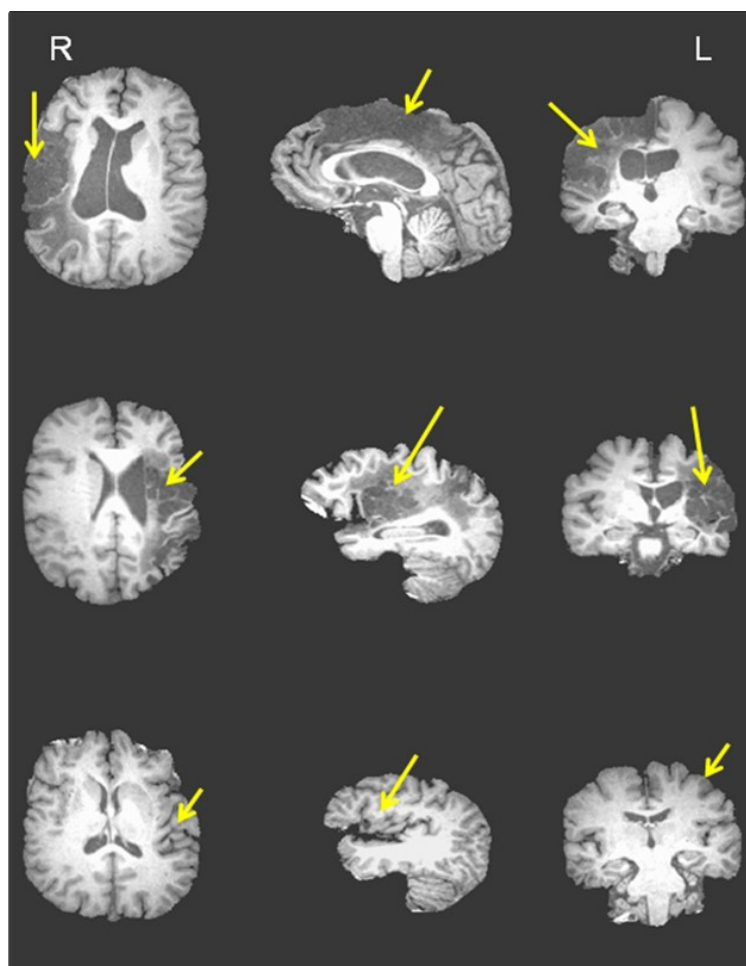


Figure 5.1 Lesion imaging for three stroke survivors  
*(From top to down, subject 3, subject 4 and subject 5. From left to right, T2-weighted MR image from axial view, sagittal view and coronal view. The yellow arrows mark the lesion location. Left side of the page is the right hemisphere.)*

### **5.3.2. Experiment procedure**

After consenting, the subject first received the medical evaluation including the basic diagnosis (stroke type, location, date of stroke and previous medical history), the symptomology (upper limb spasticity and muscle over-activity), the modified Ashworth scale [Bohannon et al, 1987] and the manual muscle test [Mendell, 1990] from a medical doctor. Then subject were invited to the mock scanner, located at the Pavilion building of Froedtert Hospital (Milwaukee, WI), which was an environment simulating the real scanner with the scanner bed, the head coil and the projectors. The subjects lay supine on the scanner bed, with their head inside the simulated head coil. A back projection board was placed at the end of the scanner bed where the tasks and instructions were projected. They could see the information on the board from the mirror over their eyes. Subject wore the UE R/G system on their affected arm/hand and practiced all the tasks as they would perform in the real scan until they were comfortable and familiar with the tasks. The purpose of mock scanning was to get the subject familiar with the scanning environment as well as the scanning procedures. On day 2, subjects were invited into the 3.0 Tesla GE MRI scanner located at the pavilion building, Froedtert hospital (Milwaukee, WI). Subjects received the real scans for 2-2.5 hours.



Figure 5.2 Snapshot of experiment set up in the scanner  
*(In the figure, Subject lay on the bed with the orthosis and glove on his/her dominant/impaired side.)*

### 5.3.3. Experiment set up

The orthosis and glove were placed on the affected hand/dominant hand of the subject prior to the subject being placed in the scanning environment. The subject lay on the scanner bed with their head inside the single channel Quadrature head coil. Inflated Pillows was placed underneath the head and a paper tape was used across the forehead from left to right to keep head stable. Velcro straps were used across the chest, hip and knee to reduce the body movement. Plastic foam was placed underneath the knee for comfort. Only the subject's hand and arm were able to move. Subject was able to see the screen via the reflected mirror on top of their eyes. Figure 5.3 demonstrated the set up in the scanner. From the device point of view, the orthosis and glove sensors cable were connected to the panel between the control room and the scanner room. All the other devices including the computers, the circuits and cables were connected at the control room. The host PC was connected to the time trigger synchronized with the scanner via a parallel port. Details of the connection were described in chapter 3.

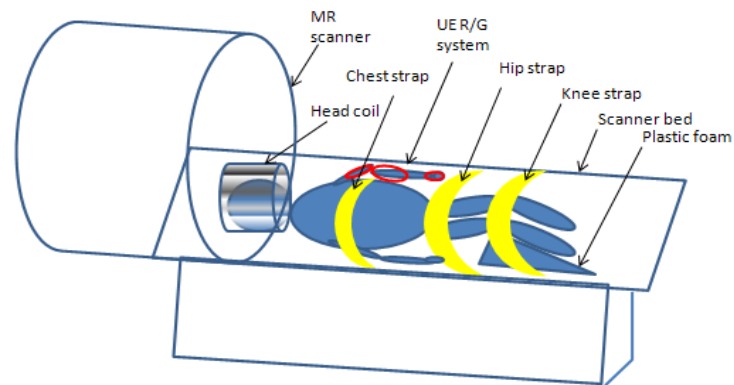


Figure 5.3 Snapshot and Diagram of experiment set up in the MR scanner.

*(The upper picture is a snapshot and the lower picture is the diagram of the experiment set up in the scanner, subject lay on the scanner bed with the UE R/G system on, impaired/non-dominant side. Straps are used on chest, hip and knee to stabilize the subject.)*

#### 5.3.4. Data acquisition

The data acquisition during the fMRI scan was divided into two parts: the movement data acquisition and the image data acquisition.

##### 5.3.4.1. Movement data acquisition

Before the subject entered the scanner room, they performed the calibration tasks in the control room to define the target information for the tasks with the details described in chapter 3. For the reach task, considering the size of the screen shown to the subject, it was hard to see the target if it was displayed at the bottom of the picture and might cause additional head movement. In this case, we kept the reach target at the center of the screen (target distance =40) and amplified the stroke subject's movement angle by the appropriate gain. The gain of movement is calculated from the following equation 5.2:

$$Gain = \frac{40}{(0.81 \text{ maximal movement angle in calibration tasks})} \quad \text{Eq. 5.2}$$

Maximal movement angle was calculated from the calibration tasks. During the scanning, the onset of the first tasks is synchronized with the start of scanner via the time trigger. The time trigger is set as period =99ms, duration =4 seconds. Each task occurred at the 4 second intervals. The movement information such as movement angle/aperture, task onset/offset time, trigger onset time, task number are saved in MATLAB.

#### 5.3.4.2. Image data acquisition

The fMRI scan contains several components: the Spoiled Gradient Recalled (SPGR) scan; localization scan, event-related tasks, resting state scan as well as Diffusion Tensor Imaging (DTI) scan. We performed the SPGR scan from sagittal axis with TE=3.9s, TI (prep) =450, TR=9.5s; Flip angle =12°, NEX=1; FOV = 240mm; Matrix =256\*224 and slice number = 144. Localization scans are the block designed task to move hand or elbow with 20 s in each block. Word instructions were projected on the screen. Table 5.2 illustrates the types of scans performed during the experiment. The

localization task scans, resting state scans and DTI scans were performed in our study, but not analyzed in this thesis.

Table 5.2 fMRI scan type and time

Scan name		Type	Time (min, sec)	Purpose
Anatomic scan		SPGR	8 ‘	To obtain the brain anatomic image
Localization*		EPI	7 ‘ 12”	To obtain the general activation pattern of each movement on both hands
Tasks	Reach	EPI	10’ 40’ each	To obtain to brain activation for the affected hand movement
	Grasp			
	Reach to grasp			
Resting state*		EPI	6’	To provide the baseline information for DTI analysis
DTI*		DTI	Three scans, 4’ each,	To obtain the fiber tracking information

The event-related task scan was a 10 minutes 40 seconds echo planner imaging (EPI) scan with TE=25ms, TR=2000ms, Flip angle=77, NEX=1, FOV = 240mm, matrix=64\*64; thickness =4.0mm, Gap =0mm, and slice number =36. Reach tasks, grasp tasks, and reach to grasp task were performed with the inter-stimulus-interval task design. The details of the tasks were described in chapter 3. Resting state EPI scan was a 6 minutes scan with the same settings as tasks scans to obtain the baseline and seed for the DTI scans. Three DTI scans were performed. Each DTI scan is 4 minutes with TE=84.4 ms/min, TR=11000ms, NEX=1, FOV=240mm, matrix =128\*128, the number of slice =38. The scan was performed in axial plane. The order of the scans might be disturbed due to the scan time limit or the device problems. Additional tasks scans were made if obvious time synchronization problem or UE R/G system problems were found during scanning.

### 5.3.5. Data analysis

Both the image and performance data were processed offline. The image data was processed with AFNI (Analysis of Functional NeuroImaging, NIH). The movement performance data processing method was the same as described in chapter 4.

#### 5.3.5.1. Performance data analysis

One subject performed the experiments in two conditions: inside and outside the scan. In order to demonstrate our ability to collect movement performance data in the scanner, we used the same method in Chapter 4 to calculate the movement data: maximal velocity, mean velocity, maximal movement angle/aperture, speed smoothness, smoothness unit, accuracy, time to peak velocity, time to target, time to maximal movement, movement time and reaction time. The movement trajectories and velocities were reconstructed and compared between inside and outside the scan conditions. Correlation coefficient was calculated between the results from two conditions.

#### 5.3.5.2. Image data analysis

The images were first pre-processed to delete the first five time series of each dataset considering the magnetic field inhomogeneity at the beginning of each scan. Volume registration was performed to generate the motion parameters of head movement in six degrees of freedom which would be used as the regressor in the General Linear Model (GLM) when calculating the activations. The EPI data was aligned to the SPGR scans in most cases except when larger lesion exists which will cause bad alignment

results. “3dDeconvolve” was used to calculate the activations from the GLM method. For the event related task design, the ideal hemodynamic response function (HRF) was defined by using the “TENT” function from the task sequence. We defined the hemodynamic response time to be 14 seconds and used 8 basis functions to form the HRF. The result of “3dDeconvolve” created a dataset with the F-statistic describing the significance of how much a model component reduced the variance of data time series residual; a t-statistic describing the impact of one coefficient and the coefficient  $\beta$  describing the response amplitude. The coefficient was chosen as the activation criterion. A threshold was visually inspected and chosen on the activation maps to make the meaningful activation results. The voxels with a coefficient larger than the threshold were defined as the active voxels. All the rest voxels were defined as the inactive voxels and were masked out. Then we used the family wise error detection method with “AlphaSim” program to calculate the overall scientific significance level. By selecting the corresponding t-value threshold, voxels that were not in the clusters were considered inactivate and masked out in the next steps. Only the activated voxels within clusters were reserved. Experience ROIs were created based on the literature in the following areas: M1, S1, SMA+PMA, dorsal prefrontal area, cingulate motor areas, superior parietal cortex, inferior parietal cortex and cerebellum. ROIs could also be generated from the functional dataset results from the activation results. The volume of activation could be calculated in each ROI and the laterality Index (LI) could be calculated with equation 5.1. LI has the range from -1 to 1. -1 represents all the activation were on the ipsilateral hemisphere, while +1 means all the activation were on the contralateral hemisphere. The smaller the LI, the activation sites were shifted more to the ipsilateral

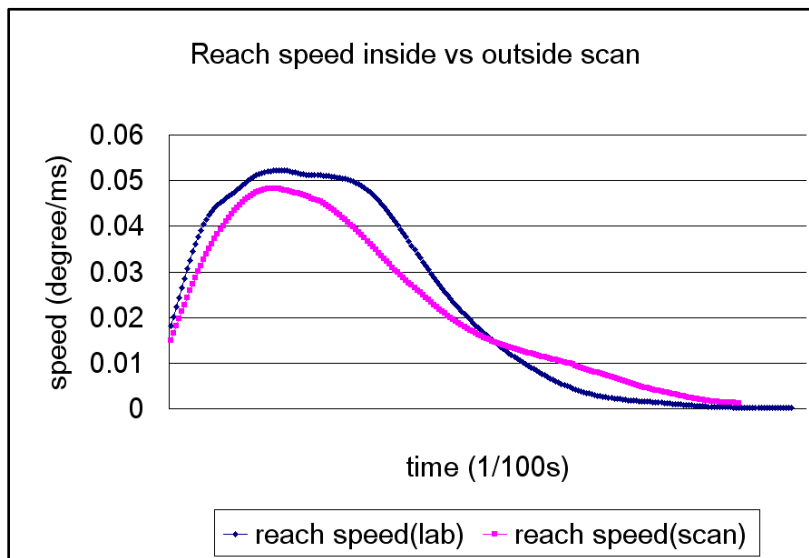
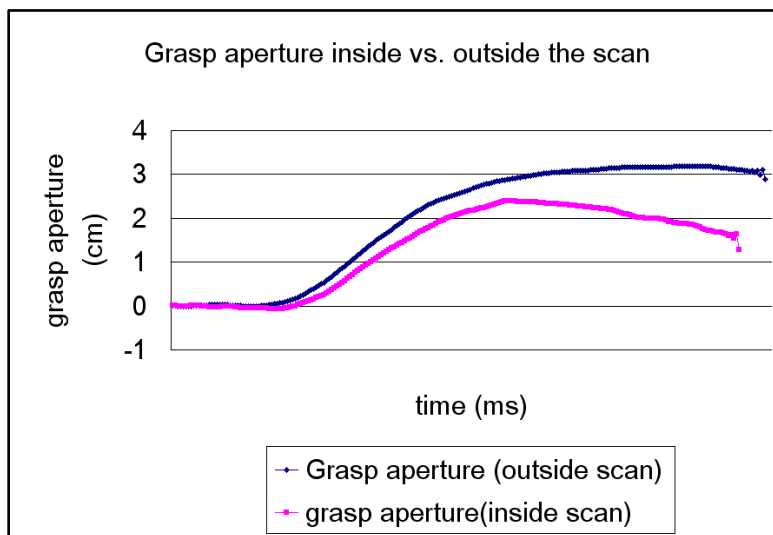
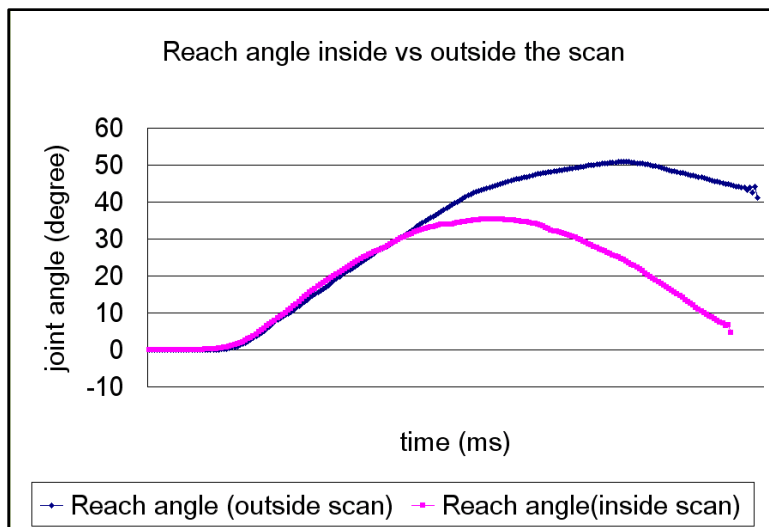
hemisphere.

## **5.4. Results**

We report our results from two sides: movement performance and brain activation patterns. A stroke survivor performed the same tasks in the scanner and in the study described in chapter 4. We compared her results from movement trajectories and velocities. In the second section, we demonstrated our preliminary findings on the brain activation.

### **5.4.1. Movement performance**

Reach, grasp and reach to grasp movement were performed by the same subject both inside and outside the scanner. Movement performances results were presented in Appendix I. From the movement trajectories and velocity trajectories (figure 5.4), we noticed no obvious differences between the conditions inside and outside of the scanner. The movements between two conditions showed similar trends and patterns which support our hypothesis that the device could measure the performance both in the scanner. The cross-correlation results between the signals inside and outside the scans for both reach and grasp movement trajectories and velocity showed high correlation coefficients with significant p-values (Table 5.3) indicating the medium to strong correlations. Therefore, we concluded that our system was able to capture the movement performance with the fMRI scans. Differences in the signal magnitudes and peaks suggested differences in movement but these differences did not detract from performance of the task.



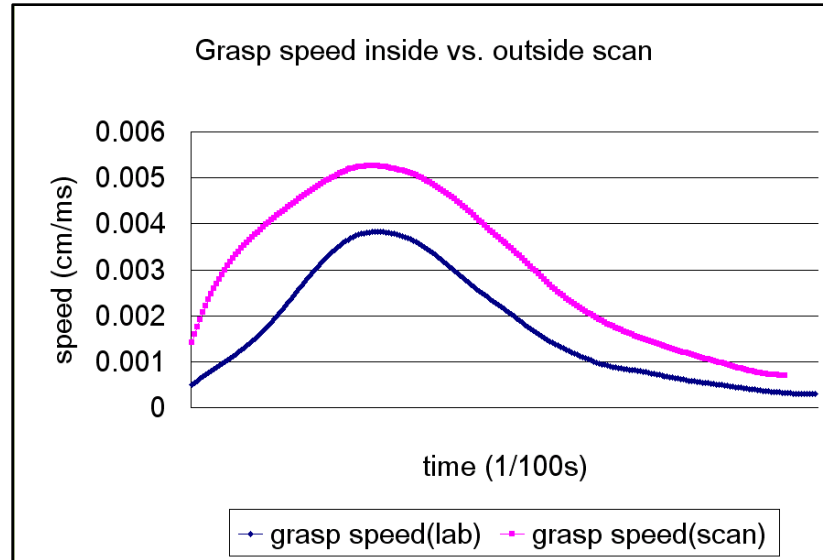


Figure 5.4 Comparisons of movement trajectory and velocity in grasp and reach movement inside and outside of the scanner.

(X axes represent the time, Y axes represent the grasp aperture and reach angle in the movement trajectories figures and hand grasp velocity and elbow reach velocity in the velocity figures. The red lines represents movement inside the scan and the green lines represents movement outside the scan.)

Table 5.3 The cross-correlation results of single inside vs. outside the scan.

	Grasp Aperture	Grasp Velocity	Reach Angle	Reach velocity
Correlation coefficient	0.97	0.96	0.73	0.99
P-value	<0.01	<0.01	<0.01	<0.01

## 5.4.2. Brain Activation

### 5.4.2.1. Model fitting

The brain activation was evaluated from two aspects: 1). To identify the ideal

hemodynamic response function with good fit in the proposed activation areas and bad fit in the non-activation areas. Figure 5.5 demonstrates the model fits. Good fits were found in the precentral gyrus in the upper figure. In the ipsilateral parahippocampal gyrus where no activations were expected, the model fitting were poor (lower figure).

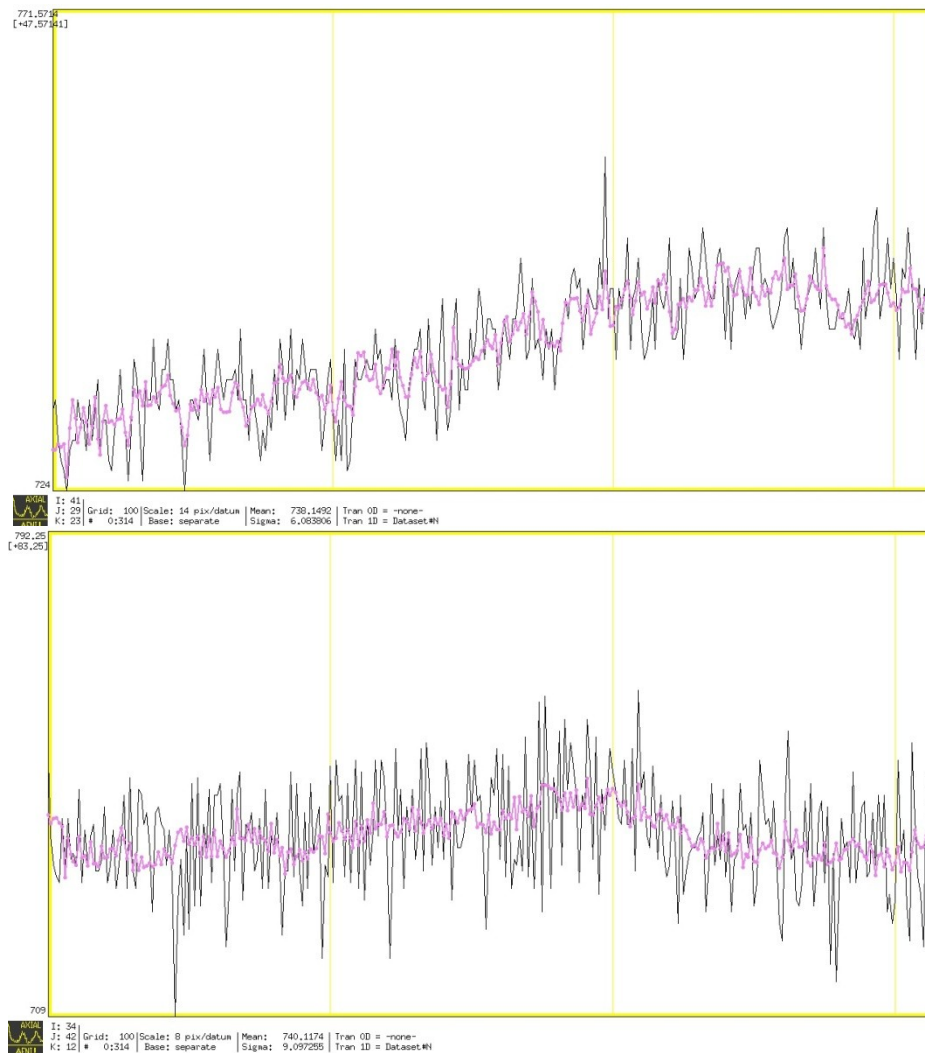


Figure 5.5 Model fit of reach-to-grasp movement  
*a) contralateral precentral gyrus; b) ipsilateral Parahippocampal gyrus. The black line represents the time series, the purple dot-lines represents the ideal hemodynamic response function generated from the TENT function.*

#### 5.4.2.2. Brain activation patterns

Brain activations were analyzed for each subject for reach, grasp and reach-to-grasp tasks. We present the examples for each type of our results for a normal and stroke subjects (figure 5.6). Specifically, in the grasp task (figure 5.6a), normal subject showed activation in precentral and postcentral gyrus of both hemispheres, SMA, inferior and superior occipital gyrus, middle temporal gyrus, superior parietal lobule, inferior parietal lobule of both hemispheres, contralateral Supramarginal gyrus, contralateral thalamus, contralateral inferior temporal gyrus and both cerebellum and cerebellar vermis. The stroke subject 4 showed activation in precentral and postcentral gyrus, SMA, superior and middle frontal gyrus, middle cingulate cortex, calcarine gyrus, lingual gyrus, fusiform gyrus, superior parietal lobule, inferior parietal lobule and middle temporal gyrus in both hemispheres. We also found activation in inferior frontal operculum, rolandic operculum, superior occipital gyrus, supramarginal gyrus and thalamus in the ipsilateral hemisphere and superior medial gyrus, middle occipital gyrus and inferior temporal gyrus in the contralateral hemisphere.

In the reach tasks (figure 5.6b), the normal subject 2 showed strong contralateral activations in superior parietal lobule and bilateral activations in precentral gyrus, SMA, middle cingulate cortex, postcentral gyrus, inferior parietal lobule, Paracentral gyrus, superior temporal gyrus, middle temporal gyrus, inferior temporal gyrus and CRB. The stroke subjects displayed ipsilateral activations in middle frontal gyrus, middle orbital gyrus, inferior frontal operculum, inferior frontal triangularis, Rolandic operculum, insula lobe, Calcarine gyrus, inferior parietal lobe and superior temporal gyrus. She also showed bilateral activation in precentral gyrus, superior frontal gyrus, SMA (more contralateral), middle cingulate cortex, lingual gyrus, fusiform gyrus (more ipsilateral), postcentral (more

ipsilateral), precuneus (more ipsilateral) and middle temporal gyrus (more ipsilateral).

In the reach to grasp tasks (figure 5.6c), we discovered the strong activation in contralateral primary motor areas, specifically in precentral gyrus, postcentral gyrus, bilateral activation in Supramarginal gyrus (more Ip) and CRB and ipsilateral activation in superior temporal gyrus and middle temporal gyrus. The stroke subject 4 showed contralateral activation in primary sensorimotor areas (along pre and postcentral gyrus) and frontal gyrus, inferior frontal gyrus, inferior parietal lobe as well as temporal lobe. He also showed bilateral activation in superior frontal gyrus, SMA, middle cingulate cortex, superior temporal gyrus, inferior temporal gyrus and ipsilateral superior parietal lobe. To sum up, we noticed the activation in the precentral and postcentral gyrus, the secondary motor areas, cingulate motor areas, and the inferior parietal lobule in all of our subjects. We also noticed differences in laterality of activation between normal and stroke survivors.

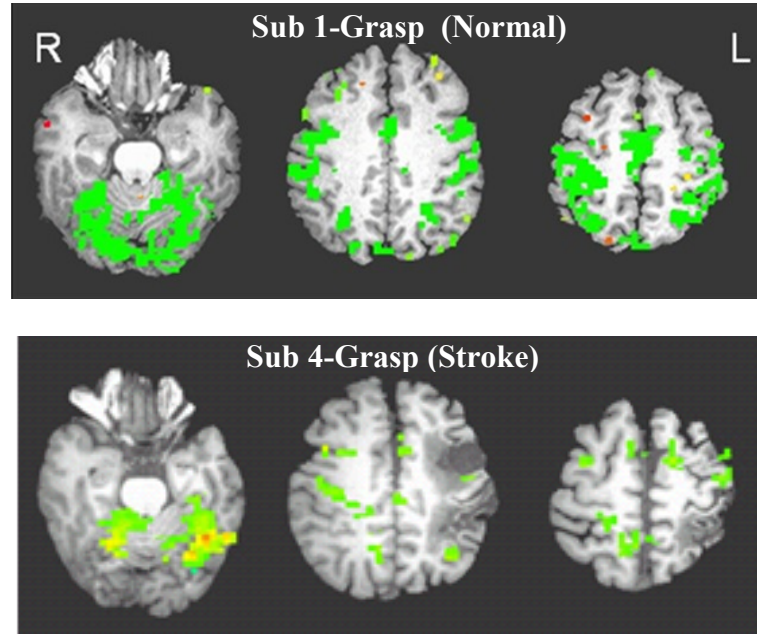


Figure 5.6a Examples of brain activation in a normal and a stroke subject's grasp movement (The images were taken from the axial view , from left to right,  $Z=47$ ,  $Z=102$ ,  $Z=115$ . Activation sites are marked in green color.)

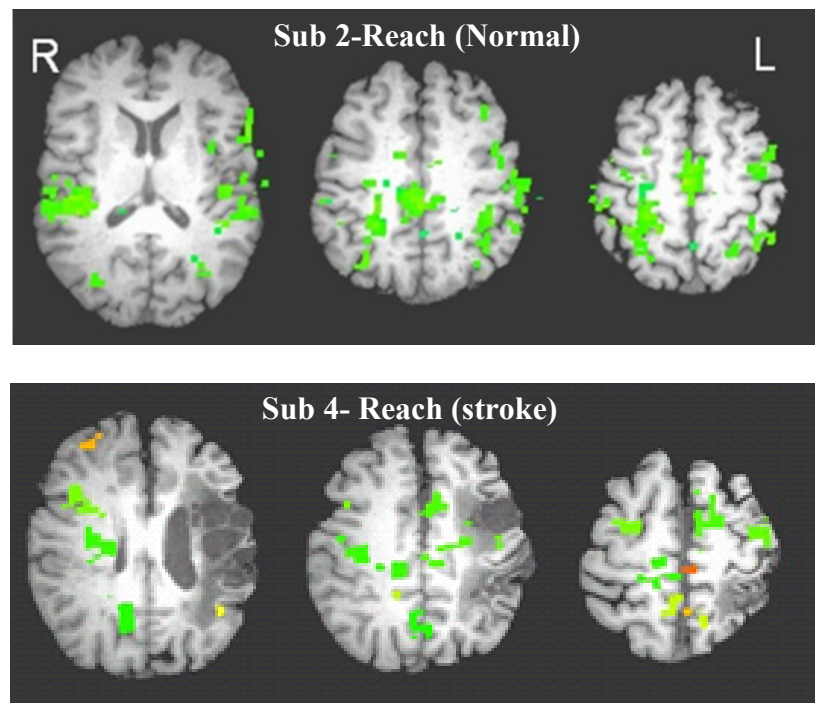


Figure 5.7b Examples of brain activation in a normal and a stroke subject's reach movement

*(The images were taken from the axial view , from left to right, Z=81, Z=106, Z=115. Activation sites are marked in green color.)*

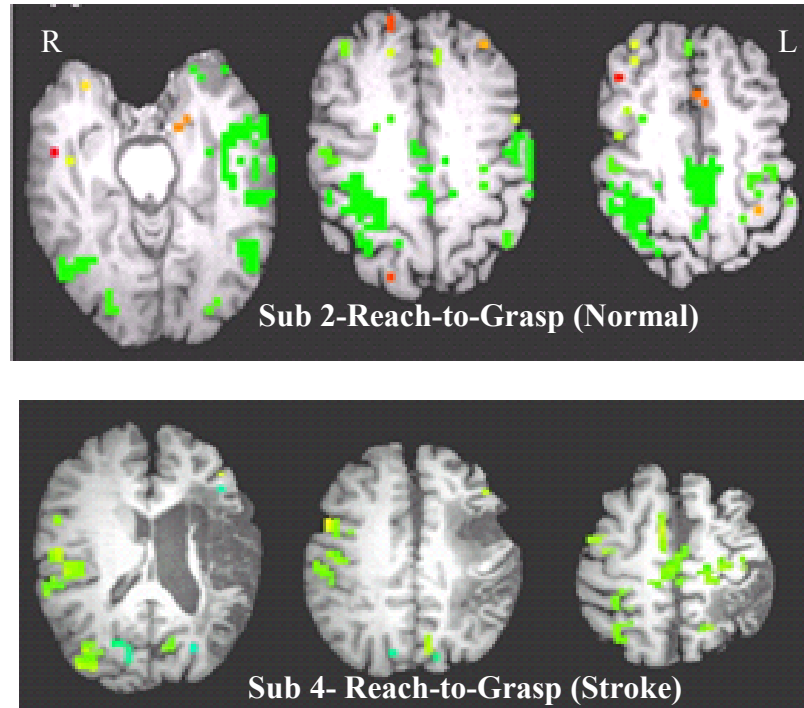


Figure 5.8c Examples of brain activation in a normal and a stroke subject's reach-to-grasp movement  
*(The images were taken from the axial view , from left to right, Z=84, Z=106, Z=115. Activation sites are marked in green color.)*

### 5.4.3. Head movement

The head movements were studied for each subject to improve the validity of the results. Head movements were calculated from directions of X, Y, Z, pitch, yaw and roll. Table 5.4 reported the range of head movements of each subject calculated from maximal movement –minimum movement in each direction. The typical tolerance of head movement is within 2 mm in each degree of freedom. As we could see from the table,

only subject 5 showed a head movement slightly larger than 2mm in X direction in reach to grasp movement. Figure 5.7 illustrates the head movement of subject 5's reach to grasp movement. It is obvious in the figure that subject 5 made a single large head movement in one time series. In the post-processing data analysis, it is helpful to take out the signal at the particular time or the adjacent time voxels. In that case, the influence of head movement could be minimized.

Table 5.4 Head movement range of each subject

Unit(mm)	Subject	X	Y	Z	Pitch	Yaw	Roll
Grasp	1	0.4904	0.5197	0.5149	1.2763	0.5702	0.7066
	2	0.3072	1.0946	0.3661	1.0905	0.1741	0.6315
	3	0.4676	0.7256	0.7212	0.669	0.2732	0.2797
	4	0.776	1.4376	0.8789	1.4742	0.6254	0.8049
	5	1.163	0.8231	0.472	0.9977	0.5509	0.4089
Reach	2	0.5332	1.0629	0.6374	1.64	0.3028	1.0454
	4	0.6492	1.0829	0.8187	0.8011	0.6122	0.4985
	5	0.7501	0.9561	0.8664	1.3343	0.7995	0.9337
Reach to grasp	1	0.4159	0.569	0.4675	1.4731	0.6017	0.8777
	2	0.6192	1.2921	0.8266	1.8783	0.315	1.2204
	4	0.4454	0.7442	1.0899	1.3336	0.6214	0.6166
	5	2.1025*	1.2694	2.9304	1.3252	3.1724	1.0576

*The range of headmovement are reported in each direction in the table. The value is calculated from the difference between maixmal value and minimum value in the direction. The stared value indicate value larger than 2mm.*

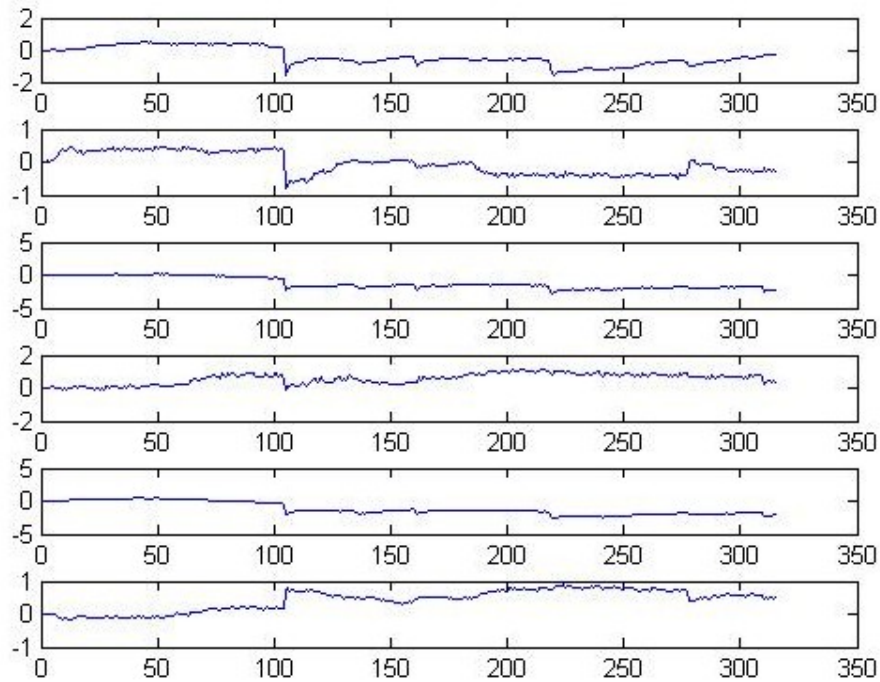


Figure 5.9 Subject 5's head movement in reach to grasp movement (*X axis is the time axis, sample frequency is 0.5Hz, y axis is the movement axis (unit: mm). From top to down, the figures represents movement in X, Y, Z direction, pitch, yaw and roll.*)

However, we anticipated some low functioning stroke survivors tended to have very large head movements, especially in the event related tasks. Their movements might not be only shown in some particular voxels but related to the event related tasks. This would have a large influence of the movement data and might results activation maps with additional activation at the edges on the brain. How to eliminate the influence of head movement for the low functional subject became an important issue in the future experiments.

## 5.5. Discussion

We have demonstrated that the UE R/G system was usable by subjects inside and outside (in a clinic) the scanner. The movement trajectories didn't show any obvious difference between these two conditions. Similar trends on movement trajectories and velocities were shown. Significant high correlations were found for the movement results inside and outside of the scanner. Although no statistical analysis was performed because of the limited sample size, based on the existing result, we think that the movement could be evaluated from inside the scanner. Kinematic metrics can be derived from these trajectories and these along with the significant regression models derived in Chapter 4, we anticipate being able to use the system in future studies.

We also demonstrated that task-related activation can be found in a number of brain regions such as sensorimotor areas, secondary motor areas, and cerebellum. Activations were found in M1, S1, SMA, CMA, dorsal prefrontal areas, inferior and superior parietal lobule, which was consistent with the literature. However, there were several aspects in our data analysis that required careful consideration in data analysis:

- 1). *Delay in the HRF in strokes and image alignment:* In the hemodynamic response function, the stroke survivors spent more time to arrive at their peak response (14 seconds) than the normal subjects (8-12 seconds). Unusual response curve with prolonged dips followed by a very late positive peak was also found in the some recent studies [Roc et al, 2006 Fridriksson et al, 2006, Bonakdarpour et al, 2007]. The shape difference of the HRF might be due to the properties of evolving stimulus as well as the underlying neuronal activity. The vascular lesion might affect the blood flow dynamics which impact the HRF. Hence, it is highly recommend to record the HRF of each subject by conducting each experiment with a long trial event related study. The hemodynamic

parameters can then be used to enhance the data analysis. In our experiment, we accounted for the delay of peak in our GLM and calculated for the delay of peaks. Optimizing the HRF would be an option to improve the brain activation analysis in the future studies. The other issue of data processing is the EPI and SPGR data alignment in volume registration. We noticed that because of the large lesion site of stroke survivors, by performing the EPI to SPGR brain image alignment might add additional problems in the data analysis. Therefore, it is crucial to choose the best alignment strategies (EPI to SPGR or EPI to base) to make the most meaningful motion corrections.

2) *The stroke survivor's head movements*: It was obviously from our result that the event related reach/grasp tasks design was able to capture the motor activation of stroke survivors. The head movement was within the tolerance for the normal and medium to high subjects as we demonstrated in this thesis. However, the example of large head movement problem with low functional subject is also shown figure 5.8. The large head movement might be induced by the fact that the task is providing the visual feedback and the subject is making all effort to complete the tasks which caused the unnoticed associated head movement. This might cause false positive activation in the results. And since the movement is task-related, it is hard to eliminate its influence in the post-processing analysis. Hence, how to adjust the task complexity and task display to induce appropriate attention of the movement and provide proper feedback as well as keep limited head movement is an important issue for further investigation. The other crucial issue about the experiment is the mirror movement. Although subjects with obvious mirror movement are generally excluded from the study, the low functioning subjects are the potential target subject groups for the study and the mirror movement is

typical among these stroke survivors. Hence, how to monitor and eliminate the mirror movement especially for the low functioning subjects is another important issue.

3) *Task design*: The third issue about our experiment design is the timing control of the event related tasks. Currently, the tasks are controlled through an external CMOS time trigger and each task is strictly restricted to 4 seconds. In other words, each task begins only when it recognizes an external pulse from the trigger. The details of task design is explained in chapter 3. However, based on our experience, there is a condition that some time triggers are missed by the task program. This will result in the task timing disturbed from the original ISI event related experiment design. And in the data analysis, the disturbed task timing will result in meaningless activation maps. The program has been updated to solve the problem. However, more experiments are needed to guarantee the proper function of the task timing and task design. This will be crucial to the reconstruction of the data.

4) *Device modification*: Another issue about the system is the necessity and possibility to provide the assisted movement. Because the strokes subject's limited movement, especially for the low functional subject, they might lack the ability to open the hand but they can close their hand; or their elbow flexor is preserved but the elbow extension movement is limited. To perform the continuous elbow flexion/extension, hand open/close movement might be difficult for them and might induce additional head movement. To provide certain assistance for the movement, e.g. help them with hand opening movement, could help subjects successfully complete the tasks and might result in better image quality.

## **5.6. Conclusion**

The case study demonstrates our ability to quantify with the UE R/G system subjects' motor performance on reach, grasp and reach to grasp movements as well as elicit brain activation during the experiment. Data collected within the scanner demonstrates similar movement trajectories as those collected outside in the lab environment. Brain activations were found in the several areas such as primary, secondary motor areas, cerebellum. In order to improve the data analysis in the future, we need to exclude the subjects with large mirror movements and design the movements to be easy to accomplish that would not require extra effort. It is also important to adjust the most appropriate time to peak parameters in the TENT function according to each individual's results and volume registration strategies need to be decided individually. Further investigations need to be performed to improve data collection and data processing methods in order to demonstrate the relationship between the activation patterns and the stroke survivor's movement performances as well as their recovery level.

## Chapter 6

### Conclusions and Future Directions

## 6. Conclusions and Future directions

The main goal of this thesis was to design, develop, calibrate and validate an upper extremity reach and grasp movement evaluation system and apply it to the brain activation studies with stroke survivors. The uniqueness of the system is that it is a system that provides both the task environment for studying how reach and grasp movements relate to brain activations patterns pre and post stroke therapy and an assessment environment to evaluate the kinematics of the reach and grasp movements of stroke survivors. We have successfully accomplished our goal and design. This thesis consists of four main components:

***Component 1:*** System design and development. In Chapter 3, we described the system development including hardware and software design. We rebuilt of the elbow orthosis with optical encoder and integrate it with the existing FES glove into a Simulink task design and built up the system to provide the reach and/or grasp tasks with visual feedback.

***Component 2:*** MR safety test and calibration. We performed the MR safety test of system to ensure its safety in the 3.0T GE MR scanner. We also performed a calibration study with the elbow orthosis to prove that it can accurately measure the elbow joint angles.

***Component 3:*** Validation study. As described in chapter 4, we conducted a validation study with 12 stroke survivors to prove that our system is able to measure the motor performances of the stroke survivors and that kinematic metrics derived from these movement trajectories were not only correlated to clinical tools used by therapists, but

could also predict functional level. We identified the stroke impairment level measured by the clinical assessment tools was closely related to their motor performances measured by our devices. We also found that lower functional subjects had lower movement velocity, smaller maximal grasp aperture (or smaller maximal reach angle), larger error, less smooth movement in reach or grasp movement. We identified regression equations for grasp recovery and reach recovery that may have potential uses in identifying functional recovery levels pre and post therapy.

**Component 4:** Usability and Application in fMRI studies. We first demonstrated our system and experimental design is able to capture the movement of stroke survivors inside the scanner. We then demonstrated our ability to study the reach and grasp movement related brain activations of stroke survivors with a case series. During the process, we finalized our experiment design and data processing method. Activations are found in regions such as sensorimotor areas, secondary motor areas, cingulate motor areas, superior and inferior parietal cortex and cerebellum. We determined that there were limitations in our ability to collect good scans with low functioning stroke survivors and care must be taken in the analysis of our data due to possible delays in the bold signal and timing shifts during data collection.

Overall, we conclude that our system is an MR compatible system that can be used to evaluate stroke survivors' movement and it can also provide the task environment to study the stroke survivor's reach and grasp movement related brain activations. This system lays the foundation for the other study on-going at the Rehabilitation Robotics Research and Design lab: fMRI and robot-assisted practice of activities of daily living. The goal of the study is to assess the short-term functional gains after practice of skilled

reaching and grasp tasks, quantify the neuronal changes associated with short-term gains and identify the trends across the high and low responders in terms of patterns of change in cortical activity and white matter connectivity. Specifically, the system will be applied to evaluate the stroke recovery of a 4-week robot assisted therapy. The ADLER system is a novel therapy system that provides the task-oriented upper extremity RAT. Clinical assessment, biomechanical assessment (kinematic assessment) and the brain activation evaluation will be performed before, after and one month after both therapy. The effect of RAT will be compared to the occupational therapy from these three aspects. And the stroke recovery mechanism will also be compared between stroke survivors from different impairment levels.

Future use of the system will need to resolve some of the identified challenges; these challenges are mainly from the following aspects: 1) The system's sensitivity needs to be further improved to capture the low functional subject's grasp movement; 2) The sensor artifact needs to be eliminated for better device performance; 3) The inconsistency of the task timing requires further investigation; 4) The fMRI scanning of low functioning subject who only have limited elbow or hand movement must be re-visited due to possible effects of large head and mirror movements. One solution is to provide a task environment that could help subjects perform the tasks without too much head movement and mirror movement; another is to determine better data processing techniques that could eliminate these effects; 5) Finally the fMRI data analysis process needs to be improved with focused on eliminating unwanted artifacts induced by unexpected head movements.

## References

AFNI website, <http://afni.nimh.nih.gov/afni/doc/edu>

American heart association Heart disease and stroke statistics, 2009 Update

Avago Technology, AEDR-8400 reflective surface mount optical encoder datasheet, 2006, [www.avagotech.com](http://www.avagotech.com)

Aisen et al, The Effect of Robot-Assisted Therapy and Rehabilitative Training on Motor Recovery Following Stroke, *Arch Neurol.* 1997;54(4):443-446.

Bandettini P.A, Jesmanowicz A, Processing strategies for time-course data sets in functional MRI of the human brain, *Magnetic resonance in medicine*, 30;161-173 (1993)

Barnes M.P, Dobkin B.H, Recovery after stroke, Cambridge; New York; Cambridge University press, 2005

Beer RF, Dewald JP Rymer WZ. Deficits in the coordination of multioint arm movements in patients with hemiparesis: evidence for disturbed control of limb dynamics. *Exp Brain Res* 2000; 131;305-19

Bhatt E. Nagpal A, Effect of finger tracking combined with electrical stimulation on brain reorganization and hand function in subjects with stroke, *Exp Brain res* (2007) 182:435 -447

Bohannon RW, Smith MB. Interrater reliability of a modified Ashworth scale of muscle spasticity. *Phys Ther* 1987;67(2):206-7.

Bouzit, M. Burdea Grigore, et al, The Rutgers Master II – new Design force-ffedback Glove, *IEEE/ASME Transactions on mechatronics*, Vol. 7, No.2, June 2002

Buell S.J and Coleman, P.D, Quantitative evidence for selective dendritic growth in normal aging, but not in senile dementia, *Brain res*, 214:23-31, 1981

Burgar C.G, Development of robots for rehabilitation therapy, the Palo/Alto VA/Stanford experience, *Journal of rehabilitation research and development* Vol.37 No.6 November/December 2000 Page 683-673

Castiello U, The neuroscience of grasping, *nature reviews, neuroscience*, Sep, 2005, Vol 6

Cao Y, D'Olhaberriague L, Pilot study of functional MRI to assess cerebral activation of motor function after post stroke hemiparesis, *Stroke*, 1998; 29-112-122

Carey JR, Kimberley TJ, analysis of fMRI and finger tracking training in subjects with chronic stroke, *Brain*, 2002 Apr; 125 (Pt4):773-88

Chae, et al delay in initiation and termination of muscle contraction, motor impairment, and physical disability in upper limb hemiparesis muscle *Nerve* 2002;25

Chang JJ, Wu TI, Wu WL Su FC, Kinematical measure for spastic reaching in children with cerebral palsy, *clinical Biomechanics* 20 (2005) 381-388

Chen, C, Tang, F, et al, Brain lesion size and location: effects on motor recovery and functional outcome in stroke patients, *Arch Phy Med Rehabil* Vol 81, April 2000

Chinzei K, MR compatibility of Mechatronic Devices, Design criteria", *Int Conf Med Image Comput Assist Interv.* 1999; 2: 1020-1031

Chollet F, Dipiero V, et al, The functional anatomy of motor recovery after stroke in humans: a study with positron emission tomography. *Ann neurol* 1991; 29:63-71

Colazweskir S.M, Siedentopf C.M, Functional magnetic resonance imaging of the human sensorimotor cortex using a novel vibrotactile stimulator, *neuroscience letters*, vol. 17, no. 1, pp 421-430, 2002

Colombo R. Pisano F. et al, Assessing mechanism of recovery during robot-aided neurorehabilitation of the upper limb, *Neurorehabil Neural Repair* 2008; 22;50

Coote S, et al, The effect of the GENTLE/s robot-mediated therapy system on arm functional after stroke, *Clin Rehabil* 2008; 22; 395-405

Cromwell FS, Occupational Therapist's manual for basic skills assessment or primary prevocational evaluation. Pasadena (CA); Fair Oaks Printing ;1960

Dechaumont-Palacin S. Marque P, neural correlated of proprioceptive integration in the contralesional hemisphere of very impaired patients shortly after a subcortical stroke: an fMRI study, *Neurorehabil Neural Repair* 2008; 22; 154

Duncan PW, Propst M et al, Reliability of the Fugl-Meyer assessment of sensorimotor recovery following cerebrovascular accident. *Phys Ther* 1983;63:1606-10.

Duncan PW, Wallace D, et al, The stroke impact scale 2.0 evaluation of reliability, Validity, and sensitivity to change, *Stroke*, Oct, 1999; 30;2131-2140

Dobkin B.H, the clinical science of neurorehabilitation, 2<sup>nd</sup> edition, Oxford University Press, USA, Jan, 2003

Dong, Y, evolution of fMRI activation in the perilesional primary motor cortex and

cerebellum with rehabilitation, *Neurorehabilitation and Neural Repair*, Vol, 21, No. 5, 412-428 (2007)

Eriksson et al, Neurogenesis in the adult human hippocampus, *nature medicine*, 4:1313-1317 1998

Feng, X., "Upper extremity performance assessment using an interactive, personalized computer-assisted neurorehabilitation motivating framework" *PhD Dissertation, Marquette University*, 2007

Feydy A, Carlier R, et al, Longitudinal Study of motor recovery after stroke, recruitment and focusing of brain activation, *stroke*, 2002; 33:1610

Fitts, P.M., 1954. The information capacity of the human motor system in controlling the amplitude of movement. *Journal of Experimental Psychology* 47, 381-391

Flexpoint inc, Bend sensor technology mechanical application design guide, 1997, [www.flexpoint.com](http://www.flexpoint.com)

Friston, KJ, Jezzard P, and Turner, P. (1994), "Analysis of functional MRI time series", *Human Brain mapping*, 1, 153-171

Friston KJ., Fletcher, P., Josephs, O., Holmes, A, Rugg, M.D, and Turner, R (1998). "Event-related fMRI: characterizing differential responses." *NeuroImage*, 7, 30-40

Fujii Y, Nakada T, Cortical reorganization in patients with subcortical hemiparesis: neural mechanisms of functional recovery and prognostic implication, *J neurosurg* 98; 64-73, 2003

Fugl-Meyer AR, Jaasko L, et al, the post-stroke hemiplegic patient *Scand J rehabil Med* 1975; 7-13-31

Gassert R, Burdet E, Chinzei K, MRI-compatible robotics, *IEEE Engineering in Medicine and Biology Magazine*, 2008a May-Jun; 27(3), pp 12-14.

Gassert R, Burdet E, Chinzei K, Opportunities and challenges in MR-compatible robotics, *IEEE Engineering in Medicine and Biology Magazine*, 2008b May-Jun; 27(3):15-22.

Gassert R, Dovat L, et al, A 2-DOF fMRI compatible Haptic Interface to Investigate the neural control of arm movements, *Proc of the 2006 IEEE international conference on robotics and automation*, Orlando, FL, May 2006

Gentilucci M Benuzzi F, et al, Grasp with hand and mout: a kinematic study on healthy subjects, *Journal of Neurophysiol* 86; 1685 – 1690 2001

Gladstone DJ, Danells CJ, et al, the Fugl-Meyer Assessment of motor recovery after stroke: a critical review of its measurement properties, *Neurorehabil Neural Repair* 2002; 16;232

Glover, GH, 1999. "Deconvolution of impulse response in event related BOLD fMRI." *NeuroImage*, 9, 416-429

Gould, Reeves, et al, 1999, Hippocampal neurogenesis in adult old world primates, *proc. Natl, acad, sci, USA*, 96:5263-5267

Grice KO, Vogel KA, et al, Adult Norms for a commercially available nine hole peg test for finger dexterity, September/October 2003, Volume 57

Grosskopf A, Kutzt-Buschbeck JP, Grasping with the left and right hand, a kinematic study, *Exp Brain Res* (2006) 168: 230-240.

Hallet M, Pascual-Leone A, et al, Adaptation and skill learning: evidence for different neural substrate. In: Bloedel JR, Ebner TJ, Wise Sp, eds. *The acquisition of motor behavior in vertebrates*. Cambridge, Mass; Massachusetts Institute of Technology Press, 1996:289-302

Hahn et al. Improving robustness and reliability of phase-sensitive fMRI analysis using temporal off-resonance alignment of single-echo timeseries (TOAST). *Neuroimage* (2009) vol. 44 (3) pp. 742-52

Hamzei, F, Liepert J, et al, Two different reorganization patterns after rehabilitative therapy: an exploratory study with fMRI and TMS, *NeuroImage* 31(2006), 710-720

He SQ, Dum RP, et al, Topographic organization of corticospinal projections from the frontal lobe: motor areas on the medial surface of the hemisphere, *J neurosci*, 1995; 15: 3284-306

Hesse S. Schulte-Tiggles et al, Robot-assisted arm trainer for the passive and active practice of bilateral forearm and wrist movements in hemiparetic subjects, *Arch Phys Med Rehabil* 2003;84(6): 916-20

Hu Y, Osu R., Okada M, Goodale MA Kawato M. A model of the coupling between grip aperture and hand transport during human prehension, *Experimental Brain research*, Vol 167 No.2, Nov. 2005

Huettel S.A, Song, A. W. et al, *Functional magnetic resonance imaging*, Sinauer Associates, April, 1<sup>st</sup>, 2004

Huttenlocher, P.R. *Neural Plasticity: the effects of environment on the development of the cerebral cortex*, London, England, 2002

Izawa J, Shimizu T, MR compatible Manipulandum with Ultrasonic motors for fMRI studies, Proc of the 2006 IEEE international conference on robotics and automation, Orlando, FL, May 2006

Jang S.H, You S. H, Neurorehabilitation-induced cortical reorganization in brain injury: A 14-month longitudinal follow up study, *Neurorehabilitation* 22 (2007) 117-122

Jeannerod, M., 1981. Intersegmental coordination during reaching at natural visual objects. In: Long, J., Baddeley, A. (Eds.), *Attention and Performance IX*. Erlbaum, Hillsdale, pp. 153–168.

Jeannerod, M., 1988. *The Neural and Behavioural Organization of Goal-Directed Movements*. Oxford University Press, Oxford.

Jebsen RH, Taylor N, et al An objective and standardized test of hand function *Archives of physical medicine and rehabilitation*, 1969: 50, 311-319,

Jeonghun K, Mraz R, et al, A data glove with tactile feedback for fMRI of virtual reality experiments, *CyberPsychology and Behavior*, Vol. 6, No. 5, 2003

Johansson, R.S., Westling, G., 1984. Roles of glabrous skin receptors and sensorimotor memory in automatic control of precision grip when lifting rougher and more slippery objects. *Experimental Brain Research* 56, 550–564.

Johansen-Berg H, Dawes H, et al, correlation between motor improvements and altered MRI activity after rehabilitative therapy, *Brain*, 2003, Nov; 126 (pt11):2569

Johnson M.J, Wisnesk, K.J, etc, Development of ADLER: the activities of daily living exercise robot, *biomedical robotics and biomechatronics*, 2006, bioRobo 2006, Volume, Issue, 20-22 Feb 2006, Page(s): 881-886

Kandel E.R, Schwartz J.H, principles of neuroscience, McGraw-Hill Medical 4<sup>th</sup> edition, July 1, 2000

Kanal E, Barkovich A.J, et al, ACR guidance document for safe MR practices: 2007, *AJR*:188, June 2007

Kamper D.G, McKenna-Cole et al, Alteration in reaching after stroke and their relation to movement direction and impairment severity *Arch phy med Rehabil* Vol 83, May, 2002

Kellor M, Frost J, et al, Hand strength and dexterity, *American Journal of Occupational therapy* 1971, 25 77-83

Keith RA, Granger CV, et al, The functional independence measure: a new tool for rehabilitation, *Advanced Clinical Rehabilitation*, 1987; 1:6-18

Khanicheh, A, Muto A, MR compatible erf driven hand rehabilitation device, in Proc

IEEE international conference on rehabilitation robotics, 2005, pp 7-12

Kidd D, Stewarr G, et al, The functional independence measure: a comparative validity and reliability study, *Disability Rehabilitation*, 1995; 17: 10-14

Krebs HI, Hogan N, Aisen ML, Volpe BT Robot-aided neurorehabilitation. *IEEE Trans Rehabil Eng* 1998; 6:75-87

Kerbs, H.I, Aisen, M.L et al, Quantization of continuous arm movement in human with brain injury, *Proc. Natl. Acad. Sci. USA*, Vol 96, pp.4645 -4649, April, 1999, neurobiology

Kwong, K, Belliveau JW, et al, Dynamic magnetic resonance imaging in human brain activity during primary sensory stimulation, *PNAS* 89; 5675-79

Kwon Y.H, Lee M.Y. Difference of cortical activation pattern between cortical and corona radiate infarct, *Neuroscience Letters*, 417 (2007) 138-142

Lang C.E, Wagner J M, recovery of grasp versus reach in people with hemiparesis stroke, *Neurorehabil Neural repair* 2006; 20; 444

Lang, C.E., Wagner, J.M., Bastian, A.J., Hu, Q., Edwards, D.F., Sahrman, S.A., 2005. Deficits in grasp versus reach during acute hemiparesis. *Experimental Brain Research* 166, 126–136

Lang, C.E., Reilly, K.T., Schieber, M.H., 2006. Human voluntary motor control and dysfunction. In: Selzer, M., Clarke, S., Cohen, L., Duncan, P., Gage, F. (Eds.), *Neural Repair and Rehabilitation*, vol. II. Cambridge University Press, New York, pp. 24–36

Lange, N. and Zeger, S.L, (1997), “Non-linear Fourier time series analysis for huan brain mapping by functional magnetic resonance imaging (with discussion).” *Applied statistics*, 46, 1-29

Lazar NA, *The statistical analysis of functional MRI data*, Springer, 2008

Levin M.F, Interjoint coordination during pointing movements is disrupted in spastic hemiparesis. *Brain* 1996; 119:281-93

Levy, C. E, Deborah N. S. et al, Functional MRI evidence of cortical reorganization in upper limb stroke hemiplegic treated with constraint induced movement therapy, *American Journal of physical medicine and rehabilitation*, 2001, Vol 80, No 1, Pp 4-12

Lincoln N, Edmans J. A re-validation of the Rivermead ADL scale for elderly patients with stroke. *Age Ageing* 1990; 19:9–24.

Loubinoux I, Carel C, et al, correlation between cerebral reorganization and motor

recovery after subcortical infarct, *NeuroImage*, Vol 20, Issue 4, Dec, 2003, Pages, 2166-2180

Mathiowetz V, Volland G, Adult norms for the box and block test of manual dexterity *American Journal of occupational therapy* 1985, Jun, 39(6): 386-91

Mathiowetz V. Reliability and validity of grip and pinch strength measurements. *Crit Rev Phys Rehabil Med* 1991; 2:201–212.

Marshall, R.S, Perera G.M, Evolution of cortical activation during recovery from corticospinal tract infarct, *Stroke*, 2000; 31: 656-661

Masire S, A. Celia, Robot-assisted rehabilitation of upper limb after acute stroke, *Arch Phys Med Rehabil* Vol 88, Feb, 2007

McDonnell, M.N., Hillier, S.L, Ridding M.C, Miles, T.S., 2006. Impairments in precision grip correlate with functional measures in adult hemiplegia. *Clinical Neurophysiology* 117, 1474-1480.

Mendell JR, Florence J: Manual muscle testing. *Muscle Nerve* 1990, 13(Suppl):S16-20

Michaelsen SM, Jacobs S, Roby-Brami A, Levin MF, Compensation for distal impairments of grasping in adults with hemiparesis, *Exp Brain Res*. 2004 Jul;157(2):162-73. Epub 2004 Feb 19.

Menon R.S, Postacquisition suppression of large-vessel BOLD signals in high resolution fMRI, *Magnetic Resonance in Medicine* 47:1-9 (2002)

Mountcastle V.B, Darian-Smith I, 1968, Neural mechanism in somesthesia, *Medical physiology*, 12<sup>th</sup> ed, V.B.Mountcastle, vol.2 1372-1423, St. Louis

Nair D. G, Fuchs A, Assessing recovery in middle cerebral artery stroke using functional MRI, *brain injury*, 19:13,1165-1176

Nathan D.E, Johnson MJ, “Design of a Grasp Assistive Glove for ADL-focused, Robotic Assisted Therapy after Stroke.”, *IEEE-Intl Conf On Rehab Robotics ICORR 2007*, Netherlands

Nathan DE, Johnson MJ, McGuire JR, Design and validation of low-cost assistive glove for hand assessment and therapy during activity of daily living-focused robotic stroke therapy, *Journal of rehabilitation research and development*, Vol 46, Nov 5, 2009 pp 587-602.

Nathan D.E, Development of a FES sensorized glove and modeling of human reaching and grasping for task-oriented, robotic assisted therapy, master thesis, Marquette University, 2008

Nef T, Riener R, ARMin- Design of a novel arm rehabilitation robot, in: Proceedings of the 9<sup>th</sup> International Conference on Rehabilitation Robotics; 2005 Jun 28-Jun 1; Chicago, Illinois. Madison (WI); Omnipress; 2005.P.57-60.

Nelson M, serial communications developer's guide, 2<sup>nd</sup> ed, Boston, USA, IDG books worldwide, 2000

Nowak, D.A., Grefkes, C., Dafotakis, M., Kuester, J., Karbe, H., Fink, G.R., 2007b. Dexterity is impaired at both hands following unilateral subcortical middle cerebral artery stroke. *European Journal of Neuroscience* 25, 3173–3184

Nowak DA, The impact of stroke on the performance of grasping usefulness of kinetic and kinematic motion analysis, *Neuroscience and biobehavioral reviews* 32 (2008) 1439-1450

Nudo RJ, Wise BM, et al, Neural substrate for the effects of rehabilitative training on motor recovery after ischemic infarct, *Science*, 1996; 272: 1791-4

Oldfield, R.C. The assessment and analysis of handedness: the Edinburgh inventory. *Neuropsychologia*, (1971) 9(1): 97-113.

Park C, O'Neill P. Management of neurological dysphagia. *Clin Rehabil* 1994; 8:166–174.

Paulette M, Van Vliet et al Coordination between reaching and grasping in patients with hemiparesis and healthy subject, *Archives of physical medicine and rehabilitation* vol 88, Oct 2007

Rajapske, JC, Kruggel, F, Maisog, JM, and Von Cramon, DY, "Modeling hemodynamic response for analysis of functional MRI time-series." *Human Brain Mapping*, 6, 283-300

Reinkensmeyer D.J, et al, Understanding and treating arm movement impairment chronic brain injury: progress in ARM guide, *Journal of rehabilitation research and development*, Vol. 37 No. 6, November/December 2000 page 653/662

Roby-Brami A, Fuchs S et al, reaching and grasping strategies in hemiparetic patient, *Mot Control* 1997; 1: 72-91

Rohrer B. Movement smoothness changes during stroke recovery, *The journal of neuroscience*, Sep 15, 2002, 22(18):8297-8304

Rossier P, Wade D. Validity and reliability of 4 mobility measures in patients presenting with neurologic impairment. *Arch Phys Med Rehabil* 2001;82:9–13

Rossini P.M, Altamura C, Ferreri F, Melgari J.-M., et al, Neuroimaging experimental

- studies on brain plasticity in recovery from stroke, *Eura medicophys* 2007; 43;241-54
- Roy CS, Sherrington CS, On the regulation of the blood-supply of the brain, *Journal of physiology* 11 (1-2): 85-158.17
- Schaechter J.D, Kraft E, Motor recovery and cortical reorganization after constraint-induced movement therapy in stroke patients, A preliminary study, *neurorehabilitation and neural repair* 16(4); 2002
- Schaechter J.D, Stokes C, Finger motion sensors for fMRI motor studies, *NeuroImage* 31 (2006) 1549-1559
- Schenck J.F, The role of magnetic susceptibility in magnetic resonance imaging, ROI magnetic compatibility of the first and second kinds, *Med. Phys.* 23(6), June, 1996
- Schenberg S, Sveistrup H, et al, The development of coordination for reach-to-grasp movements in children *Exp Brain Res* (2002) 146: 142-154
- Sheikh and Yesavage, "A knowledge assessment test for geriatrics psychiatry", 1985
- Small SL, Hlustik P, cerebellar hemispheric activation ipsilateral to the paretic hand correlated with functional recovery after stroke, *Brain*, 2002 Jul; 125 (Pt70: 1544-57)
- Song R, Tong KY, Hu XL, Evaluation of velocity-dependent performance of the spastic elbow during voluntary movements, *Arch phys Med Rehabil* Vol 89 June 2008
- Schmidt RA, Wrisberg CA, *Motor Learning and Performance: A Problem Based Learning Approach*. 3<sup>rd</sup> ed. Champaign, IL; Human Kinetics; 2004
- Small SL, Hlustik P, cerebellar hemispheric activation ipsilateral to the paretic hand correlated with functional recovery after stroke, *Brain*, 2002 Jul; 125 (Pt70: 1544-57)
- Standard Practice for Marking Medical Devices and Other Items for Safety in the MR Environment, ASTM Standard F2503-05, 2005.
- Stern EB, Stability of the Jebsen-Taylor Hand Function Test across three test sessions. *Am J Occup Ther.* 1992 Jul;46(7):647-9.
- Song, R. Tong K, Y, et al, Evaluation of velocity-dependent performance of the spastic elbow during voluntary movements, *Arch Phys Med Rehabil*, Vol 89, June, 2008
- Stinear, C. M, Barber A, et al, Functional potential in chronic stroke patients depends on corticospinal tract integrity
- Spaulding SJ, McPherson JJ, et al, Jebsen Hand Function Test: Performance of the uninvolved hand in hemiplegia and of right-handed, right and left hemiplegic persons,

Archives of physical rehabilitation, Vol 69, June, 1988

Suminski A.J, Zimbelman, J.L, et al, Design and validation of a MR-compatible pneumatic manipulandum, *Neurosci methods*, 2007, July 30; 163 (2):255-266

Sunderland A, Tinson D, Bradley L, Hewer RL. Arm function after stroke: An evaluation of grip strength as a measure of recovery and a prognostic indicator. *J Neurol Neurosurg Psychiatry* 1989; 52:1267-72.

Szaflarski J.P. Page S.J, et al, Cortical reorganization following modified constraint induced movement therapy: A study of 4 patients with chronic stroke, *Arc, of Phys Med and rehb*, 2006, vol. 87 No. 8, pp 1052-1058

Takahashi, C, D, Der-Yeghiaian L, et al, Robot-based hand motor therapy after stroke, *Brain* 2008 131(2): 425-437

Taub E, Miller NE, Novack TA, Cook EW III, Fleming WC, epomuceno CS, Connell JS, Crago JE. Technique to improve chronic motor deficit after stroke. *Arch Phys Med Rehabil.* 1993;74:347–354.

Taub E., Uswatte G et al, Constraint-Induced movement therapy: a new family of techniques with board application to physical rehabilitation – A clinical review, *Journal of rehabilitation research and development*, Vol 36, No.3, July, 1999

Tseko NV, Khanicheh A, Christoforou E, Mavroidis C, *Magnetic Resonance–Compatible Robotic and Mechatronics Systems for Image-Guided Interventions and Rehabilitation: A Review Stud*, *Annual review of biomedical engineering*, vol 9:351-387 August, 2007

Ward N.S., Brown M.M, Neural correlates of motor recovery after stroke: a longitudinal fMRI study, *Brain* (2003a), 126, 2467-2496

Ward N.S., Brown M.M, Neural correlates of motor recovery after stroke: a cross-sectional fMRI study, *Brain* (2003b), 126, 1430-1448

Ward N.S, Brown m.M, Longitudianl changes in cerebral response to proprioceptive input in individual patients after stroke: an fMRI study, *Neurorehabil Neural Repair* 2006a; 20; 398

Ward N.S., Newton J.M, Motor system activation after subcortical stroke depends on corticospinal system integrity, *Brain* , 2006b, 129, 809-819

Wiebers D. O, Feigin V.L, et al *Handbook of stroke*, 2<sup>nd</sup> ed, Lippincott Williams & Wilkins, 2006

Wison DJ, Baker LL et al, Functional test for the hemiplegic upper extremity, *American Journal of occupational therapy*, 1984; 38: 159-164

Wing A.M. Lough, S., Recovery of elbow function in voluntary positioning of the hand following hemiplegia due to stroke, *Journal neurol Neurosurg Psychiatry* 1999; 53: 126-34

Woodsen A.M, chapter 34 in *Occupational Therapy for physical dysfunction*, William & Wilkins, 4<sup>th</sup> edition, Jan, 1995

Wu C, Trombly CA et al, A kinematic study of contextual effects on reaching performance in persons with and without stroke: influences of object availability, *Arch Phys Med Rehabil.* 2000 Jan;81(1):95-101.

Zappe A.C, Maucher T, et al Evaluation of a pneumatically driven tactile stimulator device for vision substitution during fMRI studies, *magnetic resonance in medicine*, vol 51, no. 4, pp. 828-834, 2004

## Appendix

### Appendix A: Detailed description of clinical measurements

<p><b>Fugl Meyer Assessment (IMPAIRMENT SCALE_REACH and REACH_GRASP)</b></p> <p>The FM scale (Fugl Meyer et al., 1975) is a 226 point multi-item scale developed as an evaluative measure of recovery for stroke. It includes 5 domains: motor function, sensory function, balance, joint range of motion and joint pain. The motor domain includes measurement of movement coordination, reflex action about shoulder elbow, forearm, wrist, hand, hip, knee and ankle. Every measurement is scale between 0 and 2; 0 means cannot perform, 1 means can partially perform and 2 means performs fully. The upper extremity part of the motor function measure is 66 point in total. We only performed the upper extremity part of the assessment. Higher scores means higher recovery level and vice versa. The inter- and intra-subject reliability is proved by Fugl Meyer (Fugl Meyer et al., 1975) and subsequent researchers (Duncan et al., 1983, Gladstone et al., 2002).</p>
<p><b>Nine Hole Peg Test (IMPAIRMENT SCALE_GRASP)</b></p> <p>The NHPT (Exner, 1990) is a test of dexterity, which is considered essential for successful performance of tasks of daily living. Dexterity is also defined as the fine, voluntary movements used to manipulate small objects during a specific task, as measured by the time to complete the task (Backman cork, 1992). The NHPT was originally introduced by Kellor Frost in 1971 as a part of a study on strength and dexterity (Kellor, 1971). And later on Sammon Preston Inc (Bolingbrook, IL) made a commercial version of the devices. The reliability and sensitivity of the device was tested and reported by Grice (Grice, 2003). The subject was instructed to place 9 pegs into nine holes in a plastic panel. The maximal time of completing the tasks is 60 seconds; and the total time to place all the pegs are recorded by the therapist with a stop watch. If the subject dropped a peg or the trial was interrupt anyway during a trial, the therapist cued the subject to stop and restart the trial. The subject was tested on both affected and unaffected side, three times each side. Results are averaged across three trials. Time per peg is recorded for each subject. The score is then corrected for the affected hand by dividing the affected side result by unaffected side result.</p>
<p><b>Upper-extremity Functional Test (DISABILITY SCALE)</b></p> <p>The UE-FT (Wilson, 1984) is designed to evaluate the stroke survivors' motor capability for function. The test consists of 17 graded activities arranged in seven levels by degree of difficulty. The tasks includes movement requires elbow or shoulder flexion in the impaired arm, movement requires a high degree of upper extremity coordination and finger dexterity such as using the impaired arm to put a light bulb into a socket held at shoulder height. Subjects are graded between scale level 1 to level 7. After level 1, each task is also timed. Higher scores indicated subject have more hand function. The validity and reliability of the test has been proved by Wison et al. (Wilson et al, 1984).</p>

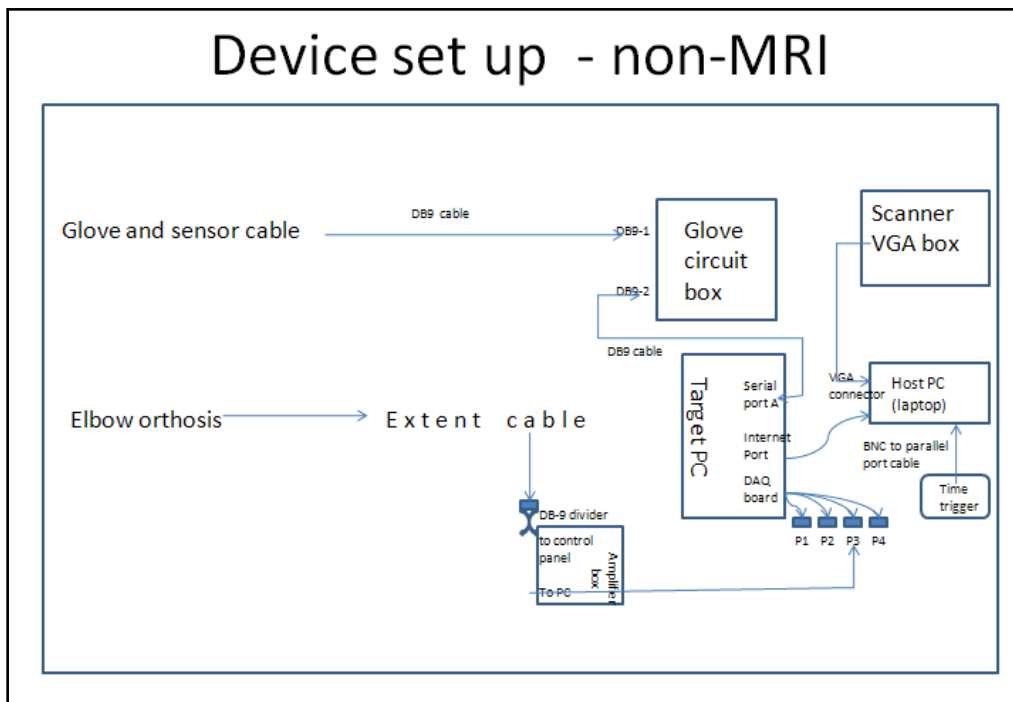
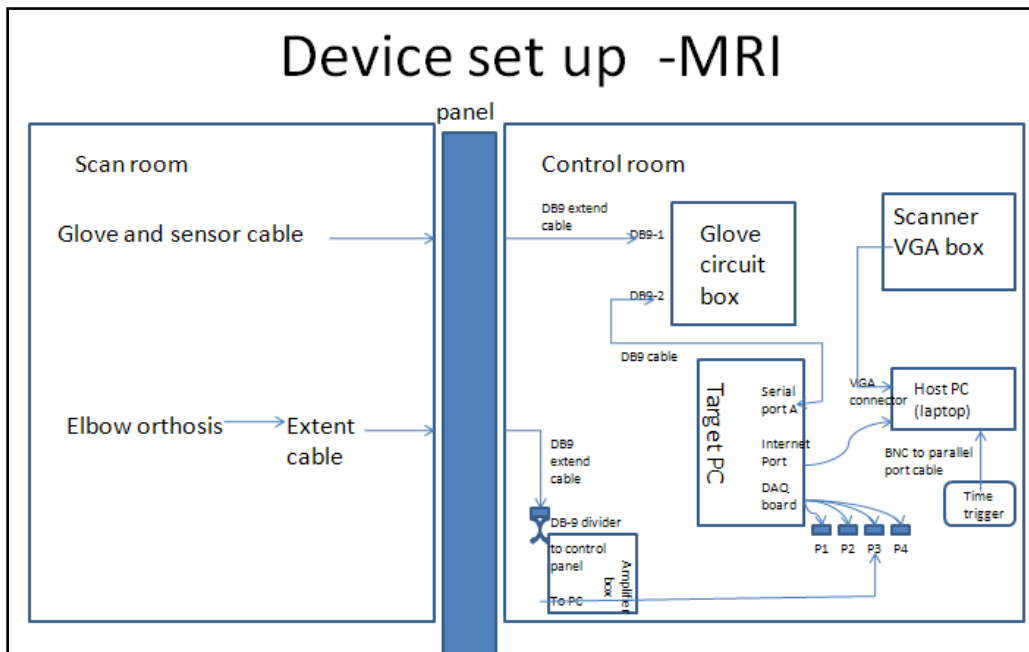
<b>Functional Independent Measure (DISABILITY SCALE)</b>
The FIM (Keith, 1987) is a sensitive and comprehensive measurement of functional outcomes of rehabilitation. Subjects are asked to give the scale between 1 (required total assistance) - 7 (complete independent) for each of the 18 items measuring their level of disability in terms of burden of care from their own perspectives. The independent score can be generated from the answers including the total score (18 items), the motor score (13 items) and the cognitive score (5 items). The items are designed from the perspective of self-care, sphincter control, mobility, locomotion, communication as well as social cognition. We used a modified version of the scale including 5 items. Subject with higher scores means they are more independent in their daily livings. Reliability and validity of FIM scales have been proved (Kidd, 1995).
<b>Box and Block Test (IMPAIRMENT SCALE GRASP)</b>
The BBT test (Mathiowetz et al., 1985) is another test for the hand manual dexterity. The therapist placed a divided box with several 2.54 cm <sup>3</sup> blocks in front of the subject. Subjects are instructed to pick up one block at a time from one side of the box with the tip of index finger and thumb and release it at the other side of the box. The total time of finishing the task is 60 seconds. The number of blocks subject moved was recorded. Subject first performed the test with the unaffected hand for three times then again with the affected side. The number of blocks is averaged across the three trials. Time per block is calculated for each side of hand. The result for affected hand is normalized by dividing the affected side score by the unaffected side score. The reliability and validity of the test is verified by Cromwell and colleagues (Cromwell 1960).
<b>Jebsen Taylor Hand Function Test (IMPAIRMENT SCALE REACH AND GRASP)</b>
The JTHT (Jebsen, Taylor et al., 1969) is an assessment tool measuring the gross function dexterity. It measures the time the subject takes to complete several hand function tasks but not the quality. The reliability and validity of the test is supported by Stern (Stern et al., 1991, Spaulding et al., 1988). The tasks includes writing, turning cards, moving small objects, simulated feeding, stacking checkers, moving light weight empty cans, and moving heavy weight full cans. After giving the instructions, the therapist timed each task by a stop watch. If the subject takes more than 5 minutes to complete a task, the result is recorded as unable to finish the task. All the tasks are performed by both affected and unaffected hand. In our analysis, the result is normalized by diving the unaffected side result by affected side result to make the higher scores represent better recovery. The hand writing part is not accounted for the final score because of the difference between dominant and non-dominant hand.
<b>Grip strength (IMPAIRMENT SCALE GRASP)</b>
The hand dynamometer is used to record the grip strength. Therapist instructed the subject to grasp as much as possible for three times with both affected hand and unaffected side. The averaged score for three trials was calculated. The final score is normalized by dividing the average of affected hand score with the average of unaffected score (Sunderland et al. 1989).
<b>Stroke Impact Scale (DISABILITY/PARTICIPATION SCALE)</b>
The stroke impact scale 3.0 is a self-report measure that includes 64 items and assesses 8 domains (strength, hand function, ADL/IADL, mobility, communication, emotion, memory and thinking and participation). Subjects are asked to give a scale between 1 to 5 to complete a questionnaire including the 59 questions and 1 overall stroke recovery score. Principle component analysis has been used to analyze the whole 8 domains and divide them into 5 factors. 1 of the factors encompasses 4 physical domains including strength, hand function, mobility and activities of daily living/instrumental activities of daily living, the rest of the domains are emotion, communication, memory, and social participation. The 4 combined

domains can be reported in one single result. For the analysis, the scores in one domain are averaged and the mean score is transform to 0-100 scale by the following equation 4.1:

$$\text{score} = \left[ \frac{\text{Mean} - 1}{5 - 1} \right] * 100$$

If larger than 50% of scores are missing in one domain, that score for that domain is reported as missing. The survey also includes a question to assess the overall percentage of recovery from the patient's own perspective. The subject reported between 0-100 percent, 0 means not recovered at all and 100% means totally recovered. The validity and reliability of SIS is proved by Duncan and its colleges (Duncan et al., 1999). In the data analysis, we only account for the 4 physical domains that are mostly related to their motor movements.

**Appendix B: Diagram of device set up**



## Appendix C: Compatibility test result

### C.1. B filed change in the compatibility test

Conditions	ROI1	ROI2	ROI3	ROI4	ROI5	ROI6	ROI7	ROI8
Glove still control	-5.18E-008	2.07E-007	5.29E-009	7.20E-008	1.08E-007	1.15E-008	2.73E-007	1.60E-007
Orthosis1 still control	7.13E-008	3.73E-007	1.26E-007	1.75E-007	1.93E-007	2.15E-008	5.76E-007	2.18E-007
Orthosis2 still control	3.17E-008	3.59E-007	7.37E-008	1.58E-007	2.29E-007	1.80E-008	4.94E-007	2.37E-007
Glove still 35cm	6.61E-008	2.61E-007	3.09E-008	1.28E-007	2.29E-007	3.87E-008	-1.43E-007	1.73E-007
Glove still 55cm	-2.29E-008	1.52E-007	-9.46E-008	-1.54E-008	7.24E-008	-1.65E-007	-1.41E-007	9.60E-009
Orthosis1 still 35cm	1.26E-007	3.15E-007	3.87E-008	1.48E-007	2.76E-007	2.36E-008	5.79E-007	1.89E-007
Orthosis1 still 55cm	-3.67E-008	1.27E-007	-7.03E-008	7.89E-010	1.19E-007	-1.20E-007	6.74E-008	4.17E-008
Orthosis2 still 35cm	-6.11E-008	4.39E-008	-7.28E-008	-4.09E-008	4.21E-008	-1.14E-007	2.04E-008	5.67E-008
Orthosis2 still 55cm	-1.09E-008	2.10E-007	2.34E-008	1.11E-007	2.23E-007	2.69E-008	-3.96E-007	2.11E-007
Glove move control	2.46E-007	2.58E-007	2.72E-007	1.85E-007	6.13E-008	1.49E-007	-2.50E-007	1.13E-007
Glove move 35cm	-7.56E-008	-9.08E-008	-2.51E-008	-1.33E-007	-2.06E-007	-2.26E-007	8.86E-008	-1.31E-007
Glove move 55cm	7.69E-008	5.50E-008	1.76E-007	7.17E-008	-4.68E-008	6.34E-008	1.79E-007	-6.58E-009
No glove move control	-1.59E-008	1.63E-007	5.34E-008	4.27E-008	4.67E-008	-7.14E-008	-4.51E-008	9.46E-008
No glove move 35cm	2.72E-008	1.41E-007	2.31E-007	8.27E-008	-1.03E-007	2.60E-008	-2.23E-008	1.38E-007
Orthosis1 move 35cm	1.15E-006	5.88E-007	9.48E-007	7.86E-007	4.16E-007	8.46E-007	-1.84E-007	5.21E-007
Orthosis1 move 55cm	3.31E-007	2.70E-007	3.18E-007	2.79E-007	2.02E-007	3.04E-007	2.82E-007	2.88E-007
Orthosis1 move control	-1.67E-008	1.21E-008	4.69E-008	-1.06E-008	-5.20E-008	-3.08E-008	-2.85E-009	5.51E-008
No orthosis1 move 35cm	7.28E-007	5.30E-007	6.93E-007	5.53E-007	3.00E-007	5.52E-007	-1.77E-007	3.89E-007
No orthosis1 move 55cm	3.89E-007	1.96E-007	3.56E-007	2.08E-007	1.94E-008	2.26E-007	-1.80E-007	1.60E-007
Orthosis2 move 35cm	5.48E-007	1.75E-007	2.19E-007	2.71E-007	3.03E-007	2.87E-007	-5.78E-008	2.26E-007
Orthosis2 move 55cm	2.57E-007	8.16E-008	2.55E-007	1.74E-007	3.91E-008	2.95E-007	1.41E-007	1.64E-007
Orthosis2 move control	-6.94E-008	-1.75E-008	5.54E-008	-1.62E-008	-8.17E-008	-1.45E-008	3.29E-008	-1.83E-008
No orthosis2 move 35cm	2.58E-007	6.24E-008	2.61E-007	6.06E-008	-1.76E-007	-3.68E-008	-2.40E-007	-4.18E-008
No orthosis2 move 55cm	1.27E-007	3.31E-008	1.65E-007	7.00E-008	-4.41E-008	9.06E-008	8.99E-008	3.00E-009

Orthosis 1 represents the old orthosis; orthosis 2 represent the new orthosis; 35cm 55cm represents the distance of device from the center of coil; control represents control room. Move means block-designed movement; still mean no movement was made.

## C.2. SNR of magnitude image

ROI	1	2	3	4	5	6	7*	8
Glove still control	259.91	227.73	220.64	250.32	276.28	259.98	5.03	203.82
Orthosis1 still control	243.03	236.46	246.93	198.77	227.27	276.59	3.06	226.23
Orthosis2 still control	272.89	267.11	200.29	255.38	271.69	264.65	4.65	233.10
Glove still 35cm	245.86	315.35	252.62	269.01	283.44	251.08	3.89	199.24
Glove still 55cm	215.45	227.61	233.09	219.56	251.50	259.67	4.76	245.10
Orthosis1 still 35cm	352.32	215.15	245.88	229.91	231.51	280.63	8.24	240.37
Orthosis1 still 55cm	253.96	316.95	227.27	225.91	280.89	290.78	3.71	251.91
Orthosis2 still 35cm	271.89	243.80	251.81	355.95	222.08	277.99	3.71	273.65
Orthosis2 still 55cm	256.38	244.17	313.21	269.52	218.91	318.92	3.70	261.43
Control condition	207.21	250.51	246.13	241.28	279.71	245.57	3.12	257.58
Glove move control	117.97	129.57	118.25	120.73	117.57	116.38	1.93	112.04
Glove move 35cm	117.41	126.28	115.10	123.36	118.27	117.20	1.96	111.62
Glove move 55cm	119.46	127.20	119.09	122.20	116.06	116.67	1.96	114.43
No glove move control	118.86	129.70	117.98	122.33	118.77	117.34	1.95	113.75
No glove move 35cm	119.19	130.40	115.23	123.25	116.36	116.47	1.97	112.30
Orthosis1 move 35cm	115.04	120.46	113.53	117.70	106.09	109.49	1.99	108.62
Orthosis1 move 55cm	121.20	126.22	116.83	122.16	117.14	115.53	1.98	113.41
Orthosis1 move control	117.02	129.22	117.77	123.49	118.51	117.97	1.93	112.37
No orthosis1 move 35cm	117.15	125.78	114.11	118.47	114.28	111.40	1.94	108.92
No orthosis1 move 55cm	120.73	127.62	117.28	123.54	116.88	115.43	1.99	114.16
Orthosis2 move 35cm	117.30	127.82	113.85	119.38	113.08	112.23	1.98	112.18
Orthosis2 move 55cm	118.68	129.16	114.81	118.78	118.33	117.51	1.93	113.09
Orthosis2 move control	120.05	127.34	118.46	120.04	117.38	115.81	1.98	112.57
No orthosis2 move 35cm	115.61	124.17	113.02	117.75	109.13	111.19	1.97	110.72
No orthosis2 move 55cm	120.31	127.69	117.99	121.03	117.82	115.65	1.93	111.52
Control condition 2	118.99	127.09	119.37	121.46	115.10	118.19	1.97	113.48

Orthosis 1 and 2 represents the old and new orthosis; 35cm 55cm represents the distance of device from the center of coil; control represents devices are in the control room. Move means block-designed movements; still mean no movement was made. Control condition 1 and 2 represents the scan with no device and no movements.

## Appendix D: Sensors' reading in the compatibility test

### D.1. Grasp aperture in the non-movement conditions

Control room		35cm from the center of coil						55cm from the center of coil					
Baseline		Flat		With new orthosis		With orthosis		Flat		With new orthosis		With orthosis	
Mean	Stdev	Mean	Stdev	Mean	Stdev	Mean	Stdev	Mean	Stdev	Mean	Stdev	Mean	Stdev
9.95	0.02	9.71	0.27	9.59	0.51	9.77	0.34	9.65	0.39	9.41	0.46	9.73	0.36
9.91	0.03	10.20	0.14	9.81	0.35	9.82	0.33	10.02	0.22	9.87	0.16	10.12	0.15
9.82	0.02	10.18	0.15	9.94	0.27	9.97	0.15	10.03	0.17	9.83	0.15	10.07	0.12

(unit: cm)

### D.2. Grasp aperture in the movement conditions

Control room		35cm from the center of coil						55cm from the center of coil					
Baseline		Move		With new orthosis		With orthosis		Move		With new orthosis		With orthosis	
Mean	Stdev	Mean	Stdev	Mean	Stdev	Mean	Stdev	Mean	Stdev	Mean	Stdev	Mean	Stdev
3.12	1.05	3.24	0.47	2.91	0.73	3.08	0.71	3.83	0.61	3.17	0.59	1.93	1.09
3.72	0.60	3.73	0.19	3.17	0.53	2.77	0.78	4.02	0.37	3.79	0.82	1.85	0.52
3.75	0.32	3.57	0.51	3.78	0.24	3.66	0.46	3.83	0.40	3.76	0.53	2.26	0.70

(unit: cm)

### D.3. Encoder reading in the movement conditions

Control room		35 cm from the center of coil				55 cm from the center of coil			
Baseline move		Move		Move with glove		Move		Move with glove	
Mean	Stdev	Mean	Stdev	Mean	Stdev	Mean	Stdev	Mean	Stdev
57.12	1.88	46.41	3.75	47.65	2.62	52.50	3.81	46.64	2.05
58.46	1.00	47.13	3.81	45.67	4.32	53.51	2.65	45.61	4.52
59.81	0.51	53.16	3.45	50.28	4.28	51.72	7.35	46.63	3.72

(unit: degree)

### Appendix E: Kinematic metrics used to evaluate movements

Metrics		Definition	Study	Movement
Velocity	Mean velocity	The 1 <sup>st</sup> order differentiation of the displacement. The mean velocity is defined as the averaged velocity during the whole movement,	Wing et al,1990 Kamper et al 2002 Colombo et al, 2008	Reach, grasp
	Peak velocity	The peak velocity is defined as the highest velocity in the movement	Lang et al 2006	
Accuracy	Direction error	The difference between the initial movement direction and the targeted direction	Beer et al, 2000	Reach
	Root mean square error	Square root of mean squared distance from acquired position to target position	Song et al., 2008	Reach
	Percent time in target (PPT) Dwelling percent time in target (DPTT)	Percentage of the time subject stayed within the target window	Feng, 2007	Tracking tasks
Efficiency	Path length ratio	The line integral of the trajectory over the time taken to reach the target, calculated by the distance between 2 consecutive points of the patient's path and normalized to the straight line distance between the starting point of the task and the target	Colombo et al., 2008, Levin et al., 1996, Kamper et al., 2002 Schneiberg et al, 2002, Lang et al., 2006	Reach
Smoothness	Segmentation	The number of speed peaks that appears in the entire movement	Krebs1999, Kamper 2002	Reach, grasp
	Speed smoothness	The mean velocity over the peak velocity	Rohrer et al, 2002	Reach , grasp
Maximal movement	Maximal joint angle	The maximal joint angle moved	Nowark et al., 2007, Kamper et al 2007,	Reach
	Maximal grasp aperture	The maximal distance between the tip of index finger and tip of thumb	Lang et al, 2005, Noward et al, 2007, Gentilucci et al, 2001	Grasp

### Appendix E: (continued) Kinematic metrics used to evaluate movements

Time	Reaction time	The time between beginning of task to the first significant movement of the subject	Johansson and Westling, 1984	Reach, grasp
	Movement time	The time between the first significant movement and the last significant movement	Lang et al., 2006, Nowark et al, 2007, Chang et al., 2005	Reach, grasp
	Time to maximal movement	The time between beginning of the movement to the maximal joint angle/grasp aperture	Gentiluchi et al., 2001 Lang et al., 2006	Reach, grasp
	Time to peak velocity	The time between beginning of the movement to the maximal velocity	Gentiluchi et al., 2001, Lang et al 2005, 2006, Chang et al., 2005	Reach, grasp
	Relationship between time to reach Peak velocity and grasp peak velocity	Percent of grasp movement when reach movement reaches its maximal angle/velocity Percent of reach movement when grasp movement reaches its maximal angle/velocity	Hu et al, 2005, Lang et al, 2006	Reach to grasp

## Appendix F: Task results

### F.1. Reach task results

Subject #		6	3	4	5	9	10	2	8	1	7	12	11
Recovery score		-6.346	-6.393	-6.065	-5.383	-4.781	-4.742	-2.663	-1.926	4.820	6.489	8.244	11.715
Maximal velocity	mean	0.053	0.092	0.066	0.070	0.023	0.088	0.157	0.048	0.084	0.143	0.148	0.189
	Std error	0.002	0.003	0.002	0.002	0.001	0.003	0.006	0.003	0.002	0.004	0.005	0.006
Mean velocity	mean	0.006	0.008	0.005	0.005	0.001	0.009	0.012	0.003	0.008	0.014	0.014	0.016
	Std error	0.000	0.000	0.000	0.000	0.000	0.000	0.000	0.000	0.000	0.000	0.000	0.000
Maximal angle	mean	29.700	32.000	27.100	30.000	5.340	37.000	52.800	22.300	51.900	73.400	49.500	53.500
	Std error	0.178	0.392	0.172	0.315	0.125	0.319	0.515	0.469	0.166	0.200	0.230	0.176
Speed smoothness	mean	0.110	0.089	0.082	0.081	0.031	0.110	0.078	0.069	0.095	0.104	0.101	0.090
	Std error	0.003	0.003	0.003	0.004	0.001	0.003	0.003	0.004	0.003	0.003	0.003	0.003
Movement unit	mean	9.780	5.360	6.730	6.750	3.840	6.790	5.080	8.780	9.800	7.700	4.800	3.740
	Std error	0.372	0.236	0.371	0.341	0.153	0.326	0.255	0.510	0.343	0.307	0.197	0.165
Error	mean	0.035	0.086	0.040	0.068	0.124	0.048	0.085	0.040	0.019	0.021	0.027	0.022
	Std error	0.004	0.010	0.004	0.008	0.011	0.007	0.009	0.022	0.002	0.003	0.003	0.002

**F.1. (Continued) Reach task results**

Subject #		6	3	4	5	9	10	2	8	1	7	12	11
Recovery score		-6.346	-6.393	-6.065	-5.383	-4.781	-4.742	-2.663	-1.926	4.820	6.489	8.244	11.715
Time to Peak Velocity	mean	0.232	0.406	0.221	0.308	0.161	0.369	0.312	0.236	0.213	0.116	0.219	0.134
	Std	0.018	0.024	0.020	0.026	0.026	0.021	0.022	0.026	0.015	0.006	0.023	0.010
Time to Peak Aperture	mean	0.858	0.928	0.875	0.856	0.711	0.927	0.902	0.906	0.939	0.911	0.900	0.872
	Std	0.009	0.008	0.009	0.009	0.035	0.008	0.009	0.013	0.006	0.005	0.006	0.006
Time to Target	mean	0.592	0.656	0.629	0.556	0.222	0.683	0.643	0.591	0.763	0.735	0.705	0.653
	Std	0.010	0.022	0.013	0.022	0.018	0.023	0.019	0.038	0.007	0.008	0.019	0.010
Reaction Time	mean	0.458	1.030	0.484	1.040	0.603	0.419	0.492	0.966	0.395	0.381	0.547	0.401
	Std	0.019	0.075	0.019	0.054	0.030	0.034	0.029	0.083	0.019	0.008	0.017	0.012
Movement Time	mean	3540.0	1750.0	2920.0	2540.0	4370.0	2920.0	1910.0	3270.0	3910.0	3310.0	1900.0	2260.0
	Std	77.400	70.300	104.00	68.500	133.00	105.00	58.100	144.00	121.00	52.900	49.600	61.900

## F.2. Grasp task results

Subject #		4	10	2	8	1	7	12	11
Recovery score		-6.065	-4.742	-2.663	-1.926	4.820	6.489	8.244	11.715
Maximal velocity	mean	0.004	0.006	0.025	0.006	0.011	0.019	0.014	0.012
	Std error	0.000	0.000	0.000	0.000	0.000	0.001	0.000	0.000
Mean velocity	mean	0.001	0.001	0.004	0.002	0.002	0.003	0.003	0.002
	Std error	0.000	0.000	0.000	0.000	0.000	0.000	0.000	0.000
Maximal aperture	mean	1.800	1.310	8.260	4.040	4.770	11.300	6.840	4.640
	Std error	0.099	0.116	0.143	0.148	0.147	0.067	0.074	0.043
Speed smoothness	mean	0.198	0.189	0.159	0.256	0.181	0.177	0.255	0.215
	Std error	0.007	0.007	0.003	0.010	0.009	0.005	0.008	0.004
Movement unit	mean	7.340	4.640	1.150	8.680	2.330	1.530	1.860	1.570
	Std error	0.319	0.245	0.052	0.502	0.213	0.113	0.137	0.101
Error	mean	0.136	0.195	0.097	0.178	0.132	0.034	0.042	0.051
	Std error	0.016	0.017	0.008	0.023	0.018	0.004	0.004	0.006
Time to peak Velocity	mean	0.559	0.660	0.404	0.687	0.670	0.480	0.366	0.473
	Std error	0.034	0.041	0.019	0.027	0.018	0.013	0.011	0.009
Time to Peak Aperture	mean	0.999	0.989	0.995	0.999	0.994	0.977	0.985	0.985
	Std error	0.000	0.005	0.002	0.001	0.001	0.004	0.003	0.004
Time to Target	mean	0.756	0.550	0.339	0.623	0.802	0.785	0.670	0.785
	Std error	0.014	0.074	0.052	0.059	0.010	0.010	0.046	0.021
Reaction Time	mean	0.013	0.002	0.167	0.004	0.062	0.081	0.035	0.029
	Std error	0.005	0.001	0.024	0.001	0.014	0.012	0.006	0.007
Movement Time	mean	2080.000	1250.000	1620.000	3020.000	1350.000	1880.000	1500.000	1420.000
	Std error	45.100	33.700	40.900	85.200	40.600	50.100	32.200	21.900

### F.3. Reach movement results in the reach to grasp task

Subject #		4	10	2	8	1	7	12	11
Recovery score		-6.065	-4.742	-2.663	-1.926	4.820	6.489	8.244	11.715
Maximum velocity	mean	0.075	0.085	0.246	0.044	0.117	0.214	0.193	0.162
	Std error	0.007	0.005	0.011	0.005	0.005	0.007	0.007	0.005
Mean velocity	mean	0.013	0.013	0.026	0.007	0.026	0.043	0.031	0.029
	Std error	0.000	0.000	0.000	0.001	0.000	0.001	0.000	0.000
Maximal angle	mean	27.100	31.600	54.200	13.900	52.600	75.100	50.600	52.100
	Std error	0.720	0.359	0.682	2.380	0.346	0.327	0.282	0.070
Speed smoothness	mean	0.186	0.156	0.111	0.164	0.235	0.210	0.167	0.186
	Std error	0.014	0.008	0.005	0.014	0.008	0.009	0.006	0.006
Error	mean	0.071	0.055	0.110	0.357	0.037	0.043	0.038	0.080
	Std error	0.019	0.008	0.013	0.110	0.005	0.005	0.005	0.021
Time to peak Velocity	mean	0.202	0.272	0.273	0.411	0.281	0.246	0.241	0.176
	Std error	0.040	0.033	0.029	0.087	0.022	0.022	0.019	0.007
Time to peak angle	mean	0.962	0.853	0.914	0.911	0.920	0.929	0.934	0.924
	Std error	0.017	0.026	0.012	0.083	0.012	0.007	0.009	0.009
Time to target	mean	0.694	0.445	0.550	0.331	0.676	0.705	0.672	0.763
	Std error	0.065	0.088	0.033	0.120	0.026	0.011	0.019	0.019
Reaction time	mean	0.250	0.234	0.463	0.794	0.263	0.727	0.307	0.187
	Std error	0.046	0.054	0.045	0.204	0.013	0.021	0.013	0.008
Movement time	mean	1590.000	1430.000	848.000	1240.000	1470.000	963.000	889.000	1270.000
	Std error	116.000	79.200	60.000	102.000	51.300	24.700	24.900	52.800

#### F.4. Grasp movement in the reach to grasp task

subject #		4	10	2	8	1	7	12	11
recovery score		-6.065	-4.742	-2.663	-1.926	4.820	6.489	8.244	11.715
Maximum velocity	mean	0.002	0.005	0.022	0.005	0.011	0.021	0.010	0.011
	Std error	0.000	0.000	0.001	0.001	0.001	0.000	0.000	0.000
Mean velocity	mean	0.000	0.001	0.004	0.002	0.002	0.004	0.002	0.002
	Std error	0.000	0.000	0.000	0.000	0.000	0.000	0.000	0.000
Maximal angle	mean	0.209	2.370	7.470	2.350	4.990	7.650	4.310	4.590
	Std error	0.037	0.284	0.277	0.422	0.304	0.146	0.154	0.037
Speed smoothness	mean	0.085	0.295	0.196	0.337	0.235	0.179	0.248	0.199
	Std error	0.005	0.022	0.012	0.018	0.008	0.004	0.009	0.004
Error	mean	1.020	0.376	0.094	0.449	0.998	0.102	0.179	0.310
	Std error	0.116	0.097	0.018	0.093	0.101	0.008	0.021	0.060
Time to peak velocity	mean	0.485	0.595	0.578	0.697	0.448	0.243	0.450	0.267
	Std error	0.070	0.064	0.023	0.060	0.024	0.011	0.030	0.016
Time to Peak Aperture	mean	0.946	0.999	0.997	1.000	0.990	0.975	0.989	0.970
	Std error	0.022	0.000	0.001	0.000	0.005	0.010	0.003	0.010
Time to Target	mean	0.001	0.663	0.498	0.233	0.364	0.426	0.404	0.703
	Std error	0.000	0.102	0.077	0.122	0.032	0.028	0.067	0.019
Reaction Time	mean	0.003	0.001	0.041	0.002	0.044	0.032	0.005	0.173
	Std error	0.000	0.000	0.011	0.002	0.012	0.007	0.002	0.020
Movement time	mean	384.000	1830.000	1750.000	2190.000	1720.000	1820.000	1300.000	1310.000
	Std error	29.800	125.000	37.200	36.700	60.600	38.900	28.000	58.800

### F.5. Kinematics results by groups

			Reach		Grasp		Reach (reach to grasp)		Grasp(reach to grasp)	
			Low to medium	High	Low to medium	High	Low to medium	High	Low to medium	High
Recovery score		Mean	-4.79E+00	7.82E+00	-3.85E+00	7.82E+00	-3.85E+00	7.82E+00	-3.85E+00	7.82E+00
		Stdev	1.68E+00	2.95E+00	1.90E+00	2.95E+00	1.90E+00	2.95E+00	1.90E+00	2.95E+00
Velocity*	Maximal velocity	Mean	7.45E-02	1.41E-01	1.02E-02	1.39E-02	1.13E-01	1.71E-01	8.41E-03	1.32E-02
		Stdev	4.00E-02	1.60E-03	1.45E-04	1.47E-04	2.73E-03	9.77E-04	3.46E-04	2.16E-04
	Mean velocity	Mean	6.05E-03	1.31E-02	1.81E-03	2.75E-03	1.47E-02	3.24E-02	1.80E-03	2.67E-03
		Stdev	3.48E-03	3.70E-03	1.59E-05	1.64E-05	3.94E-04	5.91E-04	6.74E-05	4.73E-05
Accuracy	Error	Mean	6.57E-02	2.21E-02	1.51E-01	6.48E-02	1.48E-01	4.93E-02	4.85E-01	3.97E-01
		Stdev	3.12E-02	3.59E-03	5.99E-03	6.63E-03	1.41E-01	2.07E-02	3.88E-01	4.10E-01
Smoothness	Speed smoothness	Mean	8.95E-06	1.21E-05	2.98E-05	9.98E-05	1.54E-01	1.99E-01	2.28E-01	2.15E-01
		Stdev	3.24E-06	5.96E-06	4.55E-06	1.64E-04	3.13E-02	2.96E-02	1.12E-01	3.20E-02
	movement unit	Mean	6.64E+00	6.51E+00	5.45E+00	1.82E+00	3.46E+00	2.71E+00	5.32E+00	2.70E+00
		Stdev	1.94E+00	2.76E+00	1.86E-01	5.03E-02	1.64E-01	9.94E-02	3.14E-01	2.43E-01
Maximal movement	Maximal angle (degree)/aperture (cm)	Mean	2.95E+01	5.71E+01	3.85E+00	6.88E+00	3.17E+01	5.76E+01	3.10E+00	5.38E+00
		Stdev	1.33E+01	1.10E+01	2.32E-02	4.51E-02	9.11E-01	1.27E-01	1.60E-01	1.10E-01

\* in the table, the unit for reach movement velocity is degree/ms, for grasp movement velocity is cm/ms. There are no units for recovery score, error, speed smoothness, movement unit, reaction time, time to peak velocity, time to peak movement and time to target.

### F.5. (continued) Kinematics results by groups

		Reach		Grasp		Reach (Reach to Grasp)		Grasp (reach to grasp)		
		Low to medium	High	Low to medium	High	Low to medium	High	Low to medium	High	
Recovery Score	Mean	-4.79	7.82	-3.85	7.82	-3.85	7.82	-3.85	7.82	
	Stdev	1.68	2.95	1.90	2.95	1.90	2.95	1.90	2.95	
Time	Reaction Time	Mean	0.69	0.43	0.05	0.05	0.01	0.37	0.01	0.06
		Stdev	0.28	0.08	0.01	0.00	0.00	0.01	0.01	0.01
	Movement time (ms)	Mean	2900.00	2850.00	1990.00	1540.00	1540.00	1150.00	1540.00	1540.00
		Stdev	858.00	929.00	23.11	12.00	45.2	15.7	45.20	15.82
	Time to peak Velocity	Mean	0.28	0.17	0.58	0.49	0.59	0.24	0.59	0.35
		Stdev	0.08	0.05	0.01	0.00	0.02	0.01	0.02	0.01
	Time to peak movement	Mean	0.87	0.91	0.99	0.99	0.99	0.93	0.99	0.98
		Stdev	0.07	0.03	0.00	0.00	0.01	0.00	0.01	0.00
	Time to target	Mean	0.57	0.71	0.57	0.76	0.35	0.70	0.35	0.47
		Stdev	0.15	0.05	0.03	0.02	0.05	0.01	0.05	0.02

\* in the table, the unit for reach movement velocity is degree/ms, for grasp movement velocity is cm/ms. There are no units for recovery score, error, speed smoothness, movement unit ,reaction time, time to peak velocity, time to peak movement and time to target.

### Appendix G: The location of activation areas

Area	Location
Primary motor area	Located in dorsal part of the precentral gyrus and the anterior bank of the central sulcus and mainly equate to Brodmann area 4
Primary somatosensory area (S1).	Located mainly in the postcentral gyrus in the parietal lobe of the human brain and approximately equals to Brodmann area 1, 2 and 3
Pre-motor area (PMA)	Located in the frontal lobe of the brain and extends 3 mm anterior to the primary motor cortex, near the sylvian fissure, before narrowing to approximately 1mm near the medial longitudinal fissure
Supplementary motor area (SMA)	Located in Brodmann area 6 on the medial aspect of the frontal lobe
Dorsal pre-frontal area	Located in the anterior part of the frontal lobes of the brain.
Anterior cingulate areas	Brodmann area 24
Cerebellum	Attached to the bottom of the brain , tucked underneath the cerebral hemispheres

## **Appendix H: Inclusion/exclusion criterion of subjects in the fMRI case study**

The stroke survivors met the following criteria: between 30 to 85 years old and right-handed according to Edinburgh handedness survey; suffered from a unilateral ischemic stroke with arm hemiparesis; at least 6 months post stroke; able to sit up right without support for 2 hours and able to understand the instructions; able to perform the tasks with appropriate modifications, not clinically depressed according to Geriatric Depression Scale; pass the fMRI safety screening and are not claustrophobic. The exclusion criteria for the stroke survivors are 1) brain stem stroke; 2) pre-existing neurological or psychiatric disorders; 3) spasticity  $>3$  at elbow on Ashworth scale or contracture that makes it difficult to move less than 40% of passive elbow flexion or extension; 4) demonstrated visuospatial, language or attention deficits of a severity that prevent them from understanding the task, with no severe aphasia; 5) shoulder pain or joint pain; 6) decline to participate; 7) will not comply with full protocol. The inclusion criteria for the normal control are 1) older than 20 years old; 2) right-handed according to Edinburgh handedness survey; 3) not claustrophobic; 4) no history of neurological disorder; 5) not depressed according to the Geriatric Depression Survey. The exclusion criteria for normal controls are as follows: 1) Pregnant; 2) allergic to GORE-TEX and conductivity gel.

**Appendix I: Comparison of kinematics measure of reach-to-grasp movement between inside and outside the scanner**

Metrics			Maximum velocity*	mean velocity*	maximal movement *	smoothness unit	Speed smoothness	Time to Peak Velocity	Time to Peak movement	Time to Target	Reaction Time	Accuracy	Movement time*
Grasp	Inside	Mean	1.41E-02	3.27E-03	3.04	7.00	0.24	0.49	1.00	0.61	0.00	0.50	1544.16
		Stdev	3.49E-03	7.79E-04	0.90	2.35	0.06	0.20	0.01	0.19	0.00	0.44	382.87
	Outside	Mean	1.10E-02	2.43E-03	4.99	1.95	0.24	0.45	0.99	0.36	0.04	1.00	1715.89
		Stdev	4.57E-03	8.69E-04	2.02	1.48	0.06	0.16	0.04	0.21	0.08	0.67	401.97
Reach	Inside	Mean	1.28E-01	2.43E-02	40.74	5.40	0.21	0.34	0.83	0.51	0.21	0.06	1390.42
		Stdev	3.90E-02	4.11E-03	2.99	1.74	0.07	0.19	0.10	0.29	0.15	0.05	235.05
	Outside	Mean	1.17E-01	2.61E-02	52.56	1.55	0.23	0.28	0.92	0.68	0.26	0.04	1472.32
		Stdev	3.24E-02	2.92E-03	2.30	0.87	0.05	0.15	0.08	0.17	0.08	0.03	340.50

The unit for velocity is (cm/ms) for grasp task and (degree/ms) for reach task; the unit for maximal movement is (cm) for the grasp task and (degree) for the reach task; unit for the movement time is (ms). All the other metrics don't have unit.